12-2018

The Semi-Volatile Fraction of Atmospheric Aerosols

Daniel J. Ruff
djr4705@rit.edu

The Semi-Volatile Fraction of Atmospheric Aerosols

Daniel J. Ruff

B.S. Chemistry, Gettysburg College, Gettysburg, PA, 2015

A thesis submitted in partial fulfillment of the requirements
for the degree of Master of Science in Chemistry
in the School of Chemistry and Materials Science,
College of Science
Rochester Institute of Technology

December 2018

Signature of the Author _____

Accepted by _____

Director, M.S. Degree Program Date

SCHOOL OF CHEMISTRY AND MATERIALS SCIENCE
COLLEGE OF SCIENCE
ROCHESTER INSTITUTE OF TECHNOLOGY
ROCHESTER, NEW YORK

CERTIFICATE OF APPROVAL

M.S. DEGREE THESIS

The M.S. Degree Thesis of Daniel J. Ruff has
been examined and approved by the thesis
committee as satisfactory for the thesis required for
the M.S. degree in Chemistry.

_____

Dr. Nathan C. Eddingsaas, Thesis Advisor

_____

Dr. Joseph Hornak

_____

Dr. Christopher Collison

_____

Dr. Carrie K. McCalley

_____

Date

ABSTRACT

Atmospheric aerosols are significant contributor to climate effects as well as health problems. Many of these aerosols are mostly organic where their effects are dependent on their chemical composition. Atmospheric aerosols consist of a complex mixture of organic and inorganic components. The properties of the organic components within the aerosols can vary widely including the degree of oxidation and their vapor pressure. Recent studies have shown that a large fraction of newly formed atmospheric aerosols are semi-volatile and may vaporize back into the environment. This semi-volatile fraction of organic aerosols is largely unknown due to its difficulty to model. We propose a procedure that can provide a detailed understanding of the semi-volatile fraction of atmospheric aerosols. This will be accomplished by comparing three different instrumental techniques that are ATR-FTIR, GC-MS, and LC-MS. The results of this research will provide knowledge on the composition of this fraction of organic aerosols and decrease gaps in current research models in this area.

TABLE OF CONTENTS

CHAPTER 1 - INTRODUCTION

1.1 What are atmospheric aerosols?

Atmospheric aerosols are solid or liquid particulate matter made up of a mixture of organic and inorganic compounds and water. The organic fraction can make up anywhere from 20-90% of the total aerosol.[1] This matter is suspended in the atmosphere where its potential effects are of concern. Atmospheric aerosols can negatively influence climate as well as human health. In fact, a total of 1-2% of all deaths in the developed world are caused from breathing particulate matter.[2] The Department of Health has demonstrated the significance of air quality and the consequences that particulate matter can pose.[3] The effect organic aerosols have on both climate and health is determined in part by their chemical composition. Therefore, it is important to understand the composition of aerosols to better deal with their problems. The composition of the semi-volatile fraction of organic aerosols is difficult to study and is currently an area researchers know little about.

1.1.1 Primary vs secondary organic aerosols

Organic atmospheric aerosols are formed in a variety of ways. Primary organic aerosols (POAs) are those that are released directly into the environment. This can either be from natural sources or man-made sources. Hydrocarbons are released from sources such as fungi, bacteria, and burning fossil fuels.[4, 5] As their sources can be studied, these are better understood.

Secondary organic aerosols (SOAs) are made from gas-to-particle partitioning.[4, 6] Many hydrocarbons are emitted into the atmosphere from both biogenic and

anthropogenic sources and there are estimated to be between 10,000 and 100,000 different organic compounds in the atmosphere.[6] A flux of around 1,350 Tg of non-methane carbon is emitted each year, of which 10% leads to organic aerosols.[4, 6] A gaseous organic species that is oxidized by the atmosphere may undergo a change in vapor pressure. A decrease in vapor pressure can make a gaseous species more condensable. A simple model of how SOAs can be formed from volatile organic compounds (VOCs) is shown in Figure 1.1.[1]

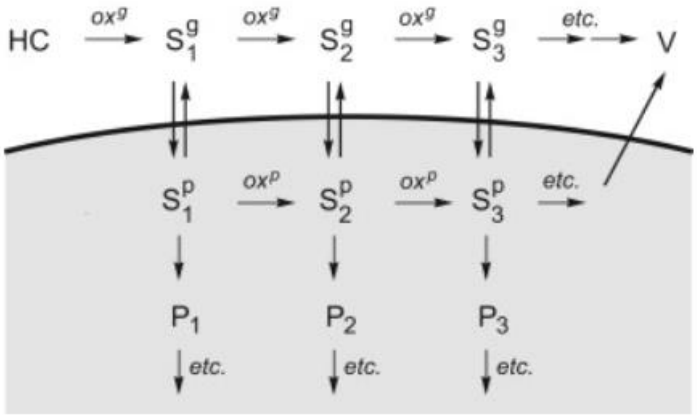

Figure 1.1: A mechanism of SOA formation and evolution showing multiple generations of gas-phase and particle-phase reactions. "S" corresponds to semi-volatile compounds, "P" corresponds to compounds formed in the particle phase, and "V" corresponds to fully volatile compounds. This is a simplified mechanism as most reactions will produce several products spanning a range of vapor pressures. Figure adapted from Kroll, J. H.; Seinfeld, J. H. *Atmospheric Environment* **2008** *42* p. 3593.

The model shows how many different products can be formed from a single species. Each reaction most likely changes volatility of the compound. Products with low volatility are considered semi-volatile as they may condense back onto pre-existing particles.[7]

1.2 Aerosol aging

Particulate matter can remain aloft in the atmosphere for up to ten days.[5] This period is a dynamic system as aerosols can move through different environments and conditions. An example of a change an aerosol may experience is the surrounding radical species. The radical species in the air from an urban setting will be different from the radical species in a rural setting. Other changes can include temperature, pressure, and humidity.[5] With such a large number of variables and random chance, the lifetime of an aerosol is extremely complex.

Over time, atmospheric aerosols have three different pathways of aging. One process of aging is through homogeneous changes within the aerosol itself.[4] Aerosols are a complex mixture containing both organic and inorganic compounds. These species can react within the aerosol, forming products with different vapor pressures.[7] A product that is formed with a lower volatility than the reactants will remain condensed in the particulate matter. If the new species is non-volatile then it will not vaporize off of the aerosol.

A second process of aging is by chemical reaction with surrounding gaseous radicals.[4, 8, 9, 10] Radicals such as HO_2 oxidize the organic fraction of the aerosol which changes its chemical composition.[4, 11] Oxidation of organic compounds can lead to a product of lower volatility than the original species. The polarity and size of a molecule are large factors for its vapor pressure.[1] Therefore, an oxidative product's volatility will be dependent on polar functional groups that are formed from reacting with atmospheric radicals. If an organic compound is oxidized completely it would form CO_2 and H_2O.[4] However, many of the oxidized species do not continue to this endpoint. How the

oxidized species behaves is determined by its new chemical composition as well as the surrounding environment.

The third pathway for aging is when the semi-volatile fraction of the aerosol vaporizes and then reacts with oxidative radicals.[1, 4] The semi-volatile fraction of aerosols consists of compounds with lower vapor pressure that are still condensable.[12, 13] They may vaporize or condense back onto the particulate matter depending on the environment. Once they vaporize into the gas phase they may react with gaseous radical species. Oxidative products may either remain in the gaseous state as a VOC or condense back to a liquid depending on the new vapor pressure.

Secondary organic aerosols are much more complicated than POAs making research into this area incredibly difficult. First off, SOAs are the result of many atmospheric reactions with many different species rather than a set source.[1, 14, 15] In addition, the products can have a large range of volatilities meaning that there may be a significant semi-volatile fraction. Another issue is the addition of functionality to oxidized species. Identifying an exact compound in a sample is problematic as this creates an extremely large number of possible chemical species with similar characteristics. Another challenge arises from atmospheric aerosols being present in such small concentrations.[16, 17] It can be difficult to study individual species as instruments need a very low limit of detection. Other obstacles in modelling the behavior of aerosols arise from attempting to replicate atmospheric conditions.[18] The atmosphere is vast and dynamic, not something easily mimicked in a laboratory setting. An aerosol's lifetime can consist of moving through a variety of different conditions at random for over a week. All current models of atmospheric conditions cannot depict a very accurate

portrayal for experiments.[1, 19] It is for these reasons that the composition of semi-volatile fractions of SOAs remain largely unknown. A better understanding of the composition of aerosols is necessary in order to identify and combat those with harmful health effects.[3]

1.3 Previous work

Atmospheric aerosols are complex mixtures where a significant organic fraction is semi-volatile.[7] The gas-particle partitioning in atmospheric conditions is a dynamic system. It is hypothesized that aging either reduces aerosol volatility by leading semi-volatiles to more stable and less volatile products, or by forming highly volatile oxidized compounds that vaporize off of the aerosol.[5] Studies have shown most POA emissions to quickly transfer to the gas phase.[4, 5, 12] The volatility and aging of primary organic aerosols was studied by Donahue *et al*.[4] One experiment was observing the oxidation of motor oil by OH radicals over time. Seen in Figure 1.2, the more volatile organics in the aerosol evaporate more readily while the less volatile organics do not.[4] The chromatograms are of nebulized motor oil particles from an experiment using a thermal-desorption aerosol gas-chromatography system. This is to compensate the loss in the gas-phase due to oxidation from the OH radicals. Loss of the less volatile species via heterogeneous oxidation by OH uptake is much slower than the gas phase oxidation. The data is indicative that an organic semi-volatile fraction is present in primary organic aerosols. This is significant as historically it was believed that POA emissions were non-volatile.

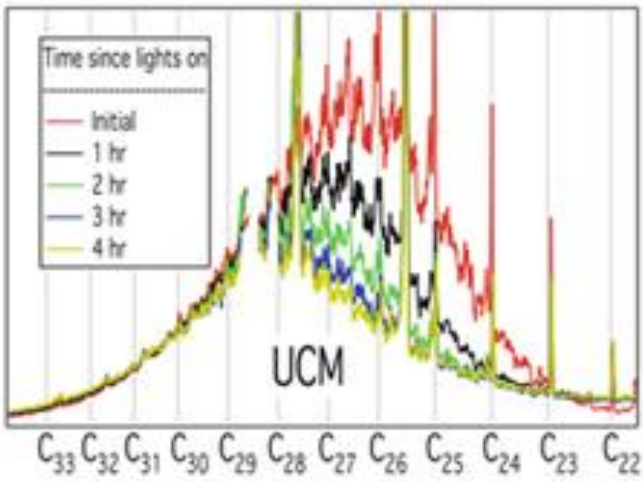

Figure 1.2: Oxidation of motor oil mixture from OH radicals. The OH radicals react with the gas-phase which drives the aerosol to evaporate. More volatile organics (nC < 28) are removed more rapidly showing the range of volatility in POAs. Figure adapted from Donahue, N. M.; Robinson, A. L.; Trump, E. R.; Riipinen, I.; Kroll, J. H. 2012.

POA emissions possessing a semi-volatile layer has also been shown in other literature. Another experiment focused on the volatility of POAs as they distribute from their source.[12] Distributions of POAs emitted from their sources have been looked at before in areas such as roadways and fires.[20, 21] The group looked at the evaporation rate of diesel in comparison to its dilution in the air. As the organic aerosol became more dilute, the more compounds evaporated off, shown in Figure 1.3.[12]

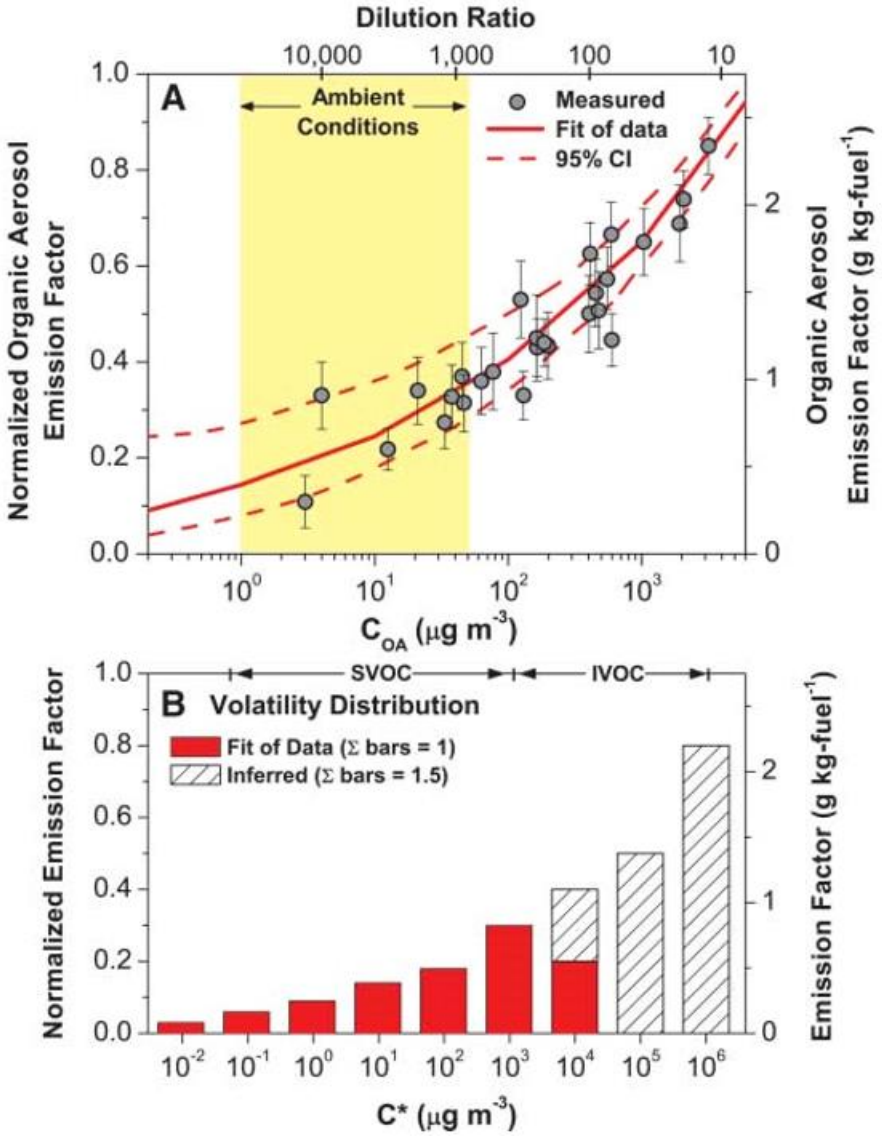

Figure 1.3: Concentration of organic aerosol (C_{OA}) after being emitted from a primary source. A) The dilution of organic aerosol compared with B) the volatility distribution. As the aerosol becomes more dilute the volatility decreases from compounds evaporating off. Figure adapted from Robinson, A. L. *et al*. *Science*. **2007**, *315*, p. 1259.

Previously POAs were thought to be non-volatile. The paper proves how actually this hypothesis is wrong as POAs are shown to have a semi-volatile fraction. As the aerosols are initially produced, they are a concentrated source of hydrocarbons. The emission factor decreases quickly as the aerosols are diluted more in the air. This

decrease in emission over time is from the evaporation of more volatile organic compounds as the gas-phase concentration is reduced. The paper that had looked at POA distribution near roadways found that the emitted aerosols become extremely dispersed within a matter of seconds.[20] This agrees with the data that there is a semi-volatile fraction in POAs that is responsible for much of the evaporation not long after being emitted.

A much more complex area to study, the volatility of SOAs has also been a major area of research.[1, 22, 23] The majority of organic aerosols are actually secondary rather than being emitted from a primary source.[24] A compound of interest is α-pinene as it is known to produce a large amount of SOAs. One particular study looked into the volatility of SOAs produced from the ozonolysis of α-pinene.[22] The number of particles and size distribution were recorded as the aerosol was heated to different temperatures in a thermodenuder, Figures 1.4 and 1.5.[22] As the temperature increased, the size and number of particles would decrease. In this experiment, at 50 °C roughly half of the SOA volume had evaporated and the average particle diameter decreased from 210 nm to 163 nm, roughly a 50% decrease in volume. At 75 °C nearly all of the volume had evaporated and the average diameter size was only 80 nm. This result is from the semi-volatile fraction of the aerosol vaporizing while the non-volatile fraction does not.

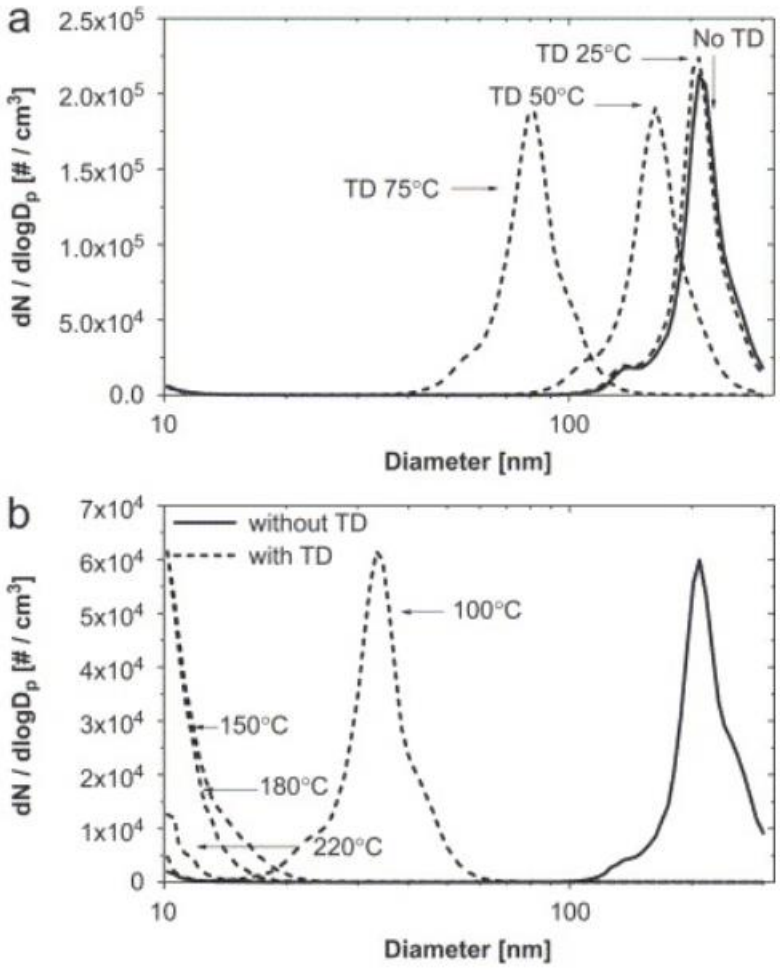

Figure 1.4: The measured number distribution of α-pinene/ozone SOA without (solid line) and with (dashed line) a thermodenuder (TD). A) at 25, 50, and 75 °C. B) at 100, 150, 180, and 220 °C. Figure adapted from Woo Jin An; Pathak, R. K.; Lee, B.-H.; Pandis, S. N. *Journal of Aerosol Science* **2007**, *38* (3), p. 305.

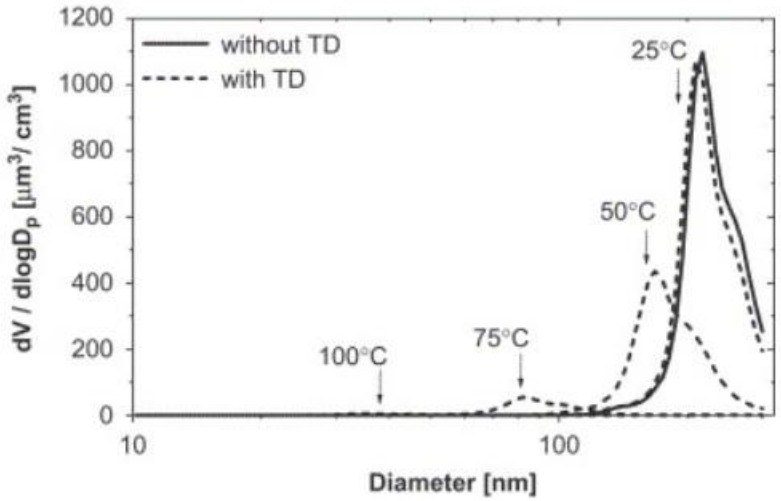

Figure 1.5: The measured volume distribution of α-pinene/ozone SOA without (solid line) and with (dashed line) a thermodenuder at 25, 50, 75, and 100 °C. Figure adapted from Woo Jin An; Pathak, R. K.; Lee, B.-H.; Pandis, S. N. *Journal of Aerosol Science* **2007**, *38* (3), p. 305.

The volatility of various SOAs in different concentrations of NO_x was studied by Lee *et al* (2011).[23] The group specifically looked at SOAs produced from α-pinene, β-pinene, and limonene at both high and low NO_x concentrations. In order to run this experiment, the laboratory setup included a smog chamber and thermodenuder. An aerosol mass spectrometer was used to measure the fraction of volume that was lost. Over the course of 4-6 hours, the fraction of total volume of SOA with increasing temperature was observed in Figure 1.6.[23]

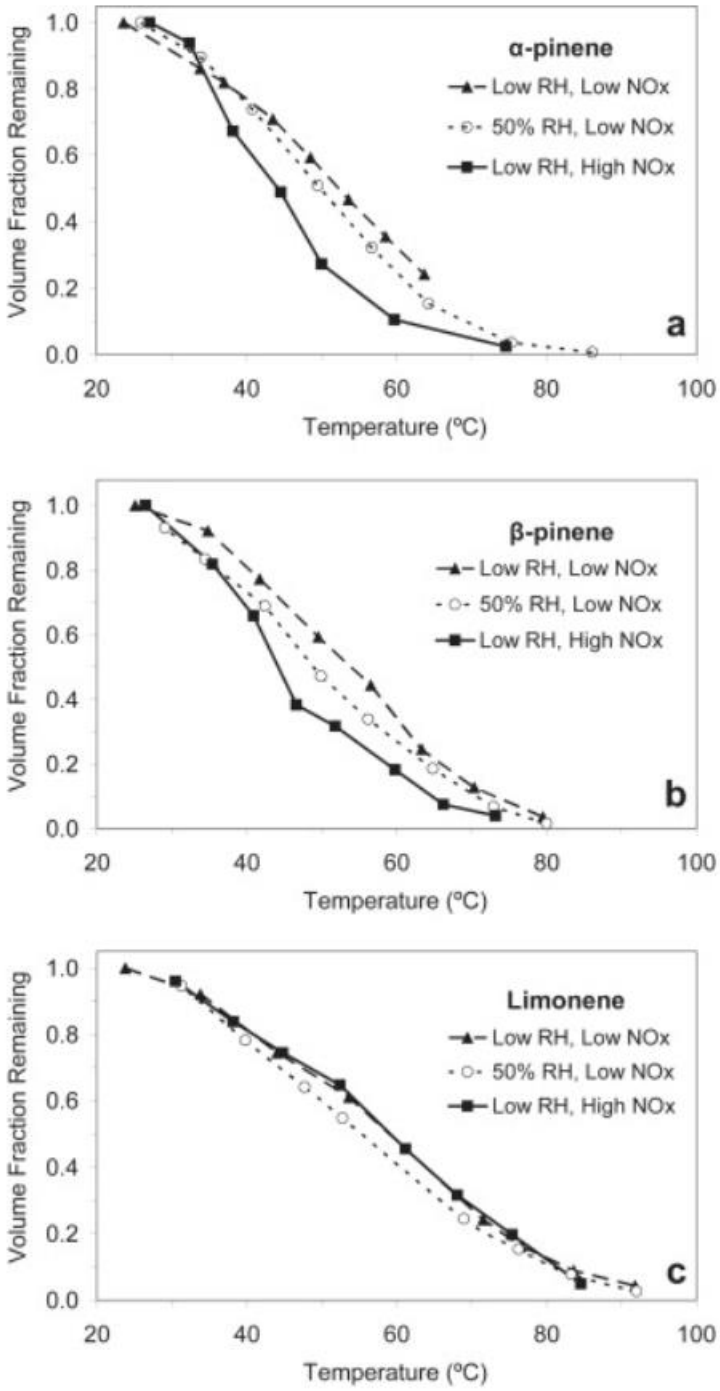

Figure 1.6: The volume fraction remaining of α-pinene, β-pinene, and limonene after low NO_x, high NO_x, and at 50% relative humidity (RH) variables with increasing temperature. Figure adapted from Lee, B.-H.; Pierce, J. R.; Engelhard, G. J.; Pandis, S. N. *Atmospheric Environment* **2011**, *45* (14), p. 2443.

The relative humidity had a slight effect as it made the aerosols slightly more volatile. Higher concentrations of NO_x produced more volatile SOAs for both α-pinene and β-pinene than lower concentrations of NO_x. The volume of aerosol decreased more rapidly in high NO_x runs than in low NO_x runs. As for the limonene, the concentration of NO_x had no significant effect on the volatility of the SOA. This result was expected as limonene produces SOAs with relatively low vapor pressures.

The semi-volatile fraction has been observed in both POA and SOA. Although this fraction is known to exist, there is still much uncertainty about its composition. To learn more about the semi-volatile fraction it is desirable to have a known method for studying SOA. Previous literature focuses largely on three instrumental techniques that include FTIR, GC-MS, and LC-MS.

1.4 FTIR

One method for studying the composition of aerosols is using Fourier transform infrared spectroscopy (FTIR) to help close current gaps in knowledge of SOAs.[24, 25, 26] One important application of using FTIR is the ability to analyze the volatility of the semi-volatile fraction as it comes off of the aerosol. Decreases in peak intensities indicate that a species in the aerosol is being removed from the particulate matter. FTIR also allows for the characterization of the semi-volatile composition as it identifies a number of key functional groups such as alcohols, amines, and carboxylic acids. Giving information on both the volatility and functionality makes using FTIR an important step in understanding the composition of the semi-volatile fraction.

Recently, there have been multiple papers on aerosol behavior with FTIR.[24, 26, 27, 28, 29] The reactive aging of films of secondary organic material was studied and an

example of their use of FTIR in collecting data is in Figure 1.7.[26] The volatility of isoprene and α-pinene were looked at by exposing them to ultraviolet radiation over time. Changes in their concentration would be observed by FTIR which is shown in Figure 1.7.

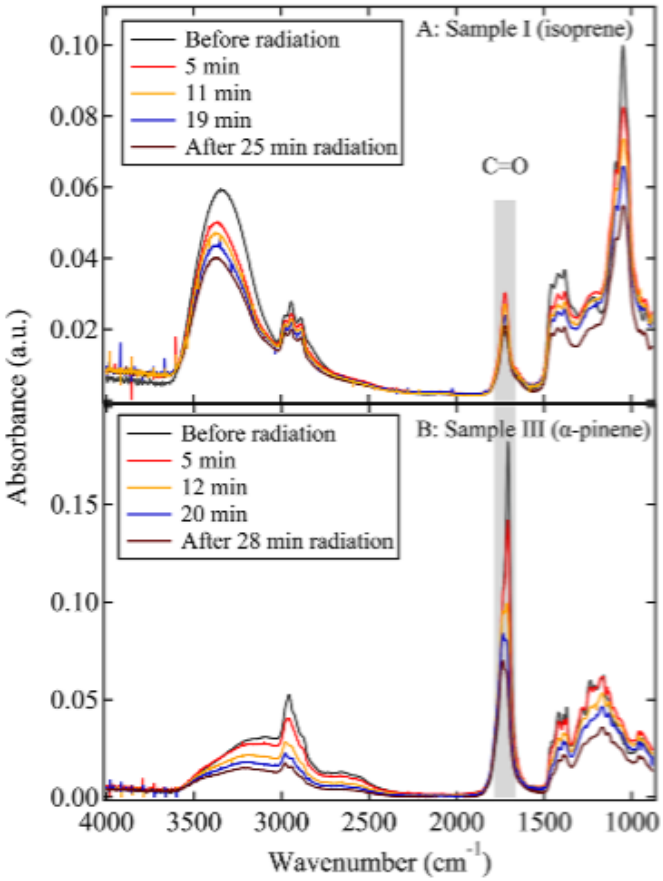

Figure 1.7: Variation of infrared spectra with increasing exposure to ultraviolet radiation. A) sample of isoprene and B) sample of α-pinene. Figure adapted from Hung, H.-M.; Chen, Y.-Q.; Martin, S. T. *The Journal of Physical Chemistry* **2013**, *117*, p. 108.

For both compounds the functional groups decrease indicating the decomposition over time from the UV radiation. FTIR is able to show the changes in both compound amount as well as how functional groups change. This finding is significant as measuring signal loss of a compound as it is removed from the FTIR can be used for analyzing the volatility of the semi-volatile fraction as it evaporates. The volatility and functionality of

the semi-volatile fraction of α-pinene was studied by a separate group using FTIR and GC-MS.[24] The ATR spectra of pinonic acid and pinonaldehyde were compared as they have been shown to be common products of α-pinene ozonolysis. The spectra includes the SOA from the ozonolysis of α-pinene immediately after introduction as well as 20 hours later under a constant flow of clean dry air. Their obtained spectra are presented in Figure 1.8.

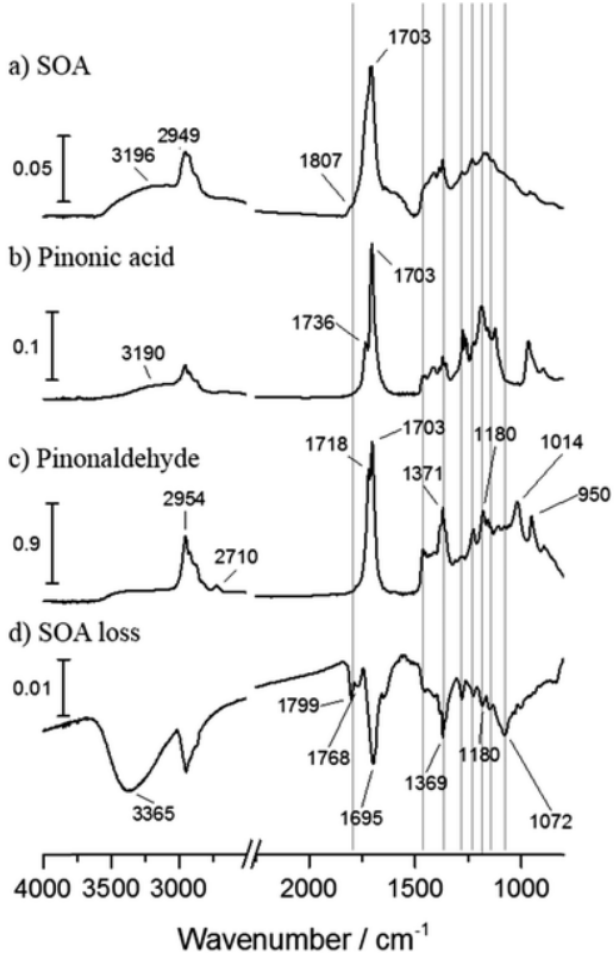

Figure 1.8: The ATR-FTIR spectra of A) the SOA from the ozonolysis α-pinene B) pinonic acid C) pinonaldehyde and D) the SOA from the ozonolysis of α-pinene after 20 hours of clean dry air flow. The negative peaks represent loss. Figure adapted from Kidd, C.; Perraud, V.; Finlayson-Pitts, B. J. *Phys Chem. Chem Phys.* **2014**, *16*, p. 22706.

The negative peaks after 20 hours represent the loss in functional groups from the SOA. Based on the functional groups that were lost, the group was able to compare this to MS data they took of the SOA to find potential candidate species that were vaporizing off of the aerosol. FTIR proved to be effective in learning the functionality of the semi-volatile fraction.

The Perraud group used FTIR to investigate how SOAs would be produced in the presence of NO_2.[27] The experiment focused on taking FTIR spectra of the SOAs formed from the ozonolysis of α-pinene with varied amounts of NO_2. The group did not attempt to collect the same mass of SOA for each sample that was run. Instead, they focused on the relative peak intensities of nitrogen containing functional groups to the C-H stretch peaks from the SOA. Peaks from RO-NO_2 are found at specific wavenumbers, such as 1280cm^{-1}, that they can compare to the carbonyl peak around 1700cm^{-1}. As the concentration of NO_2 decreased in the formation of SOA, the peaks with NO_2 containing hydrocarbons decreased relative to the other SOA peaks. This means that NO_2 is responsible for how a portion of SOAs are formed during ozonolysis. The α-pinene reacted with NO_2 when it is present to create new products containing NO_2. In this experiment, FTIR was used for its ability to determine functionality as well as being able to compare the relative intensities of certain functional groups.

A similar experiment was conducted by Gross and Bertram which looked at using FTIR for determining products from hydrocarbon monolayers with NO_3 radicals.[28] The study had one test of 1-octadecanethiol (ODT) with NO_3 and another test using undec-10-ene-1-thiol (UDT) with NO_3. For the ODT, the IR spectrum was taken while the layer remained unoxidized to use as a reference and compared this to the IR spectrum of ODT

when exposed to NO_3. The same setup was repeated for the oxidation of UDT and NO_3. Both tests confirmed that the NO_3 was responsible in the production of SOA as nitrogen containing peaks became present. An example is the ODT spectra shown in Figure 1.9.[28]

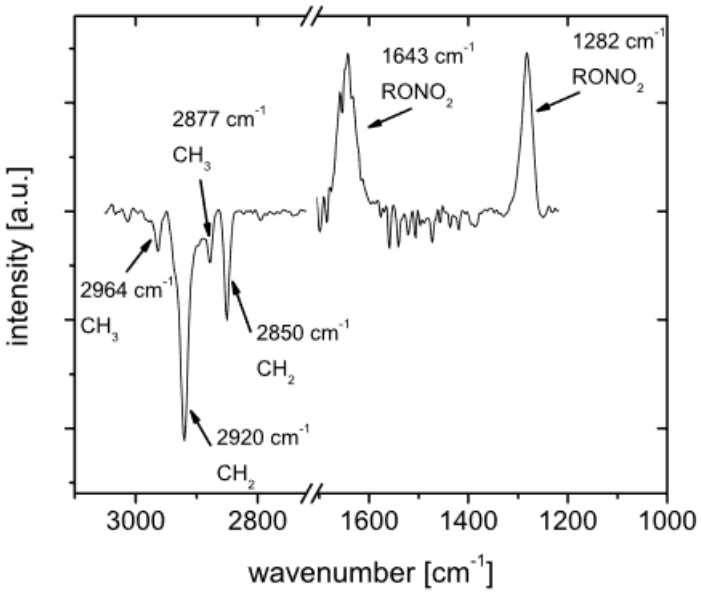

Figure 1.9: ODT IR spectrum where the negative peaks are the prominent peaks from the unoxidized sample and the positive peaks are the new peaks formed from the addition of NO_3. Figure adapted from Gross, S.; Bertram, A. K. *Journal of Geophysical Research – Atmosphere* **2009**, *114* (D2), D02307/1.

The negative peaks are the prominent peaks when ODT is unoxidized. These are normal hydrocarbon peaks in the CH_2 and CH_3 range. The positive peaks are ones that became present with the addition of NO_3. These peaks are nitrogen containing groups such as $RONO_2$. A similar spectra is seen with the UDT sample. This experiment is similar to the last paper as FTIR is used to indicate the functionality in production of SOA.

Presto *et al*. (2005) tested the effect of SOA composition under high-NO_x conditions at different temperatures.[29] An FTIR was used to compare the relative peak

heights for nitrate containing peaks and the carbonyl peak height at 22 °C and 40°C. At the colder temperature the nitrate peaks were much larger than at the higher temperature. This was determined from the relative height compared to the carbonyl peak which was fairly constant. The spectra indicate that as the temperature is raised, there is less nitrate functionality in the aerosol. This is because the increase in temperature causes more of the semi-volatile fraction to vaporize off of the aerosol. By looking at the relative absorbencies in the peaks, the group determined the relative contributions to the semi-volatile fraction for each functional group. If one functional group decreased a lot more, then compounds in the semi-volatile fraction with that functionality were more readily vaporized.

FTIR has the capabilities to analyze the functionality of the semi-volatile fraction of SOA as well as the volatility. The volatility of the SOA could be analyzed by understanding how signal loss through evaporation relates to vapor pressure. One issue with using this method is that FTIR is not able to identify specific compounds. FTIR was explored in our research to look at both functionality and volatility of SOAs but ultimately is was not effective. The work done on this method is described in Chapter 3.

1.5 GC-MS

Another method involves using GC/MS to be able to better understand the semi-volatile aerosol composition. [25, 26, 30] Jaoui and Kamens (2001) worked on identifying the specific species that are present in SOAs produced by the oxidation of α-pinene with NO_x.[30] GC-MS was used to find the specific m/*z* peaks for many possible oxidized derivatives of α-pinene. By comparing the products to the known spectra of these compounds, they were able to determine which of these derivatives were present. They

looked at both particle phase and gas phase product mixtures at different times. The first measurements were taken about one hour after α-pinene and NO_x were introduced to the smog chamber for determining first generation products. A second measurement was taken three hours after introduction to determine second generation products. Over 16 products were identified in the study and they were able to conclude that products formed in the first generation but not present later on may be responsible for the formation of secondary aerosols. From the total amount of SOA produced from α-pinene, between 54% and 71% was from identified species in the experiment. This result still leaves a significant portion of the SOA mass that is unknown.

In 2011, a paper by Goldstein *et al* proposed a method for predicting volatility and polarity of a SOA.[25] Knowledge on this subject would increase understanding of the semi-volatile fraction in the tested aerosols. GC x GC Thermal Desorption Aerosol Gas Chromatograph/Mass Spectrometer and a quadrupole Aerodyne Aerosol Mass Spectrometer were used for analysis. This method is interesting as it focuses on the traits of the semi-volatile fraction rather than attempting to identify specific species. In order to prove the chromatographic method, the group also tested specifically for 25 known compounds as well as 10 confidently identified compounds in organic aerosols. The goal was to prove that the compounds could be separated based on their polarity. They were able to group compounds from retention time based on their functionality as ketones, acids, esters, alkanes, and alkyl nitriles. One problem with the experiment is that the GC-MS heated all samples to 300 °C which does not account for the entire semi-volatile fraction. The mixture is very complex and many products that are semi-volatile would not vaporize well at 300 °C and others will not be stable at this temperature and decompose.

1.5.1 Derivatization

A method for getting around the temperature limit is derivatization. This involves reacting products under certain conditions to replace polar functional groups with more nonpolar derivatives. This in turn can significantly increase a compound's vapor pressure so that it will vaporize in the GC. Schauer *et al*. (2015) investigated the amounts of levoglucosan in Fresno, California. Levoglucosan is an important biomarker for determining biomass burning and for characterizing atmospheric polarity.[31] N,O-bis(trimethylsilyl)trifluoroacetamide (BSTFA) and trimethylchlorosilane (TMCS) were used to substitute the three alcohol groups on the compound with trimethylsilyl groups. This was done by reacting the collected material with BSTFA and TMCS in excess at 70 °C for 2 hours. A separate study used GCMS to analyze collected cloud water samples from a mountain in NY.[32] The compounds of interested were highly polar so the group used BSTFA and O-(2,3,4,5,6-pentafluorobenzyl) hydroxylamine hydrochloride (PFBHA) to target specific organic compounds. While BSTFA is used to derivatize alcohol groups and carboxylic acids, PFBHA is used to derivatize non-acidic carbonyls.

SOA can have a variety of functional groups caused by oxidation in the atmosphere. Multiple functional group derivatizations are ideal to successfully lower the vapor pressure of semi-volatiles. Flores and Doskey (2015) focused on designing a set method for doing several derivatizations for one sample.[33] They elaborate on a 3 step method for converting carbonyls, carboxylic acids, and alcohols for a single sample. Carbonyls were first converted to methyloximes ($R\text{-}C{=}N\text{-}OCH_3$) using O-methylhydroxylamine hydrochloride (MHA). Next carboxylic acids were converted to methyl esters using (trimethylsilyl)diazomethane in methanol (TMSD/MeOH). Lastly

alcohols were converted to trimethylsilyl ethers using BSTFA. Carboxylic acids could also be converted to methyl esters using BF_3 however this method was unreliable at converting species with more than 2-OH groups. By having a 3 step derivatization process the identification of compounds is more clear as there is no ambiguity between derivatized –OH and –COOH species. An example of these methods are shown in Figure 1.10. These methods were tested on a large number of different compounds to prove their ability to derivatize varying species with a reliable procedure.

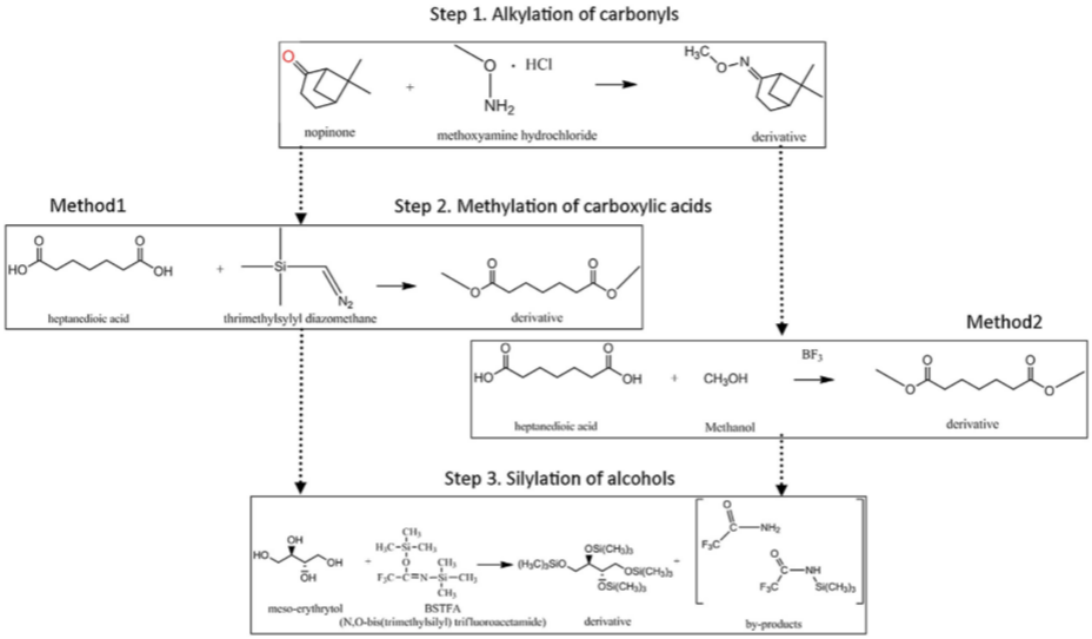

Figure 1.10: Two separate methods for a 3 step derivatization presented by Flores and Doskey. Figure adapted from Doskey, P.; Flores, R. *Journal of Chromatography A* **2015**, *1418*, p. 1.

In order to study the semi-volatile layer, compounds are often compounds collected on a sorbent. A common sorbent that is used is XAD resin for gaseous species.[34, 35, 36] However, using derivatization the aerosol compounds are not as easily

identifiable. As they have been derivatized their fragmentation pattern will be different and may not be present in an MS library. Derivatization ended up changing the fragmentation so much that there was difficulty in determining known compounds. The work with GC/MS and its problems are detailed in Chapter 3.

1.6 LC-MS

A third method involves using Liquid Chromatography Mass Spectroscopy (LC-MS) rather than GC-MS in order to analyze the products. As the sample does not need to be vaporized it eliminates the need for derivatization. Several groups have used LC-MS to study known compounds present in SOAs.[37, 38, 41] Larsen *et al*. (2001) focused on the gas-phase OH oxidation of monoterpenes.[38] Monoterpenes are known to form secondary aerosols and the group tested five of them. Limonene, α-pinene, β-pinene, 3-carene, and sabinene were each individually tested in a Teflon coated Pyrex glass reaction chamber. Using UV lamps and hydroxyl radical the monoterpenes were oxidized and their products collected onto filters. The filters were analyzed using LC-MS where they were able to determine certain known products. One figure of interest is that of the products from the reaction with α-pinene, Figure 1.11.[37] The products of pinonic acid and norpinonic acid have vapor pressures considered to be in the semi-volatile range. This demonstrates the ability of LC-MS to observe specific compounds in the semi-volatile fraction of SOA.

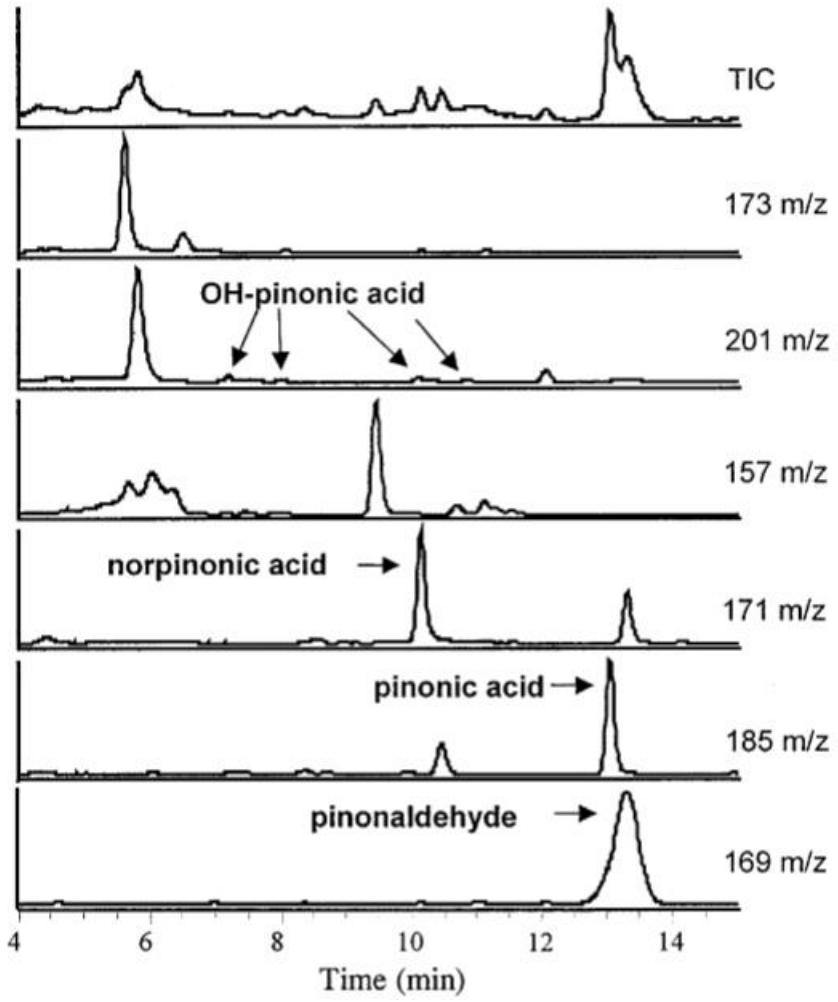

Figure 1.11: HPLC-APCI-MS chromatograms (TI and SIM) of the reaction products in the aerosol generated from the OH oxidation of α-pinene. Figure adapted from Larsen, B.; Bella, D.; Glasius, M.; Winterhalter, R.; Jensen, N.; Hjorth, J. *Journal of Atmospheric Chemistry* **2001**. *38*, p. 231.

Testing the effectiveness of LC-MS would involve successfully identifying known semi-volatile compounds from an SOA experiment. Winterhalter *et al*. (2003) looked at the oxidation of α-pinene by ozone and OH-radicals using LC-MS to identify multiple compounds.[38] Using LC-MS they analyzed and identified several products collected on filters. Shown in Figures 1.12 and 1.13, they located several prominent peaks such as pinonic acid, pinic acid, and norpinic acid.[38] Their vapor pressures are

considered to be in the semi-volatile range.[39] These peaks are important as they can be used to confirm known compounds in SOA which would mean that LC-MS is capable of analyzing specific species in the semi-volatile fraction.

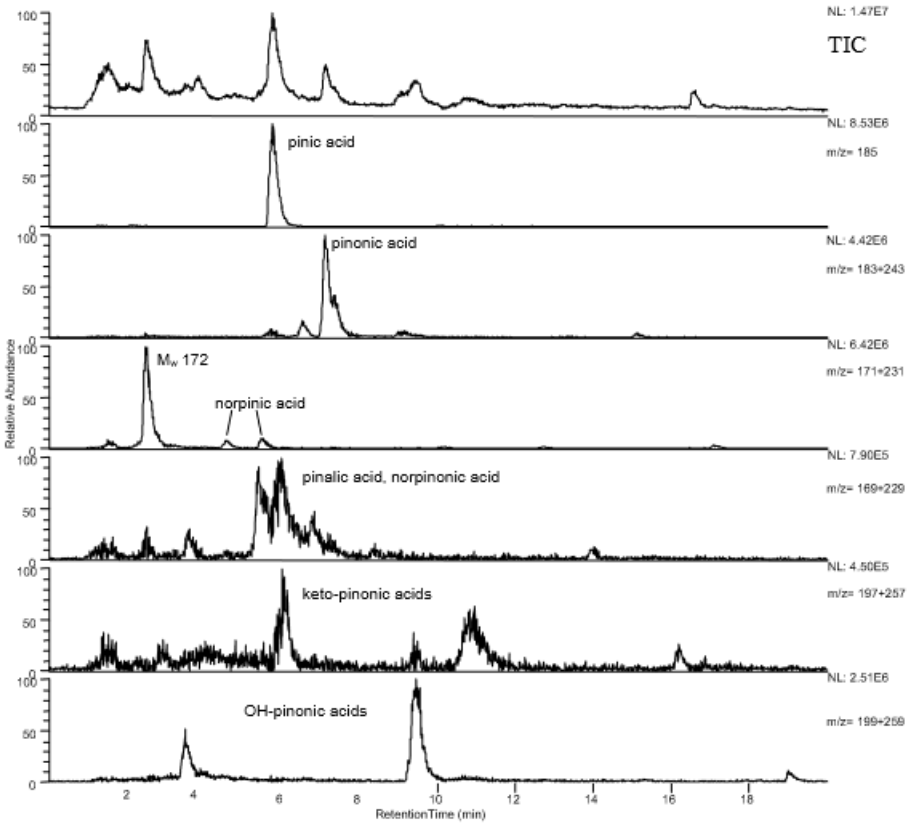

Figure 1.12: Total ion chromatogram and extracted ion chromatograms from the ozonolysis of α-pinene in ESI(-) mode. Figure adapted from Winterhalter, R.; Van Dingenen, R.; Larsen, B.; Jensen, N.; Hjorth, J. *Atmospheric Chemistry and Physics Discussions* **2003**. *3*, p. 1.

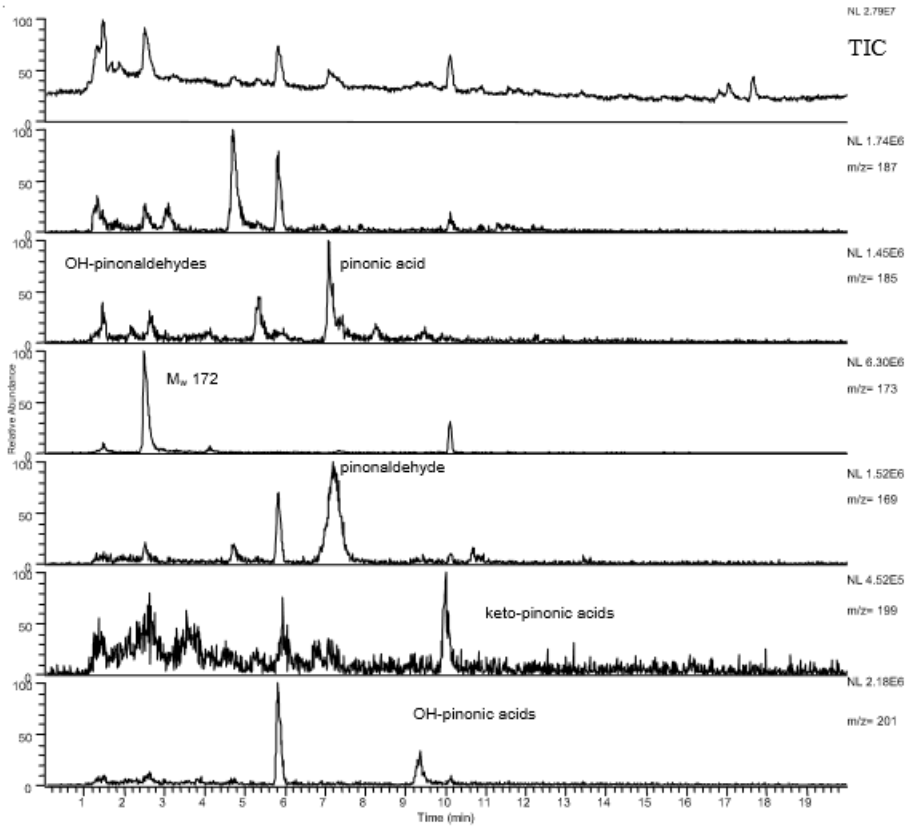

Figure 1.13: Total ion chromatogram and extracted ion chromatograms from the ozonolysis of α-pinene in ACPI(+) mode. Figure adapted from Winterhalter, R.; Van Dingenen, R.; Larsen, B.; Jensen, N.; Hjorth, J. *Atmospheric Chemistry and Physics Discussions* **2003**. *3*, p. 1.

1.7 Analysis of α-pinene ozonolysis

To date there is a significant amount about atmospheric aerosols that remains unknown. Specifically the composition of the semi-volatile fraction of aerosols, especially SOAs. Current methods have not been able to fully model and measure these complex, dynamic systems. It is imperative to continue closing gaps that models today still possess in order to ultimately identify the composition of this semi-volatile fraction. Analyzing this organic fraction is made difficult for many reasons such as the large number of possible products that can be formed and the fact that these species are mixed

with one another in the aerosol.[1, 14, 16, 41] A logical step forward is exploring a method that can be used more widely.

One specific reaction known to produce SOA that has a significant amount of prior research is the ozonolysis of α-pinene.[22, 23, 24, 26, 27, 30, 37, 38, 41, 42, 43] α-pinene is an abundant compound that is known to react with gaseous species such as ozone to form a number of semi-volatile compounds that end up within SOA. There are numerous compounds that can be created from a variety of pathways. Figure 1.14, taken from Jenkin (2004), shows some of the products from the ozonolysis of both α-pinene and β-pinene.[42]

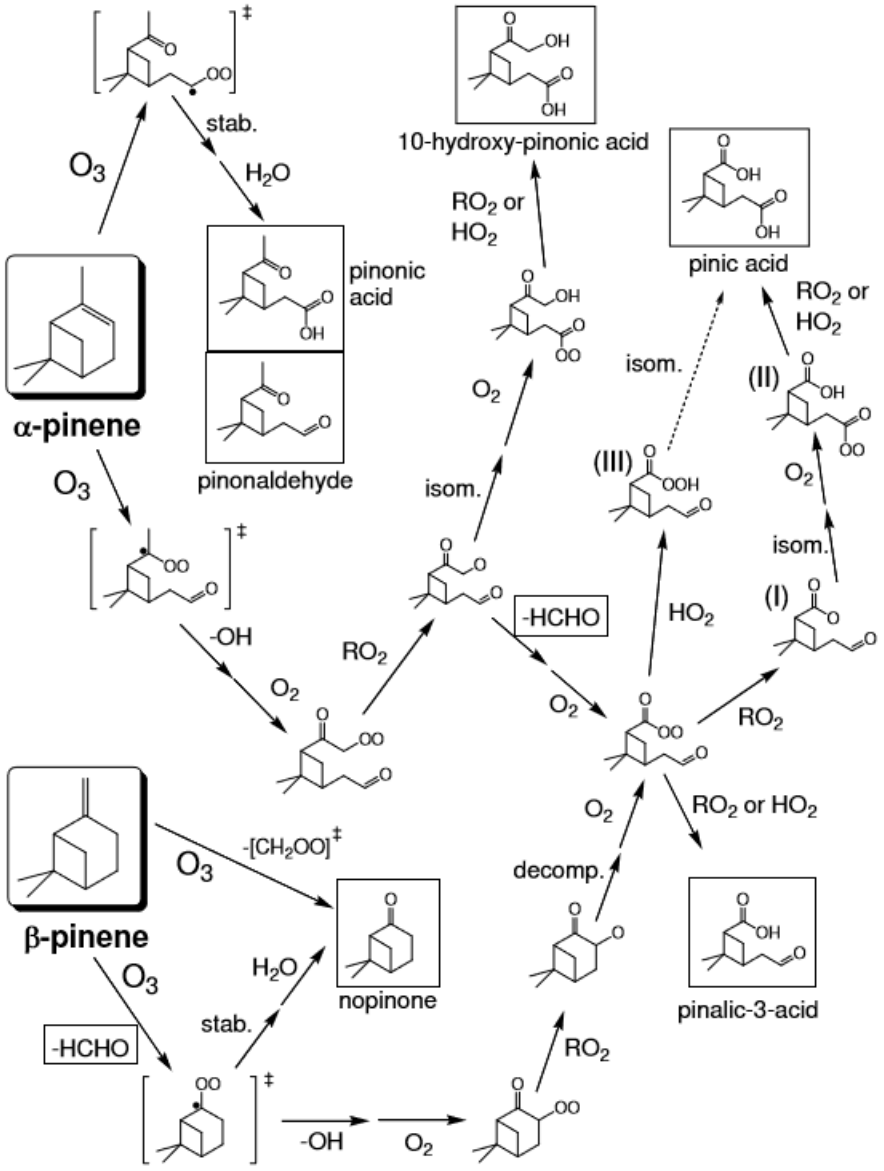

Figure 1.14: The reaction pathways of the ozonolysis of α-pinene and β-pinene. This contains just a few of the major compounds. Jenkin, M. *Atmospheric Chemistry and Physics* **2004**. *4*, p. 1741.

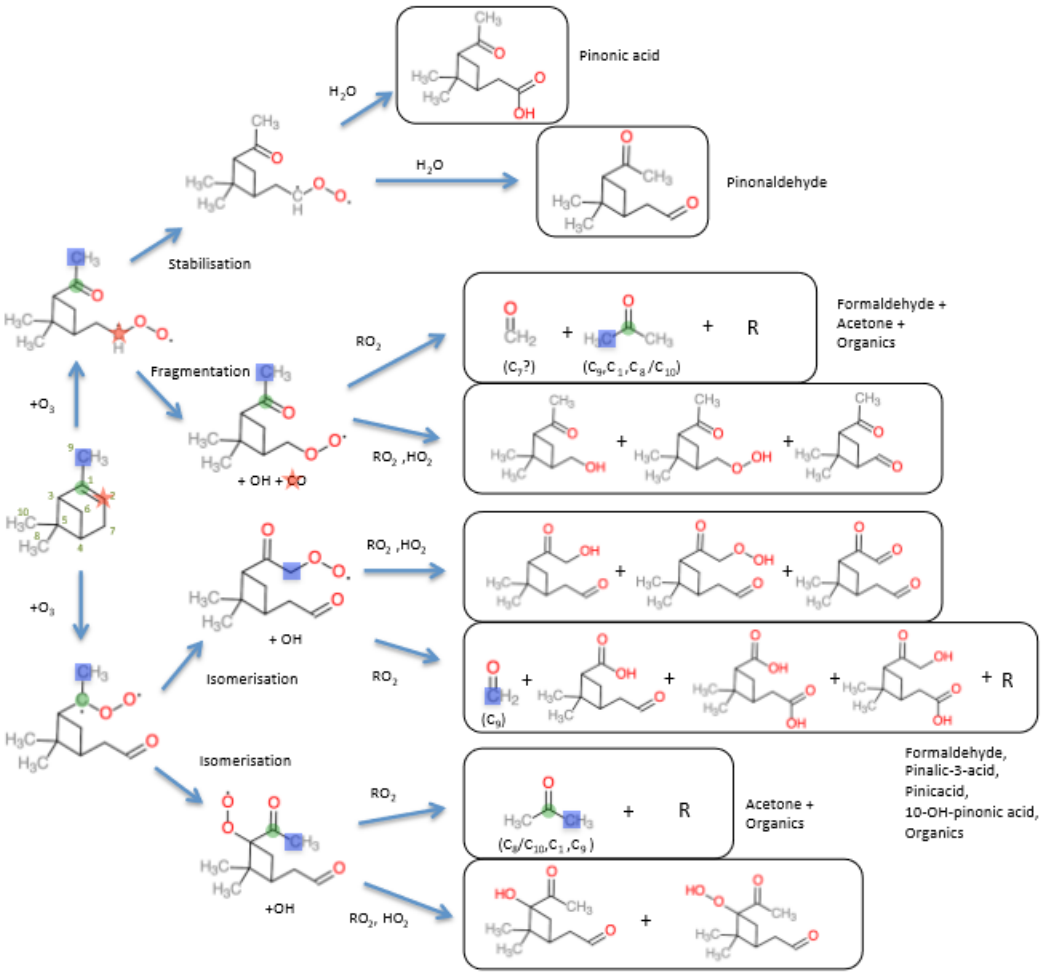

Figure 1.15: Another reaction pathway of the ozonolysis of α-pinene. A number of products can form including large oxygenated products that have lower vapor pressures. Meusinger, C. *et al*. *Atmospheric Chemistry and Physics* **2017**. *17*, p. 6373.

Figure 1.15, taken from Meusinger (2017), shows how even more species can be formed.[43] The O:C ratio usually increases the more the compound is oxidized. This can result in larger compounds with a lower vapor pressure than α-pinene that partition to the particle phase. As many of these semi-volatile compounds have been previously observed, their presence would help indicate whether a new method is successful in studying the semi-volatile fraction from the ozonolysis of α-pinene.

1.8 Objectives

The end goal of this research was to reach two important outcomes to help in this area of study. First, which instrumental method is the best for studying the semi-volatile fraction? Second, what information can be learned from this method? The first objective is detailed in Chapter 3 while the second objective is detailed in Chapter 4. Chapter 2 explains the setup that was used to be able to study the SOA. A flow reactor was used to conduct the ozonolysis of α-pinene. Initially, we worked with FTIR to study the general composition of the semi-volatile fraction of SOA. We planned on analyzing volatility by measuring the change in signal intensity from the compounds as the evaporated off of the ATR plate. We ran into difficulty with this method which is discussed in chapter 3 and it was determined to not be the best method going forward. After difficulty with the FTIR we moved to GC-MS. A method for derivatization was made in order to study compounds with lower vapor pressures. The method worked in derivatizing known compounds so we then moved to studying the products from the ozonolysis of α-pinene. Unfortunately, we were unable to identify many significant compounds that we would expect to see. Using LC-MS we found success in identifying semi-volatile species. Several known species were confirmed by comparing data with previous papers that identified these compounds. After identifying the known compounds we examined their evaporation with changing temperatures. By knowing their volatility we were able to create a relationship between a compound's vapor pressure and how much it evaporates. We also found several prominent peak in the chromatogram that are unknown. Using the relationship we are able to get a general idea of their vapor pressure.

CHAPTER 2 - MATERIALS AND METHODS

2.1 FTIR

FTIR analysis was performed on a Shimadzu IRTracer-100 equipped with a 71 mm long germanium ATR cell (Pike Technologies) with a penetration depth of 0.61µm. The ATR flow cell is capable of varying temperature. The IR range spanned from 900 cm^{-1} to 4000 cm^{-1}, the experiments were performed at a resolution of 2 cm^{-1}. Each IR measurement took a total of 64 scans and then averaged them into the final spectrum. The FTIR and cell was purged with dry nitrogen to reduce spectral contamination from water vapor and carbon dioxide. The instrument was purged at a flow rate of 3.0 SLM, the optical path of the ATR cell was purged at a flow of 0.8 SLM, and the sample compartment had dry nitrogen flow of 0.20 SLM. The sample compartment flow not only reduced spectral contamination but also evaporated the species through isothermal dilution. The ATR cell is shown in Figure 4.1 where the dry nitrogen enters on the left side and exits the plate from the right tube.

Figure 2.1: The ATR cell with flow coming from the left, passing over the germanium plate, and exiting on the right.

Initial studies were done on test samples of known compounds. Samples were dissolved in methanol so that they could be injected onto the ATR plate. Prior to injection the nitrogen flows are run so that there is a stable background scan without H_2O or CO_2 interference. Once a background has been taken, the sample which is 250 µL is injected into the ATR cell which has a volume of 0.50 mL. The sample would have a low enough concentration that the film left of dissolved species after evaporation of the methanol would not be higher than the penetration depth. Scans are taken at set time intervals to see signal change depending on what is being tested. A compound with a relatively high

vapor pressure would vaporize faster and so scans would be taken at shorter time intervals. A compound with a lower vapor pressure would take longer to be partition to the gas phase so scans would be taken at longer intervals.

A Teflon filter was used to hold samples on the ATR cell which is explained in 3.2.2. A Teflon filter is cut so that a strip of it can be placed onto the ATR cell covering as much surface area as possible. Rather than inject samples into the cell, they are injected onto the filter strip beforehand. Once the entire sample has soaked into one side of the filter strip it is placed sample side down on the ATR plate. This requires the cell to be unscrewed with the plate exposed. Styrofoam is cut and placed on top of the filter so that when the top of the cell is screwed back on it presses the Styrofoam against the filter. This pressure keeps the filter firmly against the plate to give the best signal.

2.2 Aerosol production

In the case of the experiments discussed in this thesis, SOA from the ozonolysis of α-pinene was studied. A glass flow reactor with a volume of 6.7 liters was constructed consisting of a large flow cell (153 cm x 8.7 cm), 3 separate inlets that are combined before or within the flow cell, and one exit port where the filter sample holder is attached shown in Figure 2.2. The three inlets are for the organic reactant (α-pinene), the oxidant (ozone), and the carrier flow (nitrogen). The oxidant and carrier gas are mixed at the T union shown in Figure 2.2. The hydrocarbon is injected directly into the flow cell via a 1/8 inch Telflon tubing that is fed through the T union and extended into the cell. The hydrocarbon is introduced within the flow cell itself for a number of reasons. First, this

ensures that the reaction does not initiate prior to being inside the flow cell. Second, to ensure that the oxidant is diluted to the desired concentration prior to interaction with the hydrocarbon. Finally, by introducing the hydrocarbon to the reaction cell via a tube extended into the cell, the reaction time can be varied without changing the reaction conditions by varying how far the tube is inserted into the flow cell.

The design of the flow reactor is such that the products leaving are all of the same age (4.5 minutes) so that aerosols of the same composition can be generated and sampled in high yields and can be used to study aerosol composition of a wide variety of SOA by changing the reactant organic, the oxidant, or residence time within the reactor. The first flow was for the reactive organic, a nitrogen flow of 0.100 SLM sent through a bubbler filled with α-pinene held at a constant 19 ºC in a temperature bath shown in Figure 2.3. At 19 ºC α-pinene has a vapor pressure of 3 torr. Ozone, the oxidant, was generated by passing a flow of 0.500 SLM of ultra-zero air through an Enaly ozone generator, set at 30%, to create an excess of ozone. Lastly, a nitrogen flow at 1.40 SLM was included to give the total flow through the reactor 2.00 SLM. The α-pinene flow tube ended inside of the flow reactor where it would come into contact with the ozone and nitrogen shown in Figure 2.3. The flow conditions created a concentration of 222 ppm of ozone and 180 ppm of α-pinene in order to favor SOA production. At these concentrations the lifetime of α-pinene is only 1.54 seconds due to the excess ozone. Figure 2.2 shows the basic setup for the ozonolysis experiment.

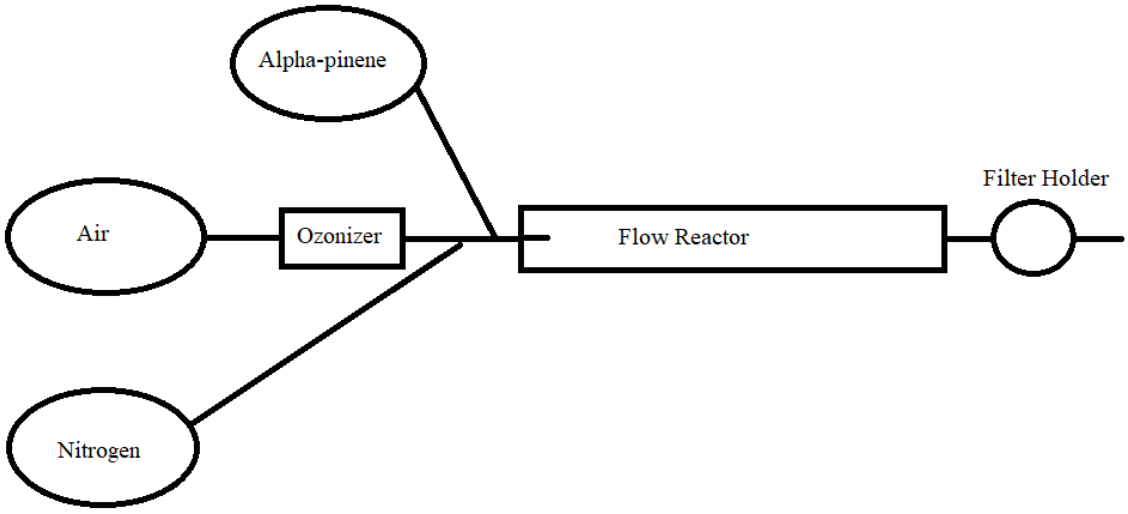

Figure 2.2: Flow chart of procedural setup for SOA from α-pinene ozonolysis.

With a flow of 2.0 SLM in a chamber with a volume of 6.7 liters the residence time was expected to be around 3.35 minutes. The actual residence time was determined by measuring the ozone concentration with an ozone monitor (2B Technologies model 202). The monitor was connected to the flow line after the filter holder. The resonance time was measured by running ozone through at a constant level and shutting it off. Then the ozone generator was turned back on once the ozone level had depleted. The time it takes for the ozone to change is the resonance time for the flow reactor shown in Table 2.1. The middle column is the time for the ozone level to begin to change and the right column is the time it takes for the change in ozone to fully finish.

Table 2.1: Table of the ozone resonance time

Ozone monitor status	Time for change to start (minutes)	Time for complete change (minutes)
Switched off	5:50	9:00
Switched on	4:50	8:30

The experimental results were longer than the theoretical result of 3.35 minutes. This is most likely due to fluid dynamics of the flow through the cell. Similar experiments were conducted by measuring water vapor concentrations instead of ozone and similar experimental results were observed.

The SOA production was estimated to be at 0.2 mg/min for ozonlysis experiments. The reactor was connected to a filter holder for aerosol collection shown in Figure 2.6. Runs were conducted for a total of 10 minutes as too much buildup of SOA on the filter would block the flow. The amount of SOA generated was regularly at 2 mg which agrees with the estimated SOA production. After the filter holder the tubing went to a fume hood in order to discharge ozone from the laboratory.

Figure 2.3: The flow reactor setup with three separate lines. The oxidant and carrier gas are the lines on the sides that combine at the T union before entering the cell. The organic reactant passes through this combination into the cell.

Figure 2.4: The α-pinene is in a bubbler which is kept in a thermoregulator at a steady 19 ºC.

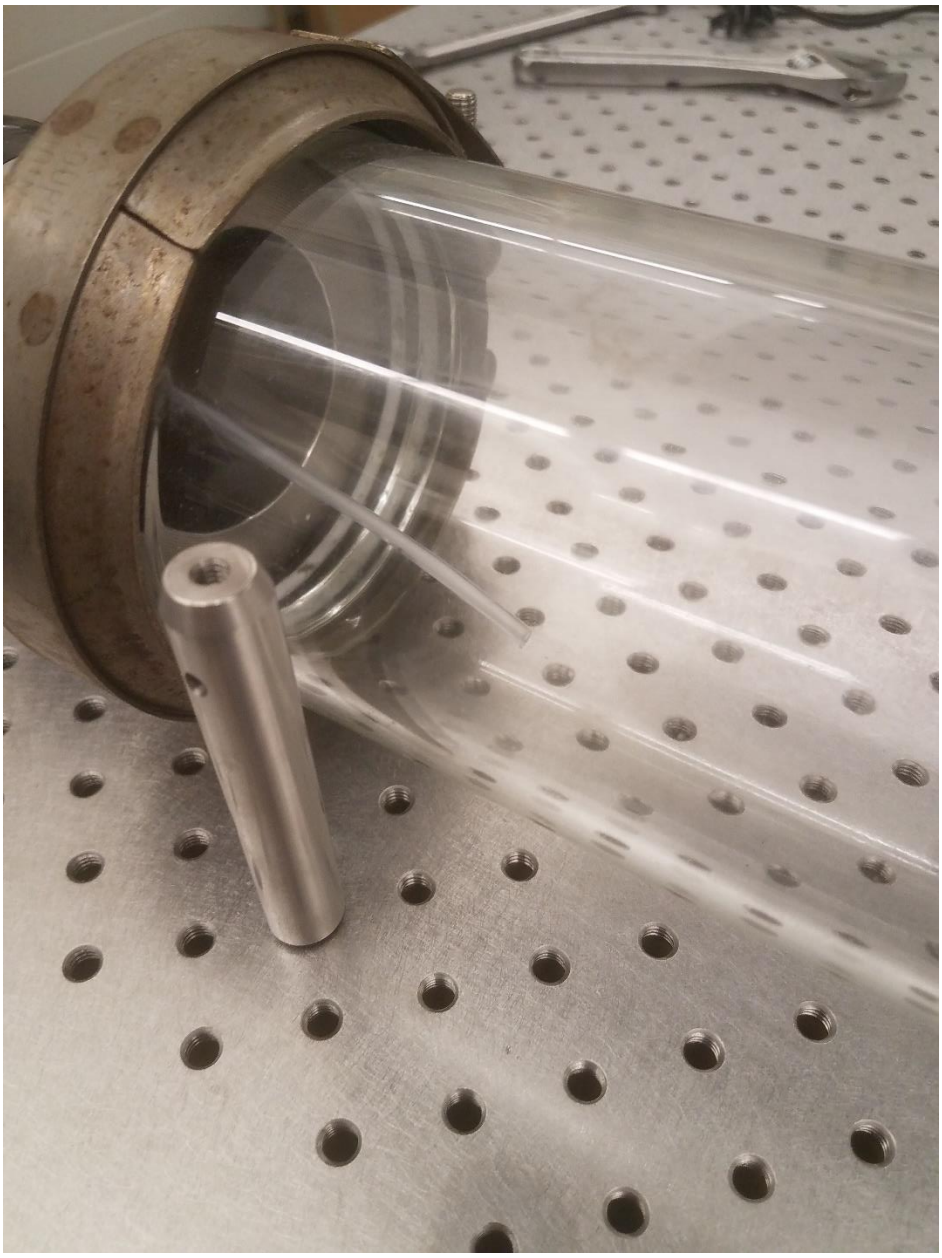

Figure 2.5: The stream of α-pinene is exposed to ozone as it enters the flow reactor.

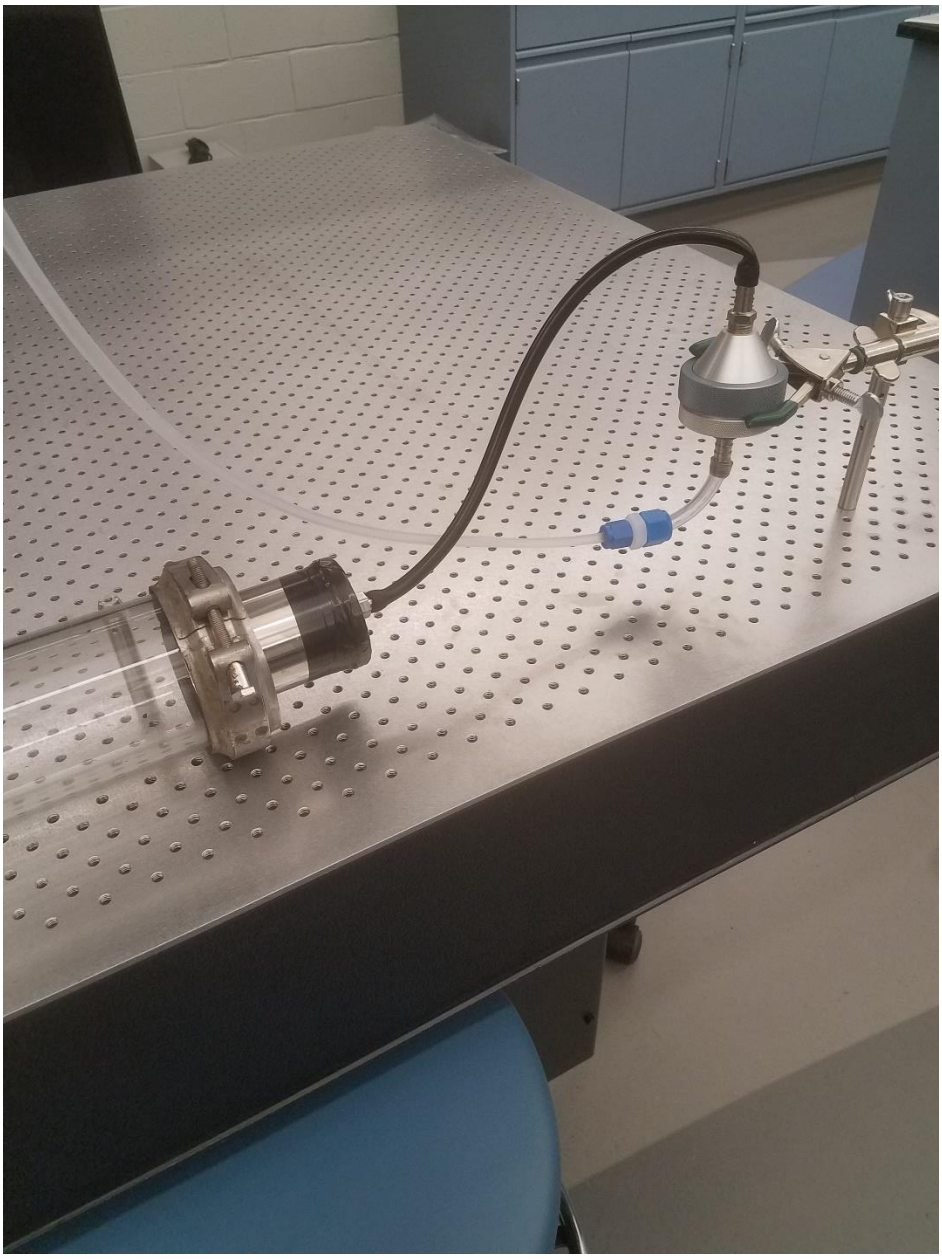

Figure 2.6: Following the flow reactor the aerosol is collected onto a filter. The line then goes to a fume hood to remove ozone.

2.2.1 Collection of SOA onto Resin

For analysis of the semi-volatile fraction of SOA by GC-MS or LC-MS, the organic fraction of the SOA evaporated from a sample during isothermal evaporation was collected onto solvent-desorption media and subsequently analyzed. A filter (Tisch Scientific, hydrophobic PTFE, 1.0 μm pore size, 47 mm diameter) was held in a filter holder with a stream of 1 SLM of dry N_2 passing through. At the base of the holder a resin tube was connected to collect any species that would evaporate off of the filter shown in Figure 2.6. To study the effect of temperature on evaporation of the semi-volatile fraction of SOA, the filter holder was wrapped in heating tape and insulated with glass wool and aluminum foil. The heating tape was placed so the filter holder could be set to a specific temperature. Increasing the temperature can be used to vaporize semi-volatiles. This setup is run for a total of 5 hours to ensure efficient volatilization of any semi-volatile species.

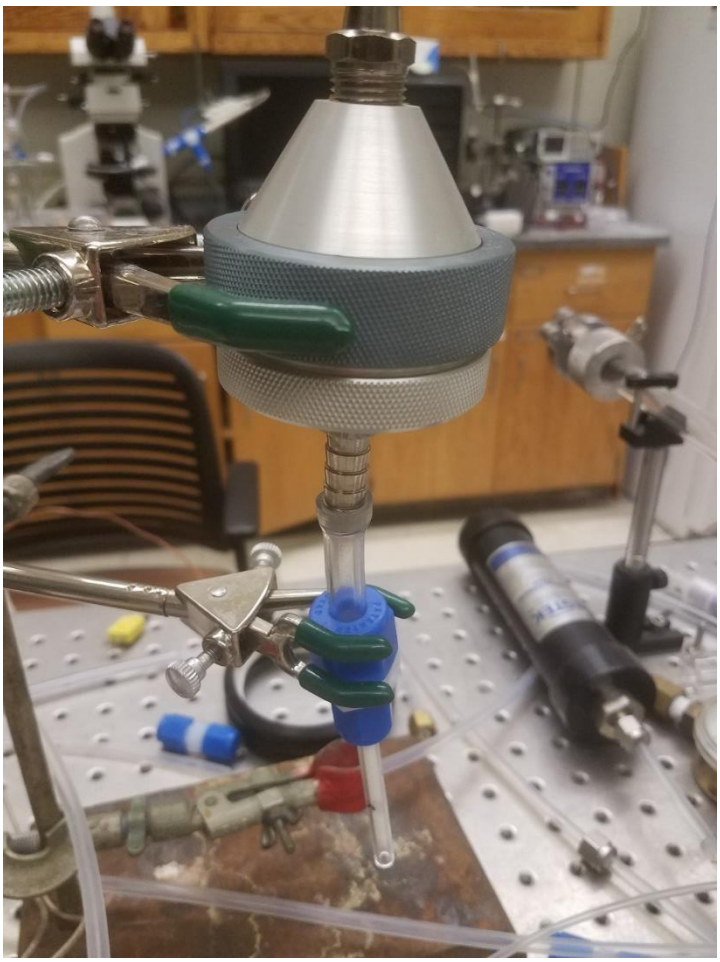

Figure 2.6: Nitrogen is blown through the top of the filter holder where then it passes through a resin tube.

2.2.2 Resin tubes

The resin tubes used for collection were not commercial sample tubes but instead ones we made ourselves. Quarter inch glass tubing was cut into sections roughly two inches long. The outer edge at each end was sanded down for ease connecting to Teflon tubing. Supelite DAX-8 resin was packed into the tubes as a single bed at 150 mg. Glass wool (Sigma-Aldrich silanized) was packed on the sides in order to hold the resin in place. Resin is cleaned by soaking it in methanol with sonication for 30 minutes. Then it is soaked in 1M HCl with sonication for 30 minutes. The solvent is then removed from

the resin through a glass sintered glass funnel filter. The resin on the filter is then rinsed repeatedly with hot nanowater (18MΩ) several times. Lastly the resin is put under a vacuum of less than 0.5 torr for a minimum of 5 hours. The cleaned resin is stored in a desiccator. Three other resins were tested in order to determine the best for collection. Amberlite XAD 4 resin, Amberlite XAD 7HP resin, and Diaion HP-2MG resin were tested along with the DAX-8 resin and the results are presented in Chapter 4.1.1.

2.2.3 Resin and filter extraction:

Resin was removed from the tube and placed in a vial and submerged in excess ethyl acetate while filters are put into a vial and submerged in excess methanol. The vials are sonicated for 30 minutes. After sonication the liquid is added to a glass LC sample vial no more than 1 mL at a time. The liquid in the sample vial is evaporated to dryness with a steady flow of hydrocarbon free nitrogen. This evaporates the solvent while the lower volatility species remain. Once all of the liquid has been transferred a 1 mL solution of 3:1 H_2O (0.1%formic acid):methanol is added to reconstitute the species in the sample vial.

2.3 GC-MS

Experiments were performed on a Shimadzu GCMS-QP2010 SE with a SH-Rxi-5Sil MS column (thickness: 0.25 µm, diameter: 0.25 µm, length: 30.0 m). The column oven temperature was held at 60 ºC for 1 minute and increased to 200 ºC at a rate of 5 ºC/min. This was held for 2 minutes before increasing at 20 ºC/min up to 280 ºC and held for 1 minute for a total runtime of 36 minutes. The GC inlet injection temperature was set at 250 ºC and were done in splitless mode with a split ratio of 12. The MS was done in electron impact mode at 70 eV. The carrier gas was helium and the total flow was 14.1

ml/min, column was 1.01 ml/min, and purge flow was at 1.0 ml/min. Pressure was at 58.0 kPa with a linear velocity of 36.6 cm/sec.

2.3.1 Derivatization procedure

Derivatization is necessary as the semi-volatile fraction consists of compounds that will not vaporize at a GC operating temperature. There are 3 separate derivatization procedures that are taken from Doskey and Flores.[33] Each procedure is used for a specific functional group (carbonyls, carboxylic acids, or alcohols) and they are done in a specific order. If the alcohol derivatization step is done before the carboxylic acid step for example, then it will derivatize the –OH in the carboxylic acids. For carbonyl compounds, a 250 µL solution of any tested compounds dissolved in methanol is added to a reaction vial along with 20 µL of methoxyamine hydrochloride (MHA). The MHA is in acetonitrile at a ratio of 10 µg per 1 µL. Then the reaction vial is capped and heated to 75 °C for 40 minutes to facilitate dissolution of MHA.

The second step is for carboxylic acids where the sample solution is completely dried using a light flow of dry Nitrogen gas. To the reaction vial 20 µL of acetonitrile is added followed by 10 µL of (trimethylsilyl)diazomethane (TMSD) and then 8 µL of MeOH. The vial is capped and sonicated for 20 minutes.

The third step is for alcohols where the sample is dried with dry Nitrogen gas as any methanol present will derivatize. Next 50 µL of acetonitrile is added followed by 100 µL of *N*,*O*-bis(trimethylsilyl)-trifluoroacetamide (BSTFA) containing 1% trimethylchlorosilane (TMCS). A stir bar is added to the vial and it is heated at 70 °C for 60 minutes with stirring. Due to the small sample size vial inserts are used for holding the final product. In some instances where there are multiple of the same functional group on

a compound the derivatization isn't fully completed. This results in not all of the specified functional group on a compound derivatizing.

Spectral identification was done through using the spectral library and fragmentation patterns. The GC-MS spectral library contains many known compounds and their derivatized forms. However, some of the SOA species are either uncommon or unknown so the library may not have the derivatized form of a product in its database. Therefore it is necessary to study the fragmentation patterns of the different derivatization methods to analyze and identify compounds not present in the spectral library.

2.4 LC-MS

The aerosol extracts, which are the SOA and semi-volatile fraction, were analyzed by LC-MS (Shimadzu Prominence-I LC-2030C) (Shimadzu LCMS-2020) equipped with a 4.6 x 50 mm C_{18}-coated silica gel (3.5 µm) column (Restek). The instrument was run in the gradient mode at 40 °C with an eluent mixture of H_2O (0.1% formic acid) and methanol (0.1% formic acid) at a flow of 0.2 ml/min. The gradient was programmed from 25% to 90% methanol in 20 minutes, held for 1 minute, and back to 25% over 3 minutes for a total runtime of 24 minutes. A scan speed of 349 u/s was used with an m/z range of 60-400. Both positive and negative ionization modes were scanned. For analyzing chromatograms, individual ions were extracted to study each species. Known compounds could be located by extracting the ion representing their molecular weight. In the positive mode the ion is M+1 and in the negative mode the ion is M-1.

CHAPTER 3 - THREE TECHNIQUES FOR ANALYSIS OF THE SEMI-VOLATILE FRACTION OF SOA

3.1 Introduction

There are a number of potential techniques to study the semi-volatile fraction of SOA. This chapter focuses on three techniques and which of them would be best suited for this research. FTIR is explored due to its ability to characterize the semi-volatile fraction's functionality and volatility. This approach may be useful as characterizing each individual species can be impractical. GC-MS is also tested as ideally it could identify specific compounds based on their fragmentation pattern. Similar to GC-MS, LC-MS is studied as well in order to analyze individual compounds but without having to vaporize the semi-volatile layer.

3.2 FTIR for the analysis of the semi-volatile fraction of atmospheric aerosols

FTIR is a suitable method for studying the semi-volatile fraction of SOA. Previous work described in Chapter 1.4 proved successful in studying the functionality loss of products from α-pinene ozonolysis over a 20 hour timespan.[24] It is difficult to study the semi-volatile fraction due to the complexity of SOA and the large number of species present. Using FTIR instead can yield a more general approach to characterize the fraction as a whole. One FTIR method is Attenuated total reflectance (ATR)-FTIR that provides increased sensitivity, surface specificity, and the ability to study how a sample changes over long timeframes. ATR relies on the concept of total internal reflection where the IR beam internally reflects with the crystal that is in contact with the solid or liquid sample providing signal of only what is on the surface of the crystal. A multipass

cell can be used to increase sensitivity. In the current arrangement, the ATR crystal is housed in a sealed, flow-through cell in order to control its atmosphere. Collected SOA can be dissolved in methanol and placed directly into the ATR cell. The methanol would evaporate quickly leaving behind less volatile species uniformly coating the ATR plate. With the aerosol coating the entire plate the FTIR can identify which functional groups are present as well as their approximate relative concentration based on the intensity of the signal.

The thin film of SOA left behind on the crystal can be studied by IR. The ATR cell is setup so that nitrogen flows over the ATR plate. The nitrogen flow evaporates the SOA through isothermal dilution. The rate of evaporation for the SOA varies as it is dependent on the vapor pressures of the individual compounds. The signal intensity of a compound would decrease as it evaporates over time off of the plate. The volatility of a functional group could be determined as a function of signal loss versus time.

In the ATR cell, the IR beam that is internally reflected penetrates out of the crystal a certain distance. This evanescent wave can reach into the sample on the plate at a specific length called the penetration depth. The distance this wave goes to is dependent on the wavelength of light, the angle of incidence, and the refractive index of the crystal. If the amount of sample is below the penetration depth then the signal of any species will decrease as it is removed from the plate. This phenomena means that the volatility of compounds can be studied. By taking multiple scans over long periods of time the compounds on the plate would eventually partition into the gas phase. As this occurs, their peak intensity would drop as less of the compound would be present. As long as the amount of matter was below the penetration depth of the FTIR then the peak intensities

would decrease as they vaporized off the plate. A linear relationship between the losses of peak intensity versus time is predicted. The method for sampling involved dissolving species in methanol, and injecting it onto the plate. With a steady stream of N_2 the methanol would evaporate uniformly leaving the less volatile compounds spread on the plate as desired.

3.2.1 Shortcoming with the evaporation on the ATR crystal

The procedure to study volatility was based on the assumption that upon evaporation of methanol, the components would form a film on the ATR plate. However, it was discovered that during the evaporation process, once methanol had evaporated to a critical volume, the remaining liquid would preferentially collect to the edges of the cell. The methanol did not simply evaporate to dryness due to the hydrophobicity of the germanium plate, once the amount of methanol was low enough, surface tension broke down and the liquid sample would collect at the edge of the cell. Upon subsequent complete evaporation of the methanol, the residual SOA material is only at the edges of the cell, mostly outside of the incident IR beam and adhered to the O-ring seal. The cell is designed to have a large surface area so the IR beam can have multiple passes through the sample. With the sample on only the edge of the plate the signal does not accurately display the loss in signal due to evaporation.

3.2.2 Using a filter to hold the sample in place

As the sample solutions did not evaporate uniformly across the ATR plate a new technique was tested. To get around the uneven distribution we placed a strip of a Tish Scientific Teflon filter (Hydrophobic PTFE 1.0 µm membrane, 47 mm diameter) within the cell to cover the surface of the ATR crystal. The sample solution would then be added

to the filter where it would be dispersed throughout the filter. When the methanol evaporates the lower volatility compounds will remain dispersed throughout the filter with greater concentration at the bottom next to the ATR crystal. A background scan is then taken, with Teflon filter and SOA sample in place. As the sample compounds evaporate they will be removed from the filter and as the background scan has the compounds present it will show an increase in transmittance, less attenuation of the light. The C-F bonds in Teflon absorbs at 1150 cm^{-1} and 1210 cm^{-1} and these features often show up in the spectra. In addition, absorption bands from analytes at this area will be interfered with and therefore these spectral regions were avoided if possible.

As the compounds evaporate the gas phase species are removed from the sealed flow through cell due to the dry nitrogen flow. This removal results in a constant evaporation at a rate proportional to the vapor pressure of the compound. Figure 3.2 is an example of FTIR scans as a function of time showing the evaporation of 1,4-butanediol over the course of 3.5 hours. The importance is being able to observe signal loss due to evaporation.

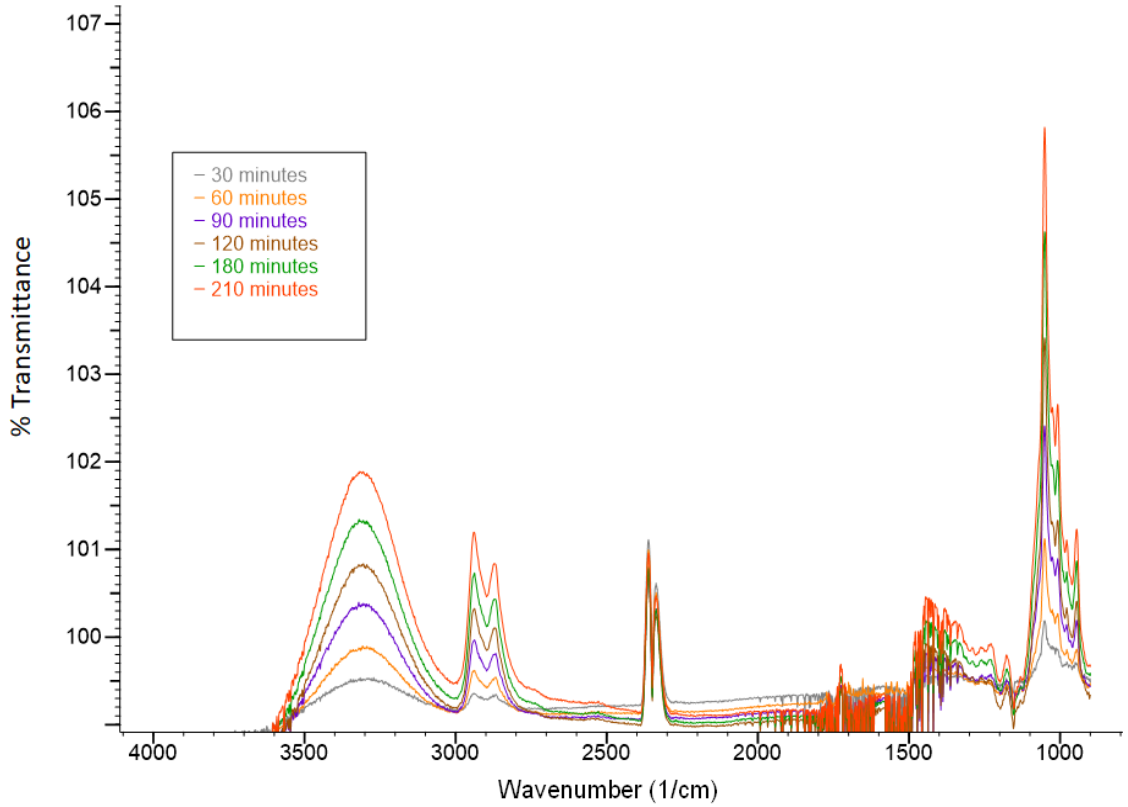

Figure 3.2: 1,4-Butanediol being removed from the filter over time. Negative water line peaks are present around 3600 cm^{-1} to 4000 cm^{-1} as well as from 1400 cm^{-1} to 1800 cm^{-1} and are unimportant. CO_2 is visible at the peaks at 2350 cm^{-1}.

The signal shows 1,4-butanediol being removed over time as expected. In order to measure the rate at which the signal is changing the peak intensity of key peaks is graphed as a function of time. The relative peak area is taken by dividing each time interval's peak area by the final peak area. This is used for comparisons to account for changes in the absorbance cross section between peaks. Figure 3.3 shows the relationship of normalized peak intensity of the O-H stretch of 1,4-butandiol as a function of time between 3000 cm^{-1} to 3600 cm^{-1}. It is important that this has a linear relationship as then a compound's signal loss over time could be used to calculate its volatility.

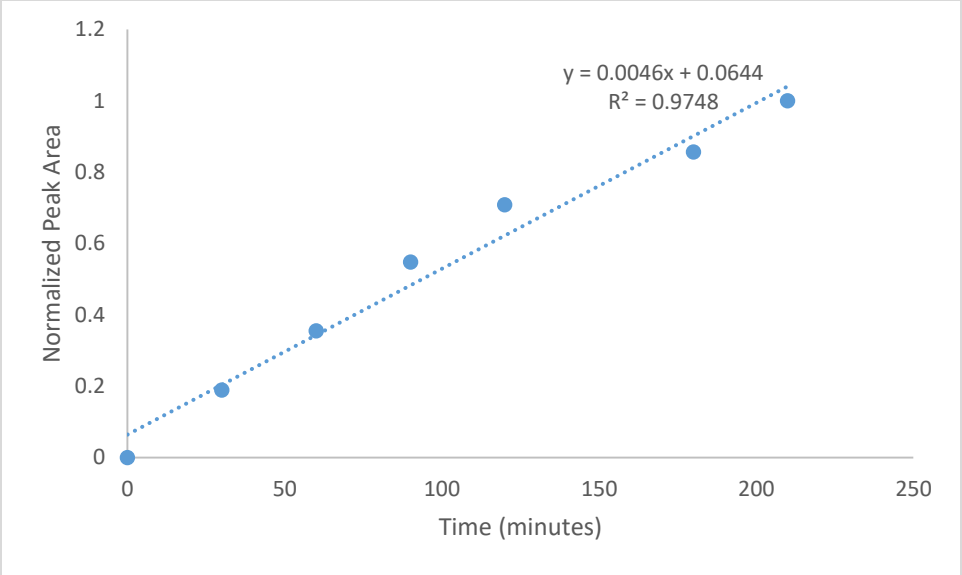

Figure 3.3: The change in the relative O-H peak area over time for 1,4-butanediol from Figure 3.2. Relative peak area is taken by dividing each time interval's peak area by the final peak area.

As can be seen, using the normalized peak area, increased transmittance as a function of time is linear indicating that the experimental procedure utilizing the Teflon filter was successful. For 1,4-butanediol the O-H stretch was used as it is a clear and significant peak on the spectrum but actually any peak from the alcohol could be used. As the relative peak areas are taken the rate of change will be the same for all peaks on a compound.

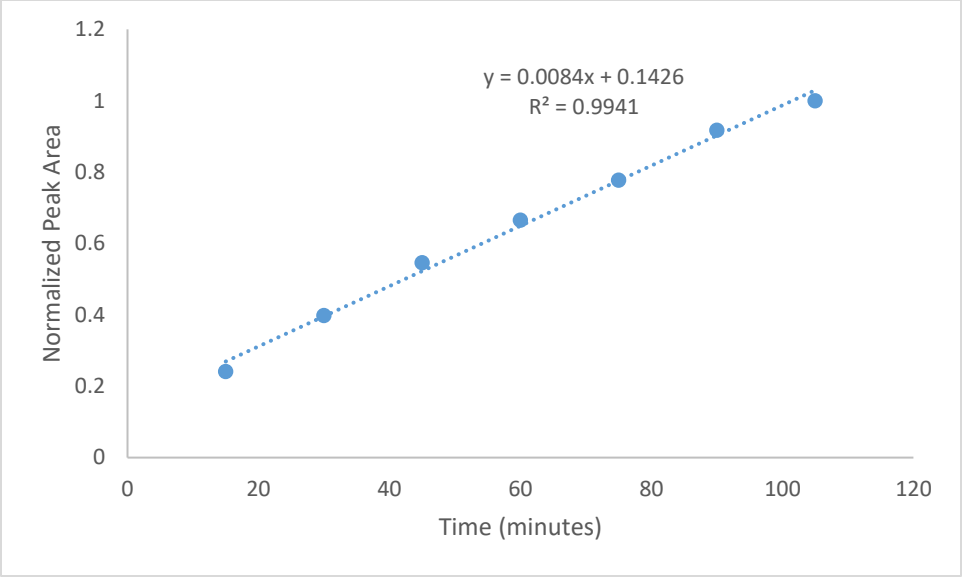

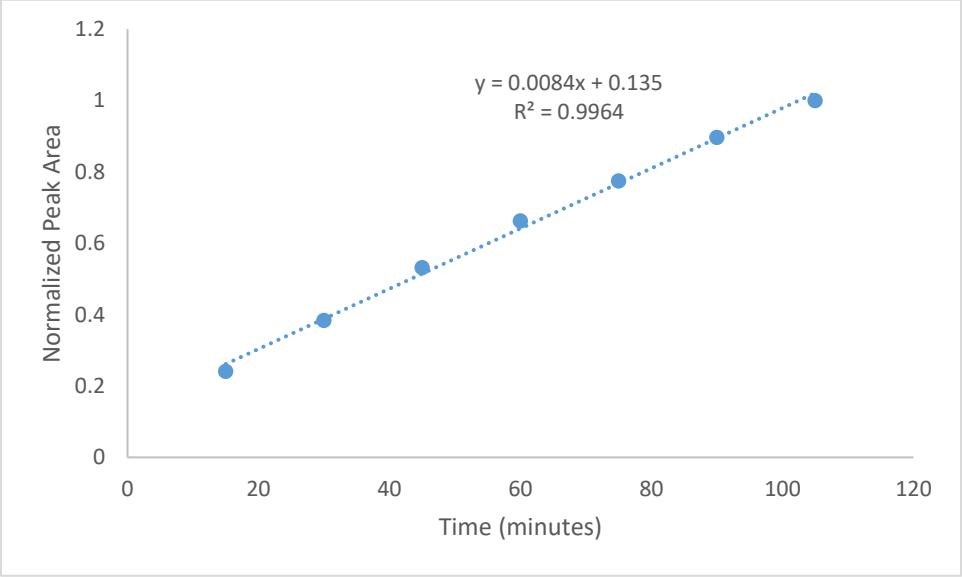

Figure 3.4: Two strong peaks from 1,2-butanediol evaporating off of the plate have the same slope. The top is at 1050 1/cm and the bottom is the OH stretch.

With the peak areas normalized the slope of loss remains consistent despite changes in the absorbance cross section. Figure 3.4 shows how two separate for 1,2-butanediol each have the same slope from evaporated loss. All peaks should have the same slope as the compound is evaporated. If the absorbance cross section is not

corrected for then different peaks on the same compound will have different absolute slopes of loss.

Numerous compounds were run spanning a range of vapor pressures from $5.01x10^{-2}$ to $5.25x10^{-7}$ torr as shown in Table 3.1. The goal was to confirm that the rate at which a compound evaporated off of the ATR plate was relative to its vapor pressure. The relative peak areas were taken for specific compounds and their rates of loss were compared. Prominent peaks with a quantifiable area were tested such as the O-H stretch in a compound containing an alcohol group.

Table 3.1: O-H stretch peak area for multiple compounds

Compound	Vapor Pressure (torr)[a]	O-H stretch slope vs time
1,2-butanediol	$5.01x10^{-2}$	$8.4x10^{-3}$
1,4-butanediol	$1.05x10^{-2}$	$4.6x10^{-3}$ $4.9x10^{-3}$
Glycolic acid	$2.00x10^{-2}$	$3.9x10^{-3}$ $4.8x10^{-3}$
Meso-erythritol	$5.25x10^{-7}$	$4x10^{-4}$

1,4-butanediol and glycolic acid were done twice.
a: taken from references 44 and 45

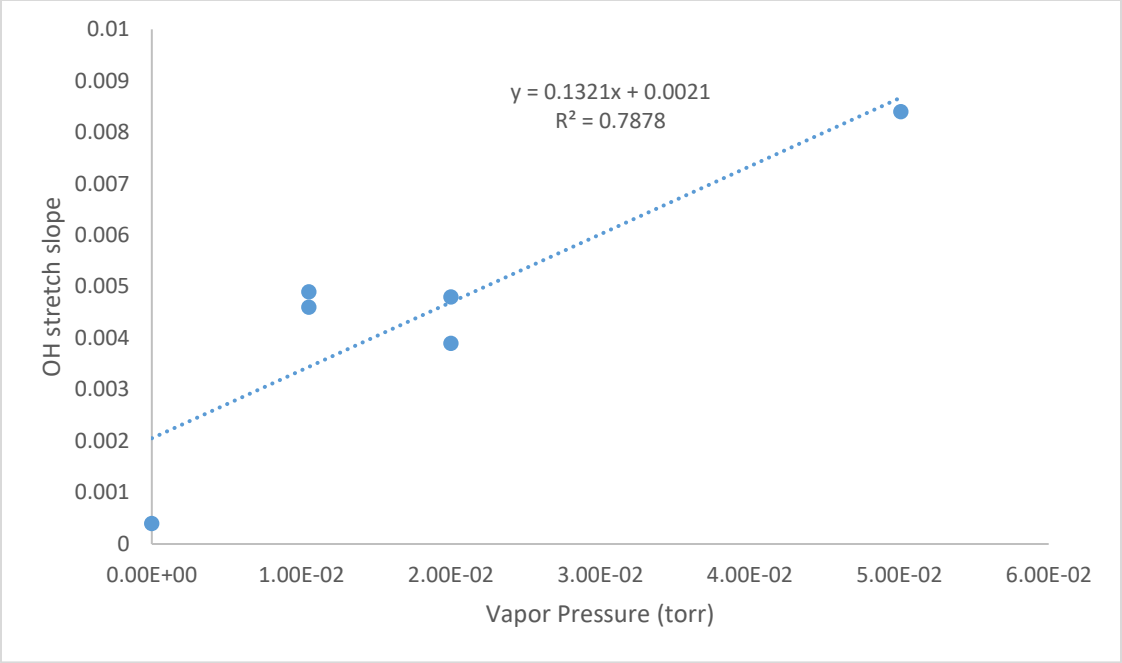

Figure 3.5: The comparison of the compounds slopes on the O-H stretch peak change vs. their vapor pressures.

The slope of loss and the vapor pressure were expected to have a linear relationship with one another. Therefore, the vapor pressure could be estimated from unknown compounds by studying their rate of the slope from evaporated loss. Figure 3.5 shows a linear regression applied to the slopes as a function of vapor pressure, but the R^2 value is only 0.7878. A single run was done for both 1,2-butanediol and erythritol while 1,4-butanediol and glycolic acid were run twice. It was desirable to have each compound run a total of 3 times in order to have a more solidified relationship. The reason they weren't is because there were complications with getting consistent data. Many experiments produced results that were not reliable such as the spectra shown in Figure 3.6.

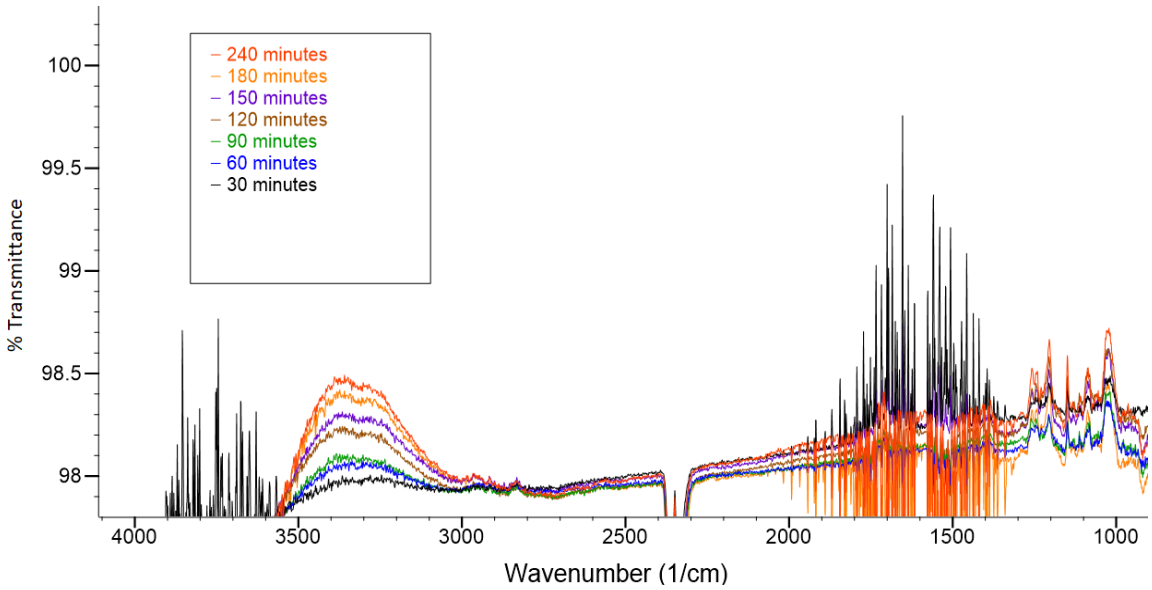

Figure 3.6: Glycolic acid being removed from the filter over time. This run was not used in Table 3.1 as the spectra is not consistent with the other experiments.

The baseline in Figure 3.6 decreases as wavenumber increases. There also should be a strong carbonyl peak around 1700 cm^{-1}. The small peak that is there is completely obscured by water lines. Although this was not impassable it was a common occurrence. There were other experiments conducted where there would be other complications, such as the compound signal not showing up at all. These runs included other compounds were run other than the 4 in Table 3.1. This may be from inconsistency with the procedure as the compound being studied is not in full contact with the ATR crystal. Instead it is close to the crystal while suspended in a Teflon filter so some experiments the IR beam may not effectively reach the sample. After many attempts it was clear this method was taking a great deal of time and many experiments were not useable.

FTIR is useful for analyzing the functionality and volatility of SOA. The complications from working with FTIR, however, led to the determination that it was not the best technique for this research. Three different techniques were tested to find the

most suitable for further studies. However, with improvements in this method, significant research could be studied and is therefore worth pursuing in the future. A possible improvement would be getting the sample to be a thin film that coats the entire ATR crystal surface.

3.3 GC-MS for the identification of components in the semi-volatile layer

A second technique that was analyzed for its capabilities to study the semi-volatile fraction of SOA was GC-MS. GC-MS is extensively used to study the composition of SOA.[25, 26, 30, 46, 47] An unknown compound's molecular weight can be determined through chemical ionization (CI) and/or its identification can be resolved using electron impact (EI) ionization and use of known compound fragmentation libraries or prior literature. However, as stated previously any sample compound in the SOA will not have the fragmentation pattern of the parent compound due to derivatization. Therefore determining an unknown compound's structure would not be as simple as a library search. When using GC-MS the compounds need to be volatile enough to make it through the column. To raise the vapor pressure of the semi-volatile fraction the samples are derivatized by substituting polar functional groups with different, more volatile groups. The volatility of these species could also be estimated by comparing the signal change of compounds between different temperatures in Chapter 2. The original compounds' vapor pressures can be studied before they are derivatized.

3.3.1 Derivatization of known compounds

As derivatization is necessary to analyze the semi-volatiles in SOA it is necessary to test each procedure. A three step derivitization method was used to selectively derivitizes different functional groups to aid in the analysis. The derivitization method

used is discussed in detail in Chapter 2.3.1. A number of known compounds were tested to perfect the derivatization method, and to find trends in the fragmentation pattern to aid in the analysis of unknown compounds. All three steps were tested by using standards with one or more of the functional groups and their expected products were successfully confirmed. The derivatized form of a compound should fragment similar to the parent compound with the exception of the derivatized groups. Certain fragments are apparent from this derivatization such as m-31 and m-59 for the acid derivatization shown in Figure 3.7. It is necessary to understand how the fragmentation pattern changes for each derivatization in order to successfully identify unknown compounds based on their mass spectrum alone.

Figure 3.7: How the m-31 peak is made on the left and the m-59 peak on the right.

For the alcohol species there is a clear m-73 peak as the trimethylsilyl is cleaved off of the oxygen on the parent molecule which is shown in Figure 3.8. Compounds with multiple functional groups can show multiple losses at the same time such as a compound with two alcohols having an m-146 peak.

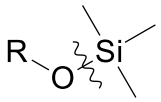

Figure 3.8: The trimethylsilyl group cleaving off of the parent alcohol.

Each derivatization step was tested and successfully confirmed. Figures 3.9-3.14 show the successful derivatization for each of the three steps and their structures. Figure 3.9 shows an acid derivatization and has the m-31 (m/z 143) and m-59 (m/z 115) peaks present. The alcohol derivatization in Figure 3.11 has a strong m/z of 73 from the trimethylsilyl cleavage. In Figure 3.13 there is an m-31 peak (m/z) 200 and an m-59 peak (m/z 172) from the acid derivatization. The m/z of 140 may be caused from an m-59 cleavage as well as the ether cleaving off from the nitrogen. The spectra each show how the fragmentation for certain functional groups occurs. Knowing the fragmentation patterns for each group is needed for determining the structure of compounds that may not have their derivatized form in the MS library.

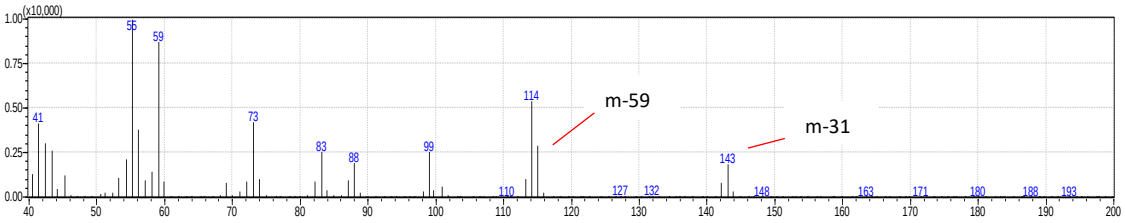

Figure 3.9: Derivatized 2-methylglutaric acid with methyl esters. Confirmed through library search.

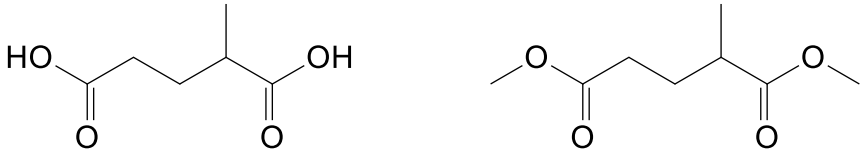

Figure 3.10: 2-methylglutaric acid on the left and its acid derivatized form on the right.

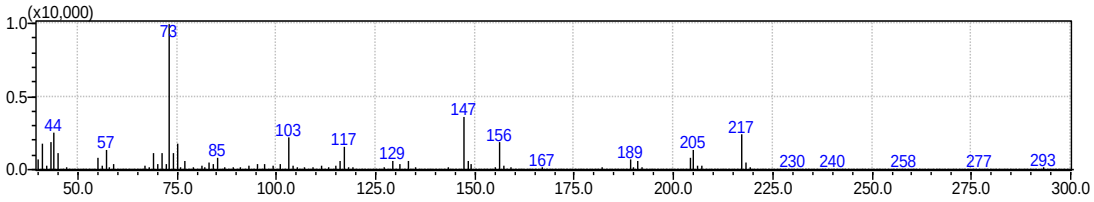

Figure 3.11: Alcohol derivatized erythritol spectrum confirmed through library search.

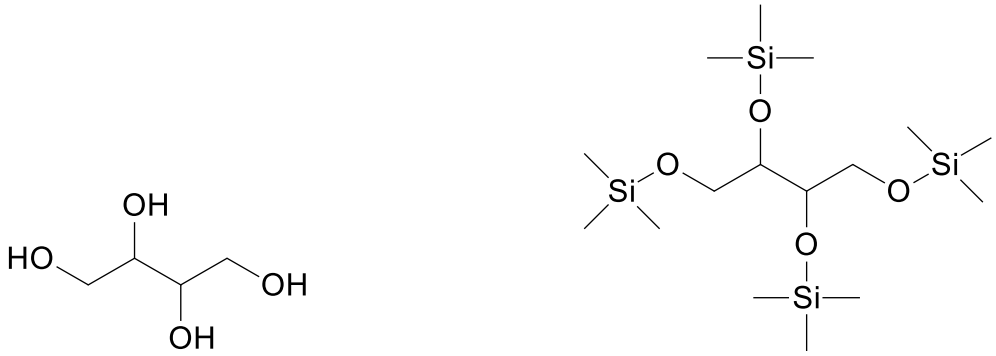

Figure 3.12: Erythritol on the left and its derivatized form on the right.

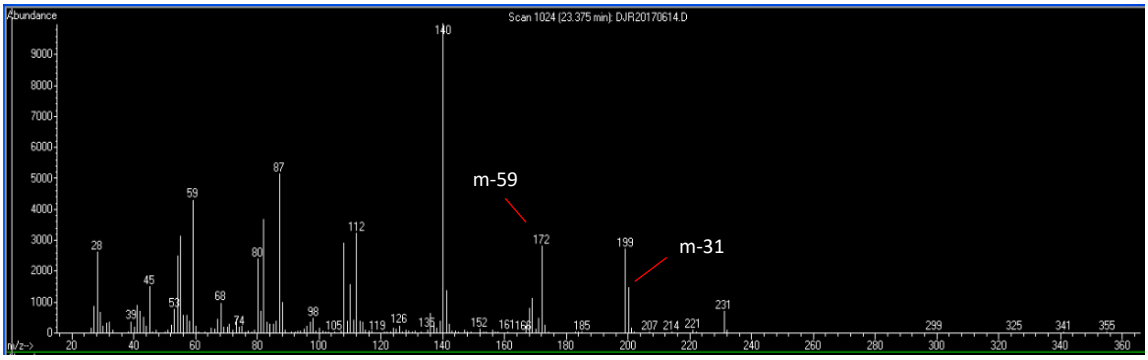

Figure 3.13: Spectrum of successfully derivatized 4-oxoheptanedioc acid including the carbonyl derivatization step. Confirmed through library search. The spectrum design is different due to using a different computer software.

Figure 3.14: 4-oxoheptanedioc acid on the left with the fully derivatized form on the right.

In order to determine the reliability of the derivatization a number of compounds were analyzed, where successfully derivatization was observed. Table 3.2 lists each compound that were derivatized and their retention times.

Table 3.2: List of successfully derivatized compounds

Compound	Vapor Pressure (torr)[a]	Calculated Derivatized Vapor Pressure (torr)	Retention Time (minutes)
10-hydroxydecanoic acid	($3.03x10^{-6}$)	$7.96x10^{-4}$	26.7
4-oxoheptanedioc acid	($3.27x10^{-7}$)	$1.39x10^{-4}$	23.4
2-methylglutaric acid	($7.64x10^{-6}$)	$5.85x10^{-2}$	13.7
3-methylglutaric acid	($7.64x10^{-6}$)	$5.85x10^{-2}$	13.6
Benzoic acid	$7.00x10^{-4}$	$4.49x10^{-1}$	11.6
Lactic acid	$8.13x10^{-2}$	$9.26x10^{-1}$	16.8
Hexanoic acid	($2.90x10^{-2}$)	2.54	6.9
Sorbitol	$9.90x10^{-9}$	$3.39x10^{-9}$	32.7
Erythritol	$5.25x10^{-7}$	$8.14x10^{-5}$	22.9
1,2,6-hexanetriol	$7.91x10^{-5}$	$6.12x10^{-4}$	23.8
1-decanol	($1.15x10^{-2}$)	$3.46x10^{-2}$	19.2
1,3-butanediol	$2.00x10^{-2}$	$2.60x10^{-1}$	11.2
1,2-butanediol	$5.00x10^{-2}$	$2.60x10^{-1}$	11.2
Hexyl alcohol	$9.28x10^{-1}$	1.95	8.7

() indicates calculated vapor pressure

a: taken from reference 44

Derivatization raised the theoretical vapor pressure for almost every compound. Calculated vapor pressures and the derivatized vapor pressures are calculated using the SIMPOL method from Capouet and Muller.[48] The method accounts for numbers of functional groups and information such as the number of carbons to predict the vapor pressure of a compound. The lowering of the vapor pressure allows for the compounds to pass through the GC column and also reduces polarity of the compounds providing relative retention times that are easier to interpret. The data agrees with the calculated vapor pressures as the retention time decreases as the compound's volatility increases. The one exception being benzoic acid having a shorter retention time than expected. This faster retention time is most likely due to benzoic acid's nonpolar structure as it passes through the nonpolar column.

With 14 different compounds successfully identified the procedures for derivatization were proven to be reliable. The reliable success of each derivatization is important as this method is necessary to identify unknown compounds. By confirming the consistency with this method we can confidently use derivatization to analyze the semi-volatile layer of SOA.

3.3.2 Difficulties identifying known SOA components

The composition of SOA from the ozonolysis of α-pinene has been well studied and is well known.[37, 38, 42, 43, 49] This provides a good test for determining the validity of a method for the analysis of SOA composition and the semi-volatile fraction. For the method to be acceptable, first it must be able to identify the species present. Pinonic acid, which is a known product, was derivatized by itself and run to see if the fragmentation pattern was predictable. The spectrum displayed a single peak which had to have been the

derivatized pinonic acid. The mass spectrum of the derivatized pinonic acid is shown in Figure 3.15.

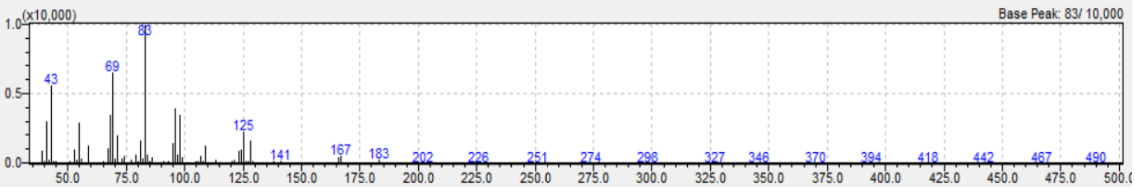

Figure 3.15: The fragmentation of derivatized pinonic acid.

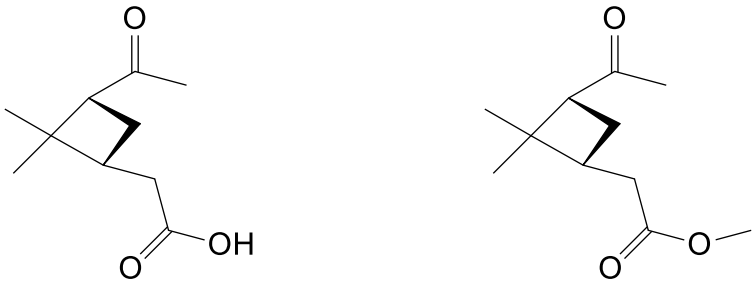

Figure 3.16: Pinonic acid on the left and the acid derivatized form on the right.

Derivatized pinonic acid is shown in Figure 3.16 where the carboxylic acid is replaced with a methyl ester. Two fragments of m-31 and m-59, at m/z of 165 and 106 respectively, are expected as there is a single acid derivatization. With a derivatized molecular weight of 198 amu the two possible expected fragments are not seen. The only noticeable fragmentation is the m/z of 125 which must be from cleaving the entire methyl ester group and extra CH_2 from the one carbon on the ring. It would be difficult to identify this compound in a sample with many unknown compounds. With only one

unique peak that indicates the compound's identity there normally would not be enough information.

The ozonolysis of α-pinene was conducted and the products were collected onto a filter described in Chapter 2.2.1. After the products were derivatized and analyzed by GC-MS, no other known compounds were able to be identified. Only pinonic acid was discovered due to the library search and having run it prior by itself. Other compounds that were expected included pinic acid, norpinic acid, norpinonic acid, and pinonaldyde. All of the predicted ions for each of these compounds were searched individually in the mass spectrum analyzer. No peaks or predicted ion fragments provided evidence of the presence of any of these compounds. A paper by Yu *et al*. (1999) identified several known compounds from the ozonolysis of α-pinene using GC-MS.[50] They also used derivatization and identified each of the five compounds listed above. However, this group used the CI mode in the GC-MS in order to find these compounds.[46] This method is much simpler as it instead uses the molecular weight of the derivatized compounds rather than their fragmentation pattern. When our samples were run using CI mode no signal was observed.

Without being able to identify known derivatized compounds through using GC-MS this method was not the most promising. Confirmation of unknown compounds would be unreliable as even known compounds are unable to be observed. The derivatization was proven successful so GC-MS may still be used later on for further research or in addition to another technique. The ability to determine individual molecular structures can be a useful tool if compounds can be identified confidently.

3.4: LC-MS for the identification of species in the semi-volatile layer of SOA

LC-MS is extensively used for the analysis of the organic composition of atmospheric aerosols as discussed in Chapter 1.6. The use of traditional SOA analysis by LCMS can be adopted to the study of the semi-volatile fraction of aerosols by first collecting SOA on a filter where the composition of the generated aerosols can be determined. This is followed by evaporating the semi-volatile layer by variation in the filter temperature and removal of the semi-volatile components using clean, hydrocarbon free air and collecting the removed species onto resins that trap the gas phase compounds produced from evaporation. The experimental detail can be found in Chapter 2.2.1. After removal of the semi-volatile fraction of the aerosols, the lower volatility species remain on the filter where they can be extracted and analyzed by LC-MS.

3.4.1 Identification of known compounds using LC-MS

LC-MS is a similar technique to GC-MS for studying the semi-volatile fraction of SOA. The procedure for each method is nearly identical so the analyses of LC-MS and GC-MS are compared. A significant difference is that LC-MS does not require derivatization in order to analyze the semi-volatile components. Therefore, LC-MS does not include the difficulty of identifying derivatized fragmentation patterns that that GC-MS does. At the same time, however, a library search can't be used to reliably determine the structure of a compound. LC-MS can provide the molecular weight of analyzed molecules and coupled with previous literature can identify known products in the semi-volatile fraction of SOA. The known compounds that were unable to be successfully identified using GC-MS are listed in Table 3.3. LC-MS was tested to conclude if these products could be found.

Table 3.3: Known products of ozonolysis

Compound	Molecular Weight	Vapor Pressure (torr)[a]	Structure	m/z
Pinic Acid	186	$3.2x10^{-5}$	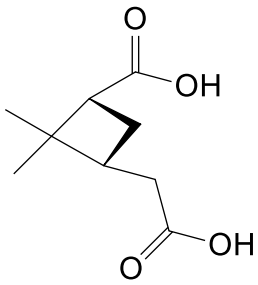	(-)185
Pinonic Acid	184	$7x10^{-5}$	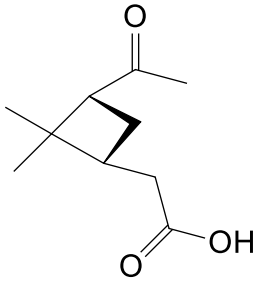	(+)185
Norpinic Acid	172	$1.3x10^{-4}$	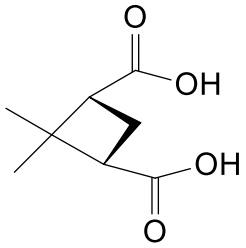	(+)173
Norpinonic Acid	170	($1.28x10^{-4}$)	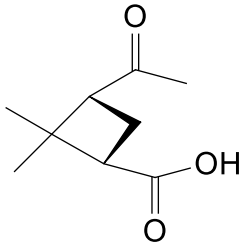	(+)171
Pinonaldehyde	168	($7.96x10^{-3}$)	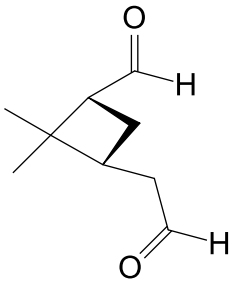	(+)169

a: () stands for a calculated vapor pressure while others were taken from literature.[51]

Two compounds' vapor pressures were not found in literature and were calculated according to Capouet and Muller.[48] Although the calculated values may not be exact, they give an estimate as to what the vapor pressure actually is. To demonstrate an example, pinonic acid has a vapor pressure of $7x10^{-5}$ torr and its calculated vapor pressure is at $4.69x10^{-5}$ torr. The m/z for each compound that was used was the peak with the best signal to noise ratio.

The SOA of the ozonolysis of α-pinene was collected onto a filter just as when GC-MS was tested. The five known compounds in Table 3.3 were analyzed by comparing their peaks to the ones in Figures 1.12 and 1.13. Although the compounds were not able to be identified using GC-MS, they are observable using LC-MS. The compounds each have the m/z stated in Table 3.3. The four carboxylic acids have both a positive and negative ion peak. In addition the relation of their retention times in Figures 1.12 and 1.13 to one another is also important for identifying each compound. After running the ozonolysis collection the filter was extracted before any evaporation of the semi-volatile layer. The chromatograms with the m/z's of each compound are presented in Figures 3.17 and 3.18. They are split into two separate Figures due to the large difference in scale.

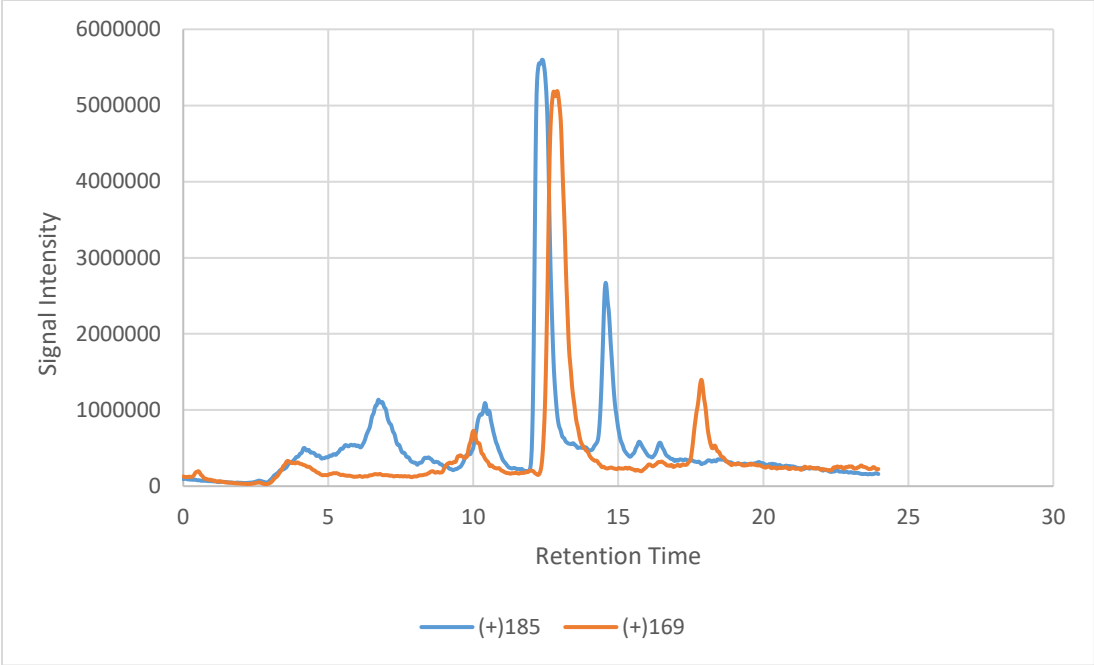

Figure 3.17: The presence of pinonic acid (+)185 at 12.5 minutes and pinonaldehyde (+)169 at 13.1 minutes.

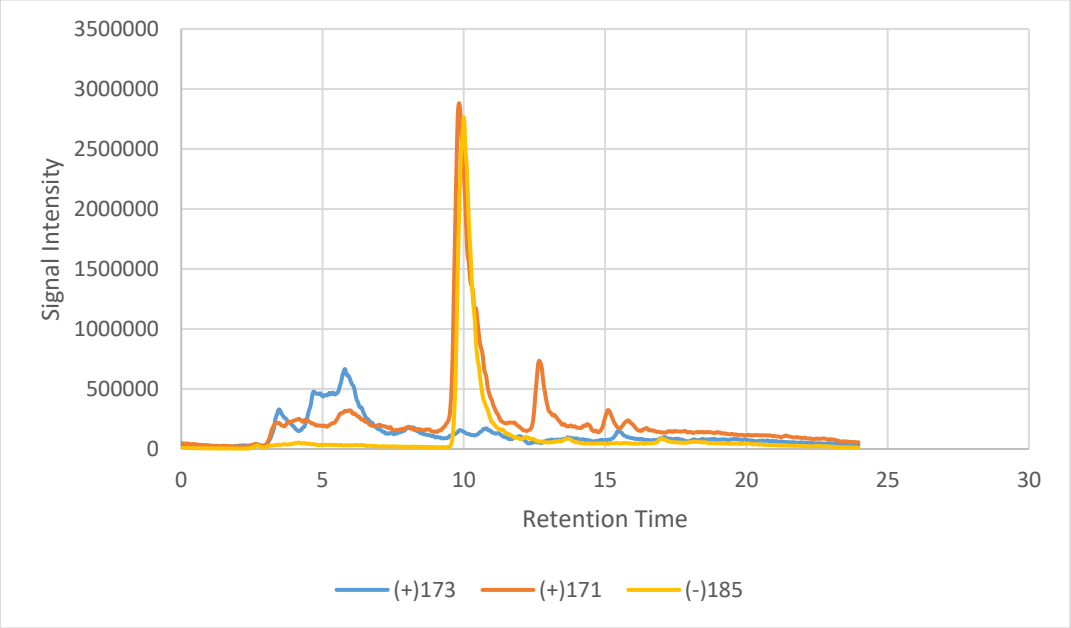

Figure 3.18: Norpinic acid (+)173 around 5 minutes, norpinonic acid (+)171 at 10 minutes, and pinic acid (-)185 at 10 minutes.

Each compound has a slightly longer retention time than in Figures 1.12 and 1.13 but this is due to differing LC-MS methods. Their relation to each other with regards to retention time and peak shape match with those presented in the paper by Winterhalter *et al*. (2003).[38] Seeing all five compounds is significant in that is shows the procedure for generating SOA, collecting it, and analyzing it for known compounds was successful.

3.5 Conclusions

Out of the three methods LC-MS was the most successful. The technique requires no derivatization and can successfully analyze known SOA products. The instrument is unable to reliably determine a compounds structure by itself as it doesn't utilize fragmentation patterns and an MS library as GC-MS does. However, compounds can still be identified through investigation of the reaction pathway of α-pinene ozonolysis and previous literature. In addition, in the future LC-MS may be partnered with GC-MS to successfully identify unknown species. The results of using LC-MS to study the semi-volatile fraction of SOA is presented in Chapter 4. FTIR proved less effective due to unreliable spectra. The sample compounds are most likely not consistently in contact with the ATR crystal which causes problems such as the sample not even being present in the spectrum. GC-MS also was less effective than LC-MS at studying SOA from the ozonolysis of α-pinene. GC-MS requires derivatization to analyze the semi-volatile fraction. Although the procedures for derivatization were successful, the confirmation of derivatized products was not.

CHAPTER 4 - ANALYSIS OF SOA FROM THE OZONOLYSIS OF α-PINENE USING LC-MS

4.1 Introduction

LC-MS proved to be more successful in studying SOA than the other two methods. The capabilities of the LC-MS needed to be studied further. The SOA from the ozonolysis of α-pinene has been extensively studied in the past. [22, 23, 24, 26, 27, 30, 37, 38, 41, 42, 43] In addition, the determination of which collection media is best for semi-volatiles is another significant area of study. Prior research with LC-MS and the products of the ozonolysis of α-pinene are important for this experiment and are covered in Chapters 1.6 and 1.7.

4.1.1 Solvent desorption resins

In order to maximize collection of the semi-volatile fraction the best desorption resin for this experiment had to be chosen. Four resins we considered were; Amberlite XAD 4, Amberlite XAD 7HP, Supelite DAX 8, and Diaion HP-2MG resin. Each resin is useful for collecting gas-phase organics and their properties are listed in Table 4.1.

Table 4.1: Different resin properties

Resin	Matrix	Particle size	Pore size	Surface Area
XAD 4	Styrene-divinylbenzene	20-60 mesh	~0.98 mL/g pore volume 100 Å mean pore size	750 m^2/g
XAD 7HP	Acrylic	20-60 mesh	0.5 mL/g pore volume 300-400 Å mean pore size	380 m^2/g
DAX 8	Acrylic ester	40-60 mesh	~0.79 mL/g pore volume 225 Å mean pore size	140 m^2/g
HP-2MG	Polymethacrylate	25-50 mesh	1.2 mL/g pore volume 170 Å mean pore size	~500 m^2/g

Properties taken from Sigma-Aldrich.[51]

Resin is used to collect the semi-volatile species as they evaporate from the filter. This separates the semi-volatiles from the low volatile compounds in the produced SOA.

4.2 Collection efficiency of different sample resins

To analyze the semi-volatile fraction of the SOA, efficient collection of the evaporated species must occur. The four different types of resin were tested to see which had the best efficiency. A filter was loaded with 100 µg each of pinonic acid, 4-oxoheptanedioc acid, and 2-methylglutaric acid. The filter was put on the filter holder and heated to 60 ºC. Hydrocarbon free nitrogen at a rate of 1.0 SLM was passed through the filter-holder to a resin tube containing one of the resin for 5 hours. This experiment was repeated each time only varying the resin. All four resins were extracted and run on

the LC-MS to compare the three compounds' peak areas and signal intensity. The data for each compound is presented in Tables 4.1, 4.2, and 4.3.

Table 4.1: Pinonic acid peak compared between resins

Resin	Peak Area	Peak Height
HP-2MG	$3.19x10^7$	$1.46x10^6$
XAD 4	$1.94x10^7$	$6.48x10^5$
XAD 7	$1.25x10^7$	$4.22x10^5$
DAX 8	$2.58x10^7$	$8.87x10^5$

Table 4.2: 4-oxoheptanedioc acid peak compared between resins

Resin	Peak Area	Peak Height
HP-2MG	$3.90x10^6$	$9.52x10^4$
XAD 4	$1.86x10^6$	$5.37x10^4$
XAD 7	$4.71x10^5$	$1.33x10^4$
DAX 8	$2.04x10^6$	$6.08x10^4$

Table 4.3: 2-methylglutaric acid peak compared between resins

Resin	Peak Area	Peak Height
HP-2MG	$7.29x10^5$	$1.91x10^4$
XAD 4	$4.46x10^5$	$1.38x10^4$
XAD 7	Not visible	Not visible
DAX 8	$1.17x10^6$	$4.68x10^4$

No single resin performed the best for each compound. HP-2MG and DAX 8 had the best collection overall out of the four resins by having larger peaks for the same amount of compound. Both resins are good options and we decided to use DAX 8 resin due to its versatility. DAX 8 resin has moderate polarity allowing it to adsorb both polar and nonpolar compounds. Other resins are typically either polar or nonpolar and therefore are specialized to a specific polarity. HP-2MG may have performed better due to its larger pore volume size and ability to hold a larger amount of material. As semi-volatile SOAs are unknown it is logical to use a resin that can efficiently collect a wider range of species.

4.3 LC-MS procedure for analysis of SOA from α-pinene ozonolysis

LC-MS was evaluated for its ability to study SOA by doing a number of experiments. The general procedure described in Chapter 2.2 involves a flow reactor with three inlets and one outlet. Two inlets are the ozone and the nitrogen carrier gas which combine prior to entering the chamber. The third inlet contains the α-pinene which is fed into the flow reactor and exposed further inside. The total flow is 2.0 SLM with an ozone concentration of 222 ppm and the α-pinene concentration at 180 ppm. The outlet leads to a filter being held by a filter holder that collects SOA. The line is then led to a fume hood to dispose of ozone. The experiment is run for a total of 10 minutes. Once the SOA has collected onto the filter, 400 µg of sorbitol which is dissolved in methanol is added to the filter. This constant sorbitol addition serves as an internal standard to account for changes between runs. Afterwards, the filter is cut into two halves where one is used for analysis on the LC-MS. This pre-evaporation half contains the SOA produced from the ozonolysis reaction. The other half remains in the filter holder where it is blown with a stream of dry

nitrogen for 5 hours. The filter holder's temperature can be increased by wrapping it in Thermo-tape in order to increase evaporation of the semi-volatile fraction. By changing the temperature of evaporation the signal change of known compounds can be observed. This leads to the ability to study the vapor pressure of a compound versus its signal change with temperature. The flow leads to a resin tube that collects the evaporated semi-volatile fraction.

First the identification of SOA products was tested by searching for the ions of known compounds listed in Table 3.3. The extracted ions for each compound were based off of their molecular weights. The retention times for each were also compared with previous literature to confirm each compound's presence. The filter holder temperature for evaporation of the semi-volatiles was set at 80 ºC. Unknown compounds could also be found from this same experiment by searching for different ions with prominent peaks.

Once the presence of the known compounds had been confirmed, the next experiment was to learn if they are still observable at a more atmospherically relevant concentration. Initial concentrations of reactants were overly high as the goal was to favor SOA production. The experiment was repeated with the ozone concentration lowered to 12.5 ppm to test if the products were still visible. The temperature of the filter holder for evaporation was at 80 ºC.

The next experiment evaluated evaporation rate as a function of temperature. Comparing the signal change of known compounds from the pre-evaporation filter and post-evaporation filter at different temperatures gave a relationship of signal change and vapor pressure. The vapor pressure of the unknown ions could be determined through this signal change relationship. Four separate evaporation runs were completed with the filter

holder temperature set at 20 ºC, 40 ºC, 60 ºC, and 80 ºC. The SOA was produced with an ozone concentration of 222 ppm.

4.3.1 Identification of SOA products

LC-MS was first tested on its ability to detect known semi-volatile compounds in the SOA. The 5 known products from α-pinene ozonolysis that were identified were listed in Chapter 3.4.1. They are presented again in Table 4.4 along with their vapor pressures.

Table 4.4: Known products of ozonolysis

Compound	Molecular Weight	Vapor Pressure[a] (torr)	Structure	m/z
Pinic Acid	186	$3.2x10^{-5}$	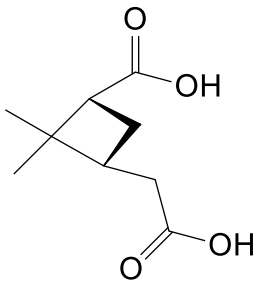	(+)187 (-)185
Pinonic Acid	184	$7x10^{-5}$	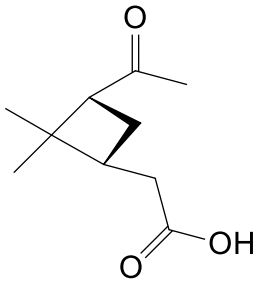	(+)185 (-)183
Norpinic Acid	172	$1.3x10^{-4}$	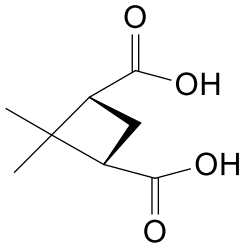	(+)173 (-)171

Norpinonic Acid	170	($1.28x10^{-4}$)	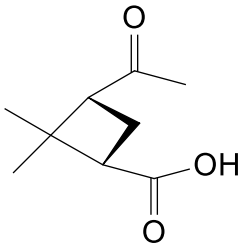	(+)171 (-)169
Pinonaldehyde	168	($7.96x10^{-3}$)	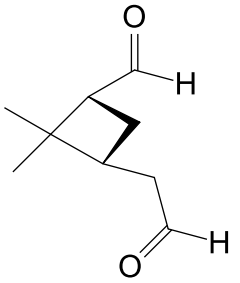	(+)169

a: () stands for a calculated vapor pressure while others were taken from literature.[48, 50]

Each carboxylic acid had a positive and negative peak in the chromatograms. Based on signal intensity and clarity, the positive peak for each compound was used for analysis except for pinic acid where the negative peak was used. Sorbitol was used as an internal standard and has a retention time of 3.0 minutes. This is known from previously running sorbitol by itself and observing the lone peak at 3.0 minutes. Studying each compound involved analyzing products from the pre-evaporation filter, post-evaporation filter, and the resin that collected the vaporized SOA. The signal of products from the post-evaporation filter should be less than the signal from the pre-evaporation filter. The point is that the amount this signal changes with respect to temperature will be directly caused by each compounds' vapor pressures. The goal is to be able to correlate signal change with vapor pressure. Therefore, unknown compounds' vapor pressures could be estimated by observing how much their signal changes. In order to accomplish this task, the identified products from Table 4.4 that were identified in Chapter 3.4.1 need to also

be quantifiable in the post-evaporation filters. The extracted ion chromatograms use the m/z in Table 4.4 to indicate the presence of each species. The pre-evaporation filter contained all 5 products shown in Figures 4.1 and 4.2.

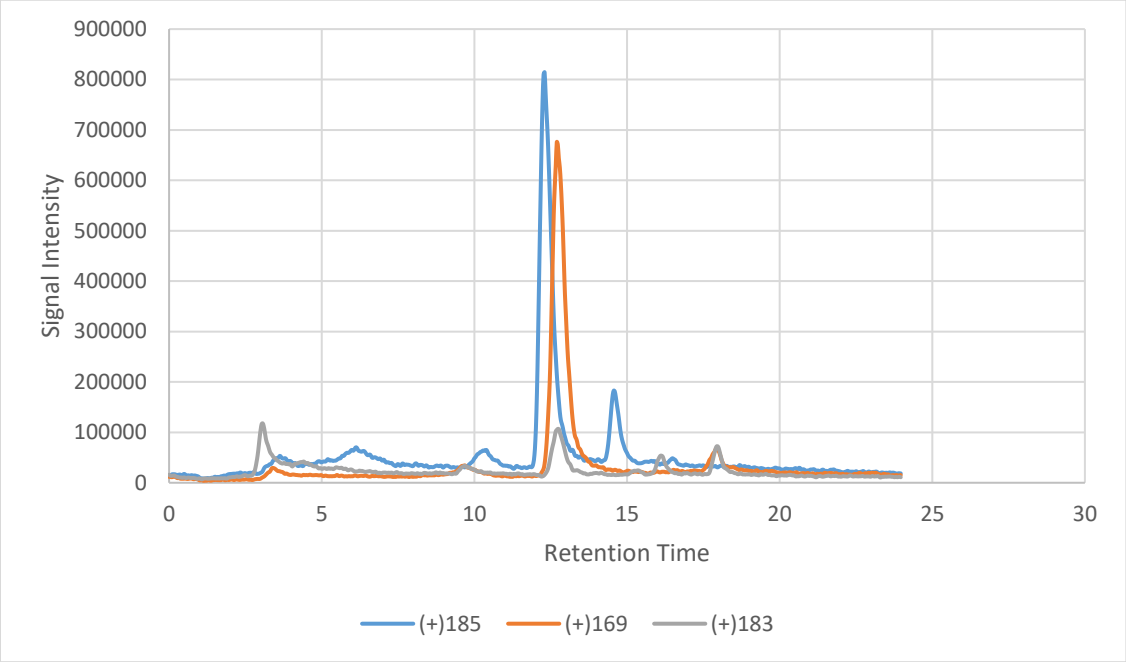

Figure 4.1: Chromatogram from the pre-evaporation filter with extracted ions of pinonic acid (+)185 at 12.5 minutes, pinonaldehyde (+)169 at 13.1 minutes, and sorbitol (+)183 at 3.0 minutes.

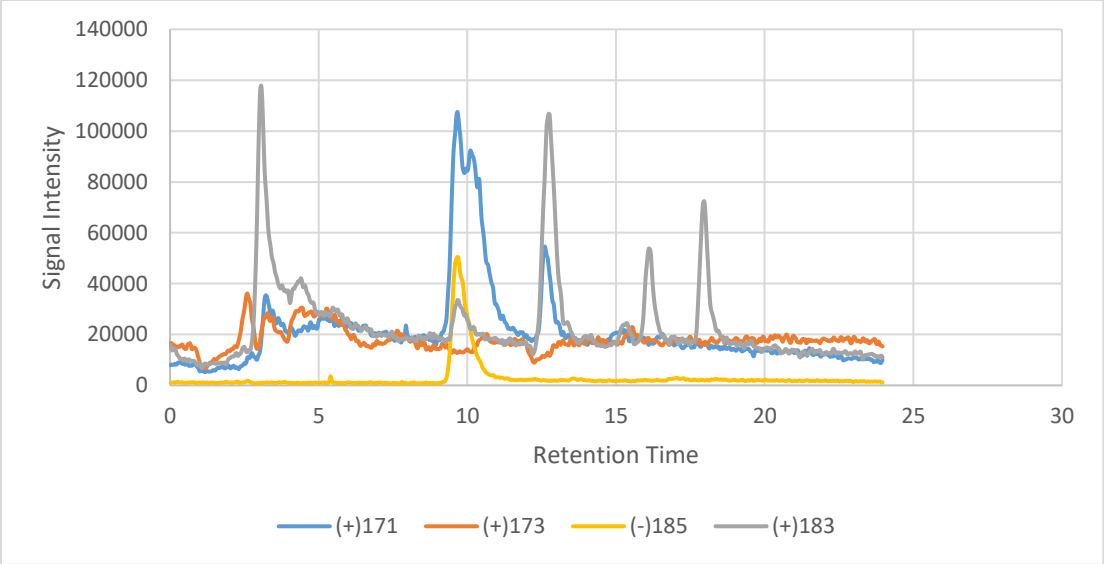

Figure 4.2: Chromatogram from the pre-evaporation filter with extracted ions of norpinonic acid (+)171 at 10 minutes, norpinic acid (+)173 around 5 minutes, pinic acid (-)185 at 9.8 minutes, and sorbitol (+)183 at 3 minutes.

The post-evaporation filter is after a 5 hour flow of dry nitrogen at 80 ºC as shown in Figures 4.3 and 4.4.

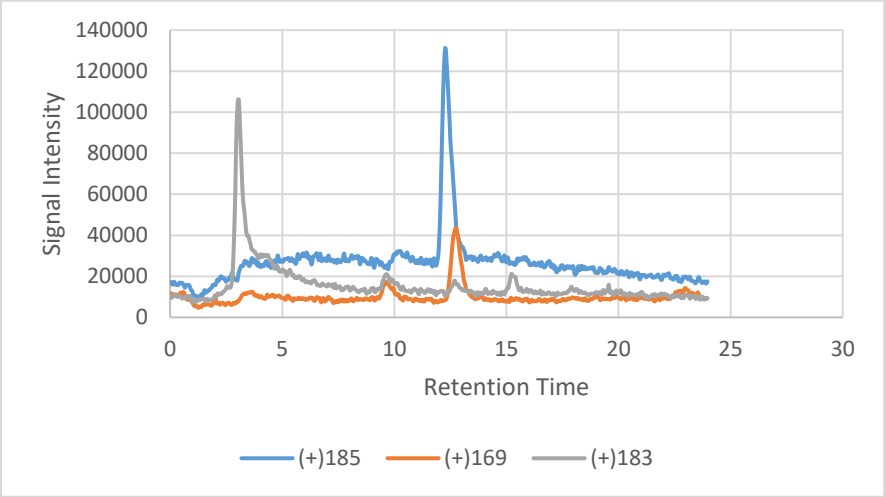

Figure 4.3: Chromatogram from the post-evaporation filter with extracted ions of pinonic acid (+)185 at 12.5 minutes, pinonaldehyde (+)169 at 13.1 minutes, and sorbitol (+)183 at 3.0 minutes.

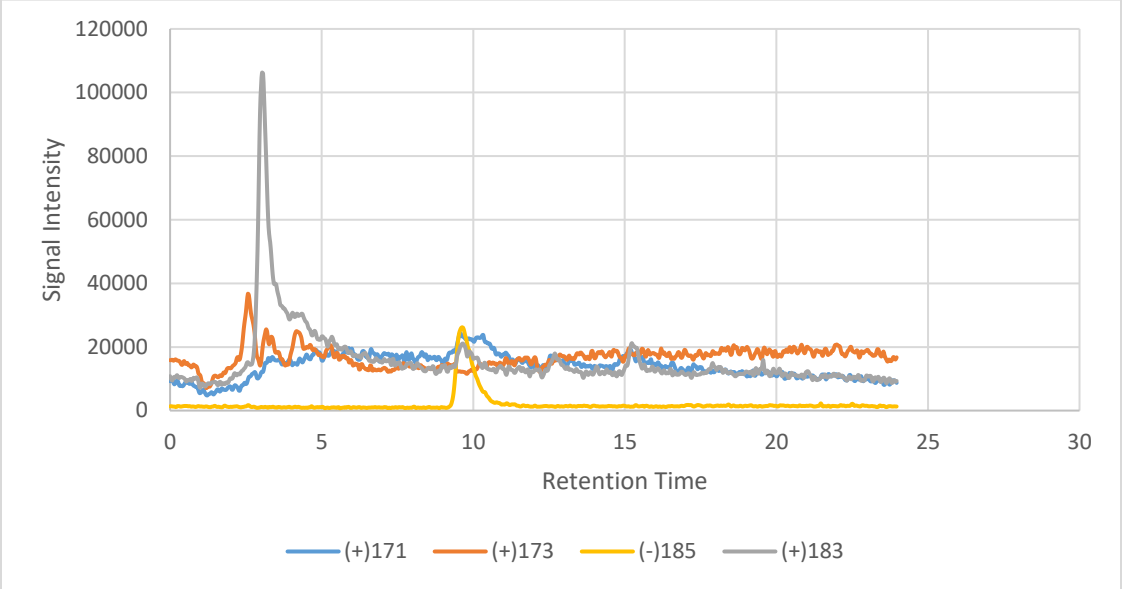

Figure 4.4: Chromatogram from the post-evaporation filter with extracted ions of norpinonic acid (+)171 at 10 minutes, norpinic acid (+)173 around 5 minutes, pinic acid (-)185 at 9.8 minutes, and sorbitol (+)183 at 3 minutes.

The compounds all had a decrease in signal compared to the pre-evaporation filter based on their relation to the constant sorbitol peak. Some compounds showed more loss such as pinonaldehyde due to its higher vapor pressure. Meanwhile pinic acid and pinonic acid did not decrease nearly as much due to their lower volatility. The semi-volatile fraction that was evaporated was collected by the resin tube. The results of the resin collection are presented in Figures 4.5 and 4.6.

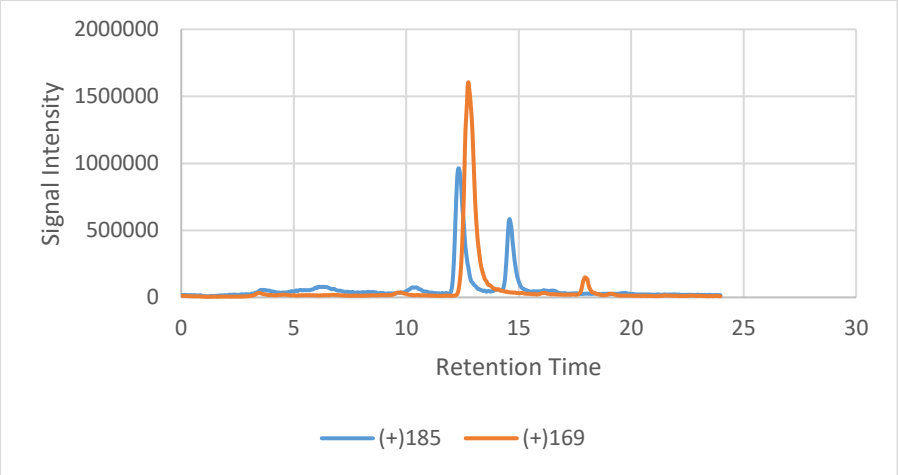

Figure 4.5: The chromatogram of the resin with extracted ions of pinonic acid (+)185 at 12.5 minutes, pinonaldehyde (+)169 at 13.1 minutes.

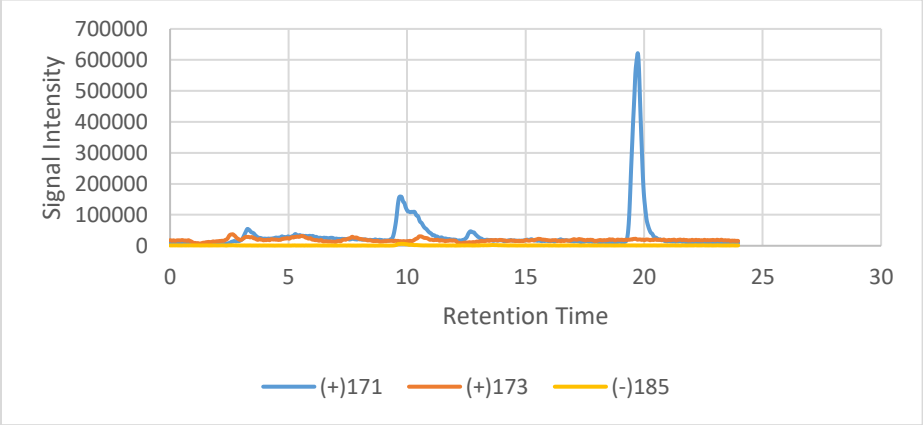

Figure 4.6: The chromatogram of the resin with extracted ions of norpinonic acid (+)171 at 10 minutes, norpinic acid (+)173 around 5 minutes, pinic acid (-)185 at 9.8 minutes.

For the resin collection, the amount of norpinic acid was not enough to be observable. Pinic acid is barely visible due to less evaporation from very low vapor pressure ($3.2x10^{-5}$ torr). The resin collection was tested as collection of the semi-volatile fraction onto a sorbent could be useful for future studies. In addition to the known

compounds, there were many unknown ions that were observed. Four prominent ions were at (+)191, (+)193, (+)207, and (+)209 which are shown in Figure 4.7. These unknown ions may be important species in the SOA that can be further analyzed. Figure 4.8 shows the TIC of which has several peaks that have similar retention times to the ions that have been extracted.

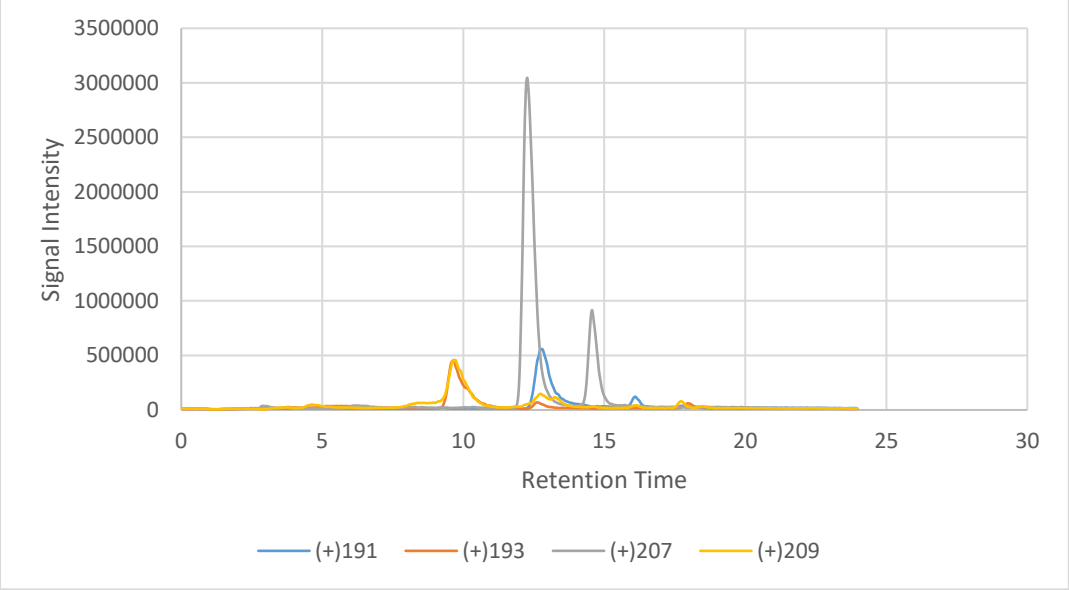

Figure 4.7: Several prominent unknown ions present in the SOA from the pre-evaporation filter.

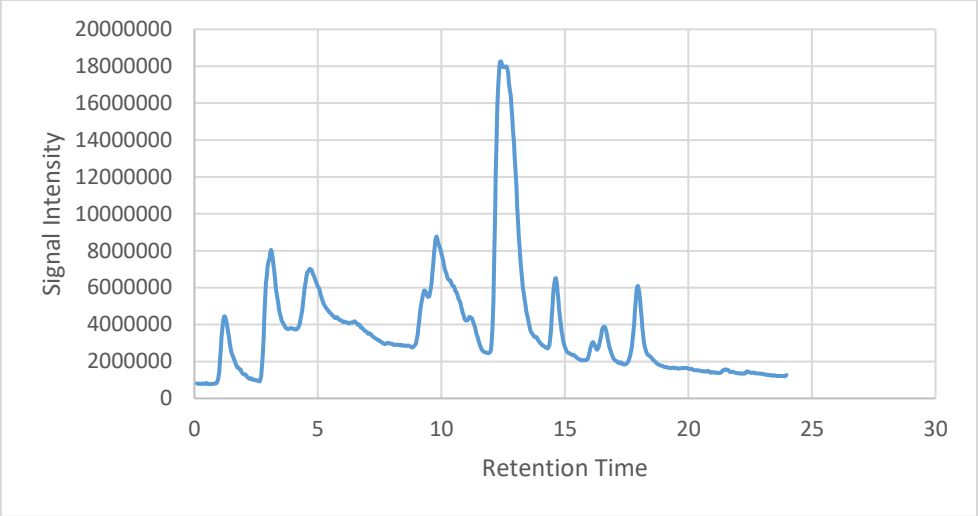

Figure 4.8: The positive TIC of the SOA from the pre-evaporated filter.

The strong peak around 13 minutes may be from the pinonic acid, pinonaldehyde, and the (+)207 ion. The peak at 10 minutes may be the result of norpinonic acid, the (+)193 ion, and the (+)209 ion. Table 4.5 lists all major ions and their respective retention times.

Table 4.5: Retention times of significant peaks

Ion peak	Name	Retention Time (minutes)
(-)185	Pinic Acid	10.0
(+)185	Pinonic Acid	12.5
(+)173	Norpinic Acid	5.0
(+)173	Norpinonic Acid	10.0
(+)169	Pinonaldehyde	13.0
(+)191	Unknown	12.7
(+)193	Unknown	9.8
(+)207	Unknown	12.3
(+)209	Unknown	9.8

4.4 Confirmation of products at a lowered concentration of ozone

The initial concentrations of ozone and α-pinene were extremely high in order to favor production of SOA. The next question is if they are observable at a more atmospherically relevant ozone concentration. The previous ozone concentration was at 222 ppm and it was lowered to 12.5 ppm. This is still much higher than actual ozone concentrations in the atmosphere as typically the troposphere background ozone concentration is in the range of 20-45 ppb.[52] The ozone generator was lowered to roughly 12% and its flow was reduced to 0.01 SLM. The nitrogen flow was increased to keep a total flow of 2.0 SLM.

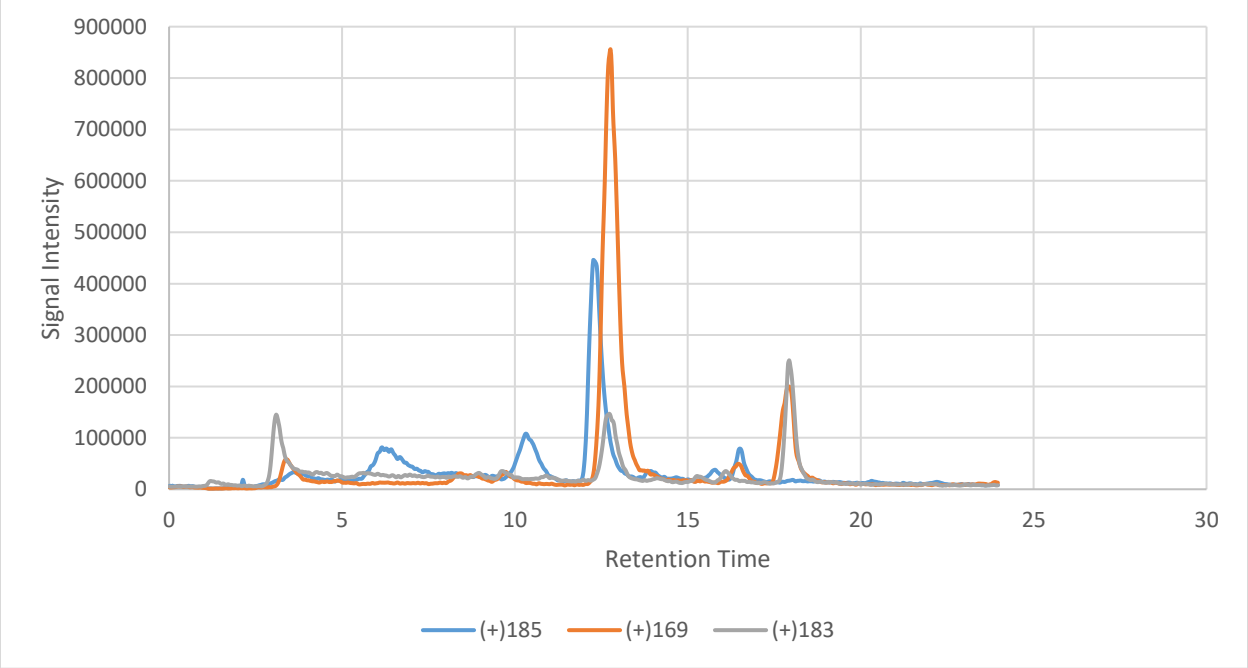

Figure 4.9: Chromatogram from the pre-evaporation filter at the lowered ozone concentration with extracted ions of pinonic acid (+)185 at 12.5 minutes, pinonaldehyde (+)169 at 13.1 minutes, and sorbitol (+)183 at 3.0 minutes.

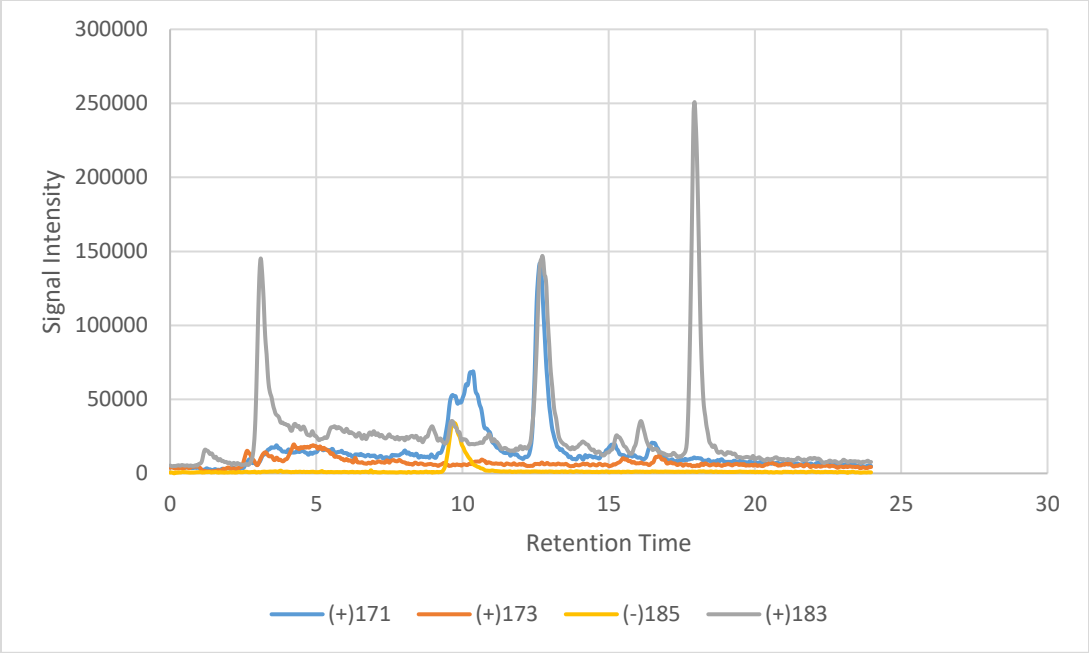

Figure 4.10: Chromatogram from the pre-evaporation filter at the lowered ozone concentration with extracted ions of norpinonic acid (+)171 at 10 minutes, norpinic acid (+)173 around 5 minutes, pinic acid (-)185 at 9.8 minutes, and sorbitol (+)183 at 3 minutes.

In Figures 4.9 and 4.10 all 5 compounds are visible in the pre-evaporation filter. Compared to the chromatograms in Figures 4.1 and 4.2 their signal is drastically lower due to the overall lowered SOA production. One difference between the high ozone and low ozone runs was the ratio of pinonaldehyde to pinonic acid. In the high ozone experiment, pinonic acid has a greater signal intensity than pinonaldehyde in the produced SOA. In the low ozone experiment, the signal intensity of pinonaldehyde is greater than pinonic acid in the produced SOA. This result may give insight to the reaction pathway of α-pinene ozonolysis depending on ozone concentration.

Each ion was extracted in the post-evaporation filter to determine if the compounds evaporated off of the filter and whether they are still visible. Figures 4.11 and 4.12 contain the 5 ions from the post-evaporation filter.

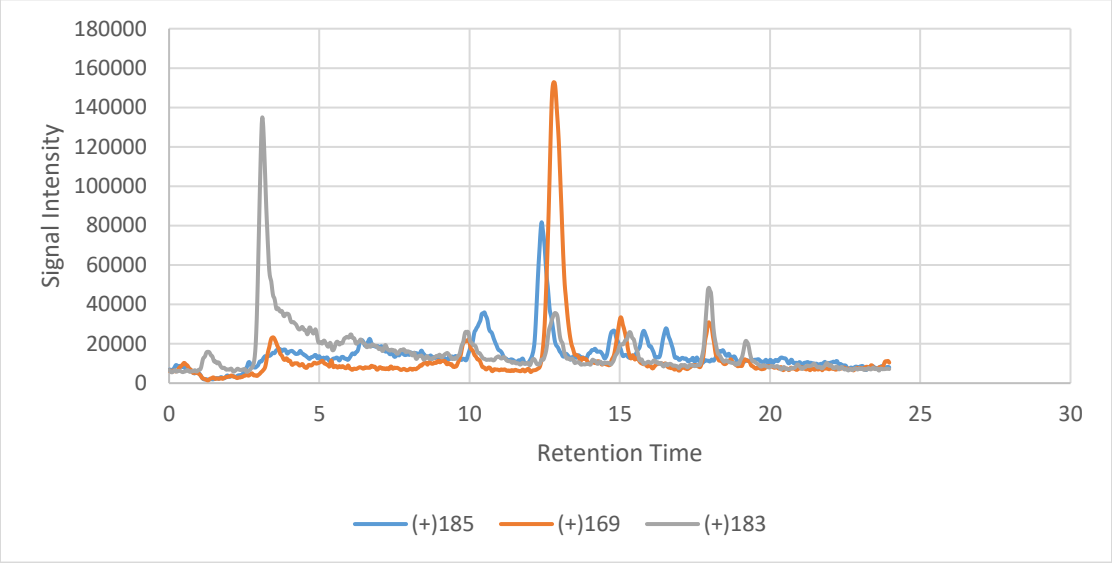

Figure 4.11: The chromatogram from the post-evaporation filter at the lowered concentration of ozone with extracted ions of pinonic acid (+)185 at 12.5 minutes, pinonaldehyde (+)169 at 13.1 minutes, and sorbitol (+)183 at 3.0 minutes.

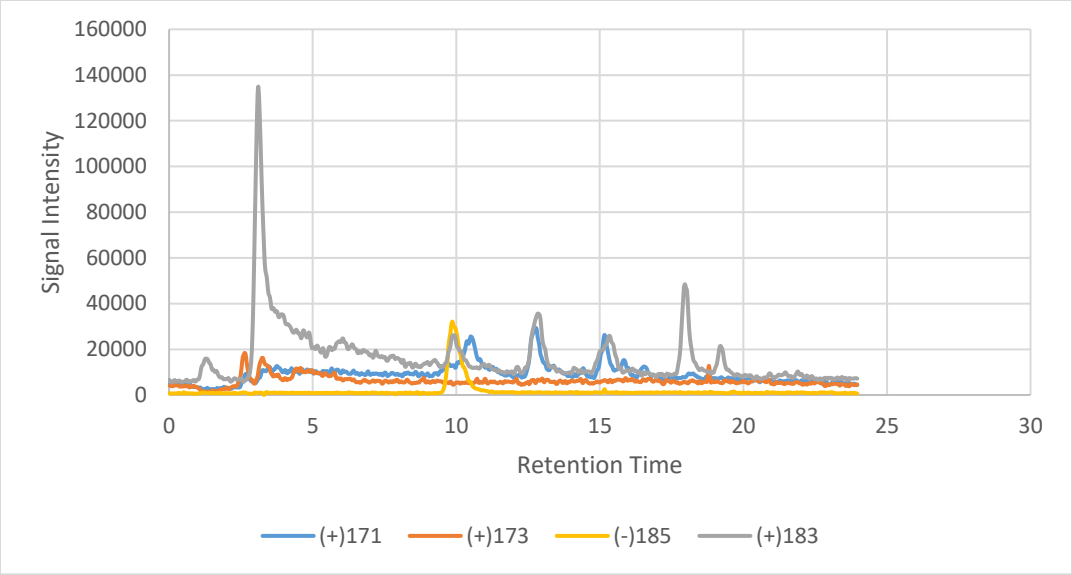

Figure 4.12: The chromatogram from the post-evaporation filter at the lowered concentration of ozone with extracted ions of norpinonic acid (+)171 at 10 minutes, norpinic acid (+)173 around 5 minutes, pinic acid (-)185 at 9.8 minutes, and sorbitol (+)183 at 3 minutes.

The post-evaporation extracted ions in Figures 4.11 and 4.12 are similar to the high ozone post-evaporation extracted ions in that they all decrease. Each ion vaporizes off of the filter to some degree leading to a decrease in signal. The evaporated semi-volatiles travel to the resin tube where they are collected onto the resin.

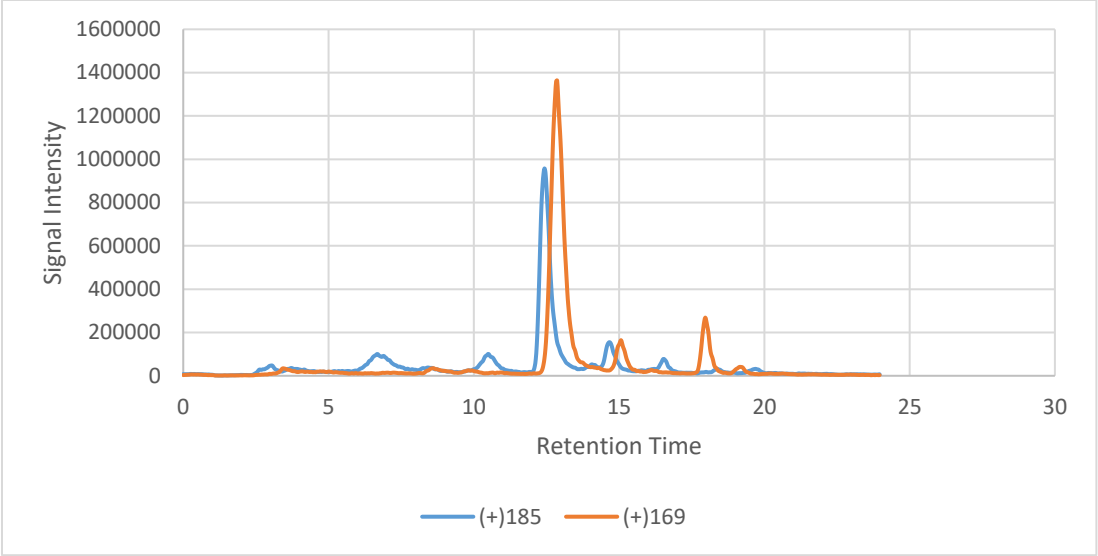

Figure 4.13: The chromatogram of the resin at the lowered ozone concentration with extracted ions of pinonic acid (+)185 at 12.5 minutes, pinonaldehyde (+)169 at 13.1 minutes.

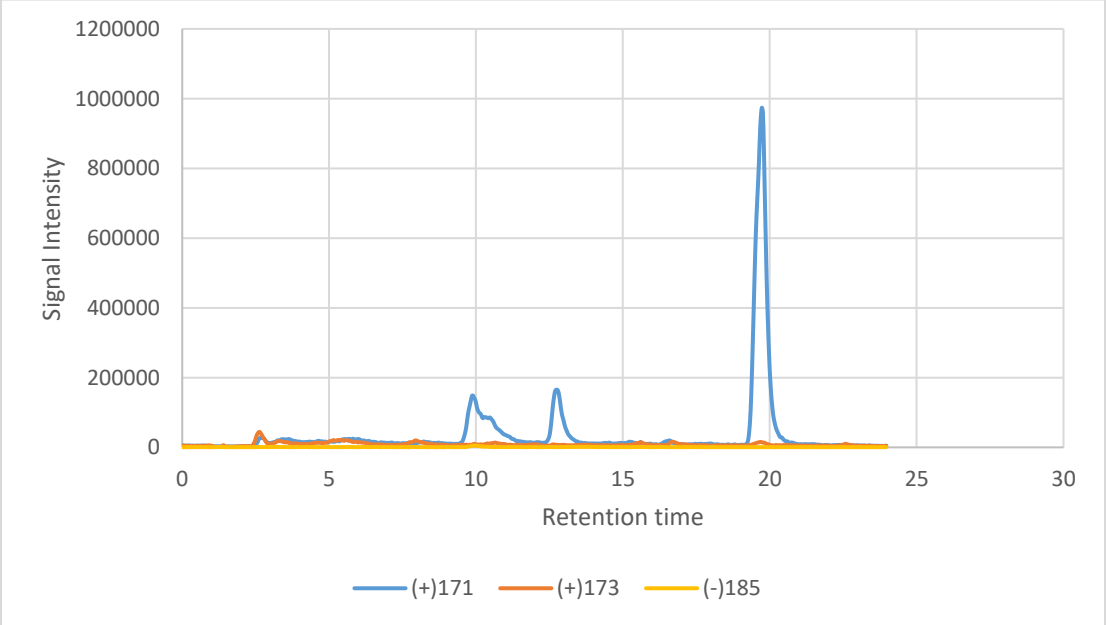

Figure 4.14: The chromatogram of the resin at the lowered concentration of ozone with extracted ions of norpinonic acid (+)171 at 10 minutes, norpinic acid (+)173 around 5 minutes, pinic acid (-)185 at 9.8 minutes.

Only 3 of the compounds are still visible in the resin when the ozone level was reduced to 12.5 ppm, as seen in Figures 4.13 and 4.14. Pinonic acid and Pinonaldehyde are visible due to their extremely strong signals while norpinonic acid is visible from its moderately strong signal and higher vapor pressure. Norpinic acid is not visible due to its smaller concentration and pinic acid is unobserved because of its low volatility. Pinic acid can be made visible on the resin spectrum in the future by increasing the amount of time that SOA is collected onto the resin. The temperature may also be increased but that may degrade some products so increasing the time of collection is more desirable.

At this low of a concentration for a 10 minute flow of the ozonolysis reaction the compounds are still produced at an observable level. This experiment was done to see if the products were still quantifiable when the ozone was set at a more atmospherically relevant concentration. Overall the chromatograms at the lowered concentration of SOA are similar to those at the higher concentration of SOA except that their signal intensities are much lower. The compounds were also observed in both the pre-evaporation and post-evaporation filters. The significance of that data is that these compounds can be used to find a relationship between signal loss with temperature and vapor pressure.

4.5 Evaporation rate as a function of temperature

With the successful confirmation of ozonolysis products stated in Chapter 3.4 the next step focused on looking at the volatility of SOA. The generated α-pinene ozonolysis SOA was subjected to different temperatures between experiments. The amount a species is removed from the filter at given temperatures would indicate how high or low its vapor pressure is. Changing the temperature directly affected the signal intensity of the five compounds for the post-evaporation filter collection and resin collection. The change in

peak intensity indicates the amount of the compound removed which allows the relative vapor pressure to be assessed between the different species.

The collection of ozonolysis products was done multiple times altering the filter holder temperature between 20 ºC, 40 ºC, 60 ºC, and 80 ºC. The SOA generation for the extraction at 40 ºC was much greater than the other runs for unknown reasons, therefore this run is not included in certain data analyses due to its inconsistency. Each compound was studied to evaluate the evaporation rate as a function of temperature. The constant sorbitol peak of (+)183 at 3 minutes is used to give a comparison between runs. Figures 4.6, 4.7, 4.8, and 4.9 each show how the peak intensity of the known compound ions changes with temperature and between filters. The loss of the compounds as temperature increases can be observed as their peak changes with respect to the constant sorbitol peak.

a.

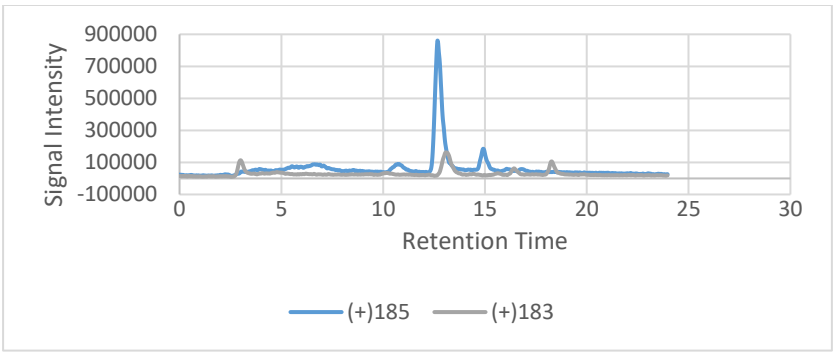

b.

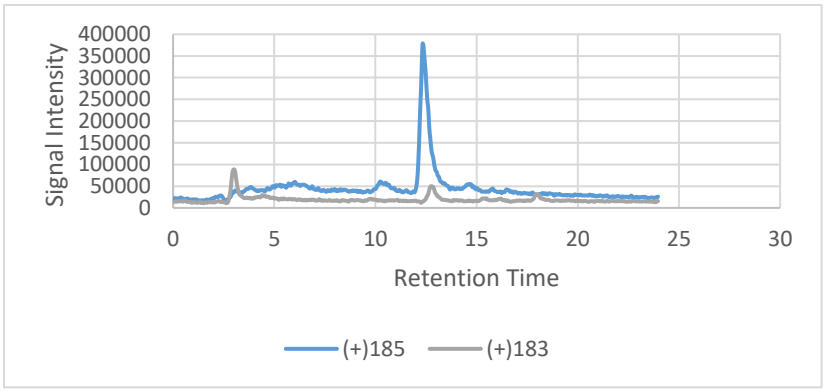

c.

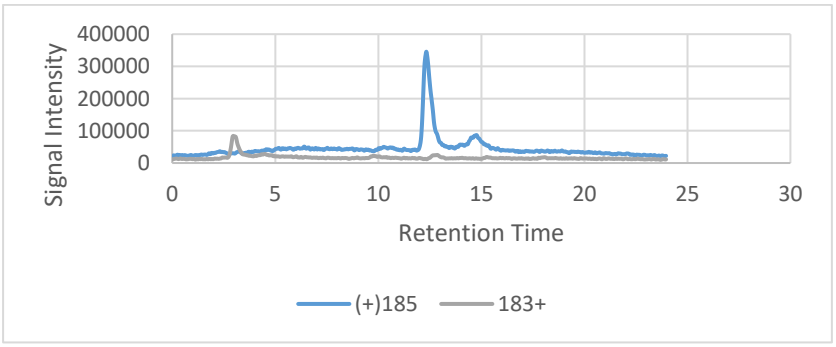

d.

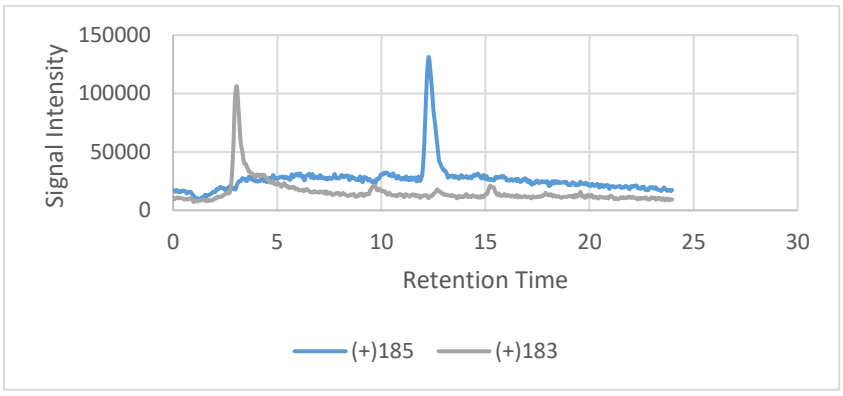

Figure 4.15: Pinonic acid (+)185 peak at 12.5 minutes with sorbitol (+)183 at 3 minutes on post-evaporation filters. The temperature for each evaporation is a: 20 ºC, b: 40 ºC, c: 60 ºC, and d: 80 ºC.

a.

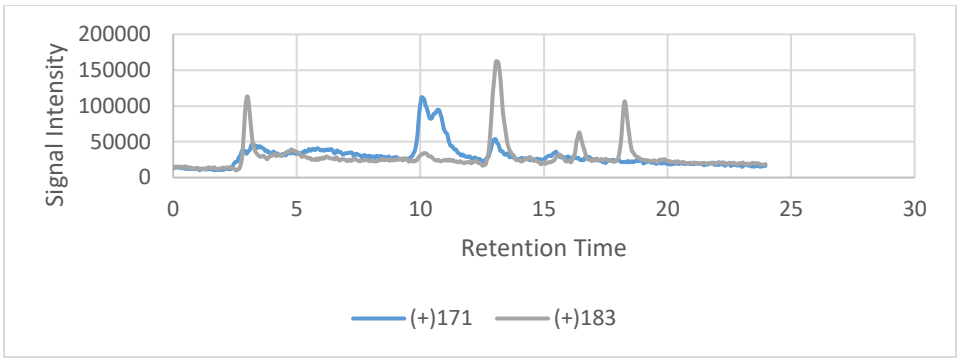

b.

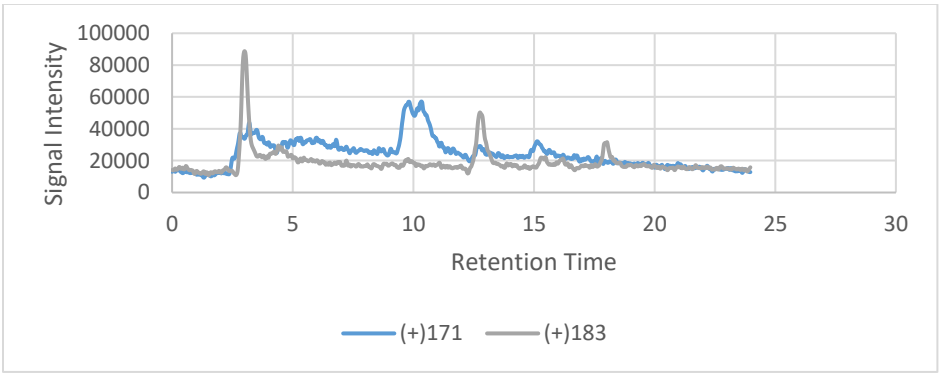

c.

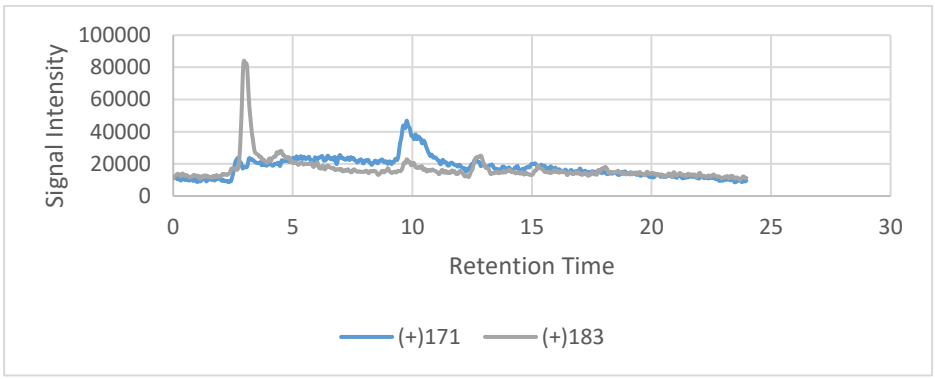

d.

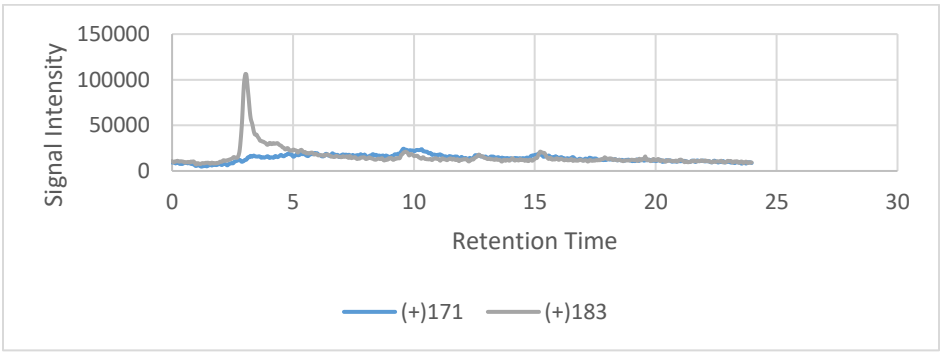

Figure 4.16: Norpinonic acid (+)171 peak at 10 minutes with sorbitol (+)183 at 3 minutes on post-evaporation filters. The temperature for each evaporation is a: 20 ºC, b: 40 ºC, c: 60 ºC, and d: 80 ºC.

a.

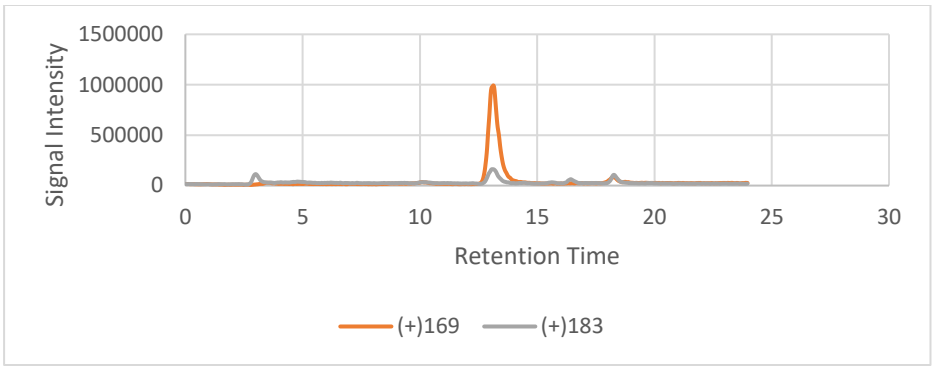

b.

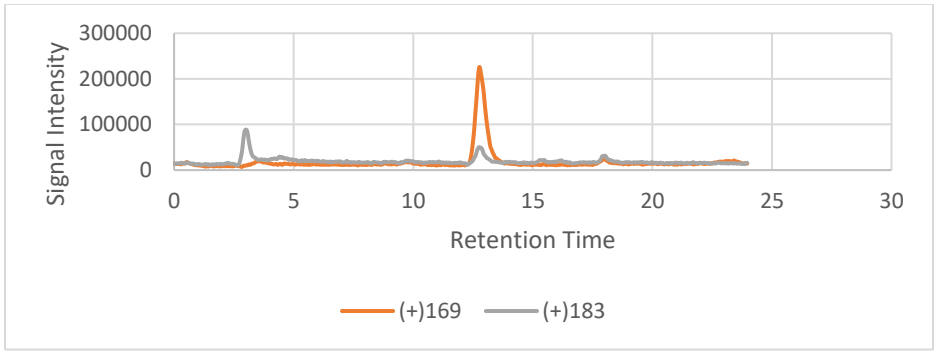

c.

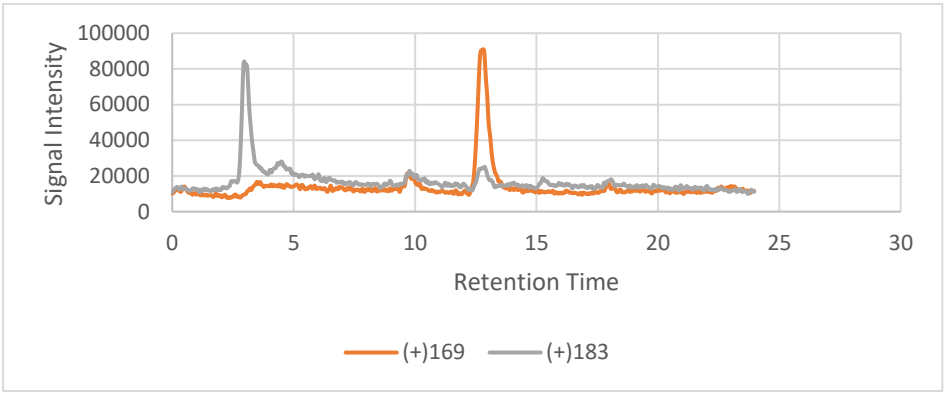

d.

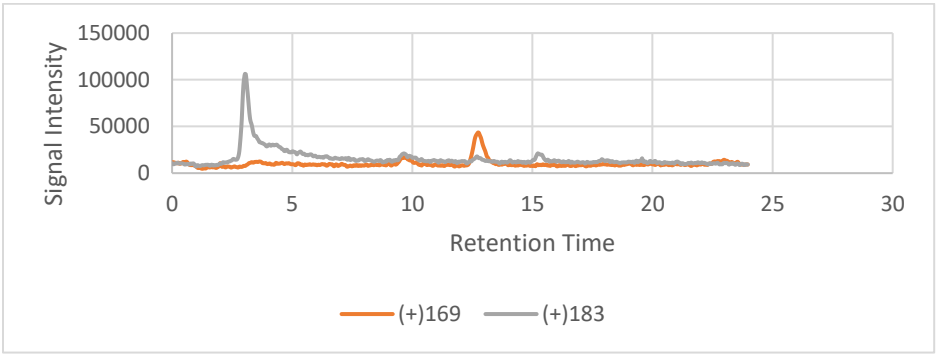

Figure 4.17: Pinonaldehyde (+)169 peak at 13.0 minutes with sorbitol (+)183 at 3 minutes on post-evaporation filters. The temperature for each evaporation is a: 20 ºC, b: 40 ºC, c: 60 ºC, and d: 80 ºC.

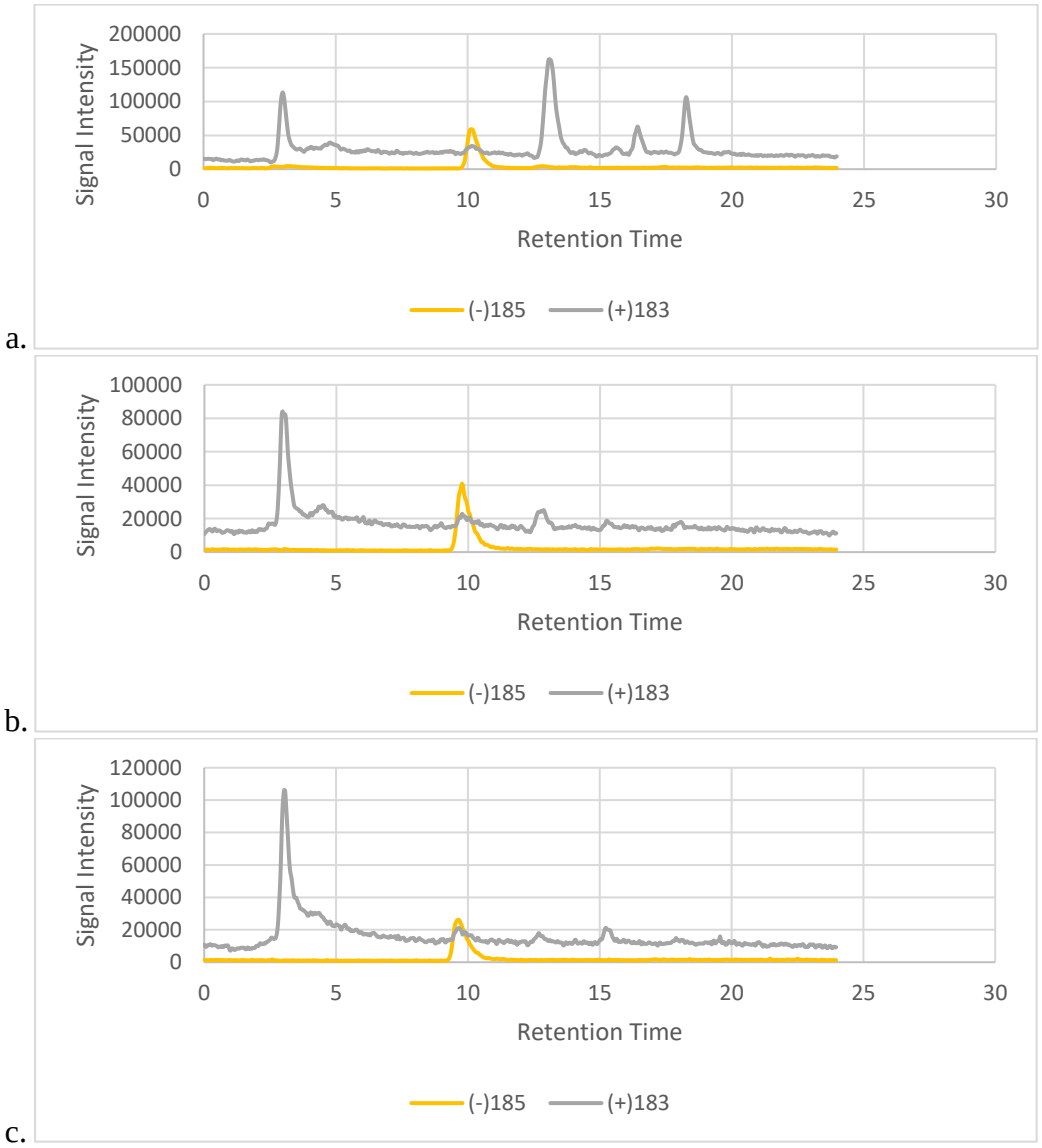

Figure 4.18: Pinic acid (-)185 peak at 10 minutes with sorbitol (+)183 at 3 minutes on post-evaporation filters. The temperature for each evaporation is a: 20 ºC, b: 60 ºC, c: 80 ºC. The run at 40 degrees is not shown as it was skewed due to excess SOA production.

The loss of a compound on the filter is determined by both its vapor pressure and the temperature of the filter holder so this information is used to develop a relationship of

evaporative loss and volatility. The ratio of the normalized peak area in the post-evaporation filter over the pre-evaporation filter for each temperature shows how much loss a compound experiences. The pre and post evaporation peak areas are normalized by first dividing each by the area of the sorbitol peak for its respective run. Next the peak for the post-evaporation filter is divided by the pre-evaporation filter peak. The normalized peak areas are used to account for change in between runs in the LC. Comparing the ratio of compound loss to the temperatures gives a linear trend according to Figures 4.10, 4.11, and 4.12. At a higher temperature the ratio should be lower as more of the compound is removed. A compound with a higher vapor pressure would have a steeper slope of loss than one with a lower vapor pressure.

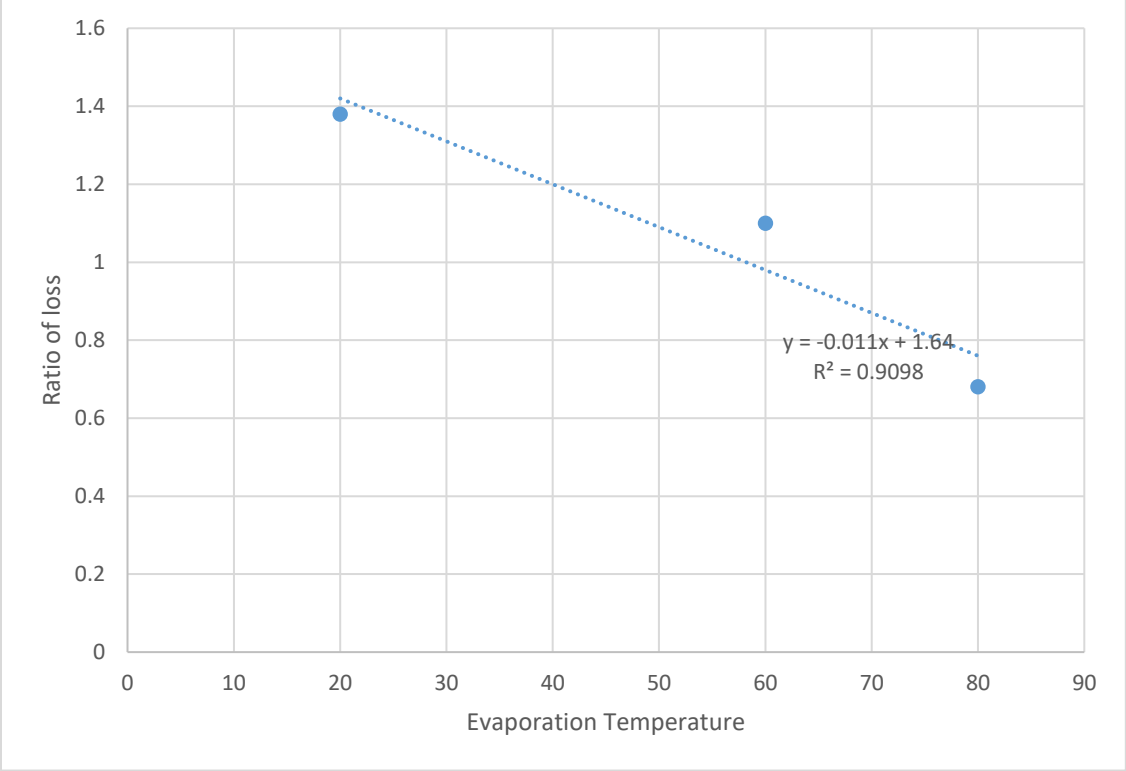

Figure 4.19: The normalized peak areas of the post-evaporation filter divided by the pre-evaporation filter for pinic acid. The rate of pinic acid evaporation determined by the ratio of compound loss.

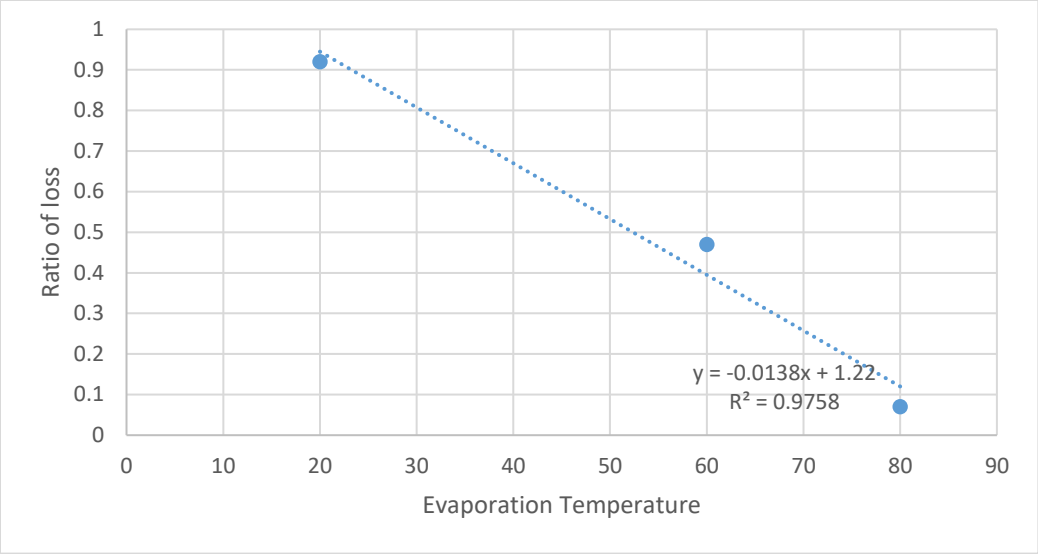

Figure 4.20: The normalized peak areas of the post-evaporation filter divided by the pre-evaporation filter for norpinonic acid. The rate of norpinonic acid evaporation determined by the ratio of compound loss.

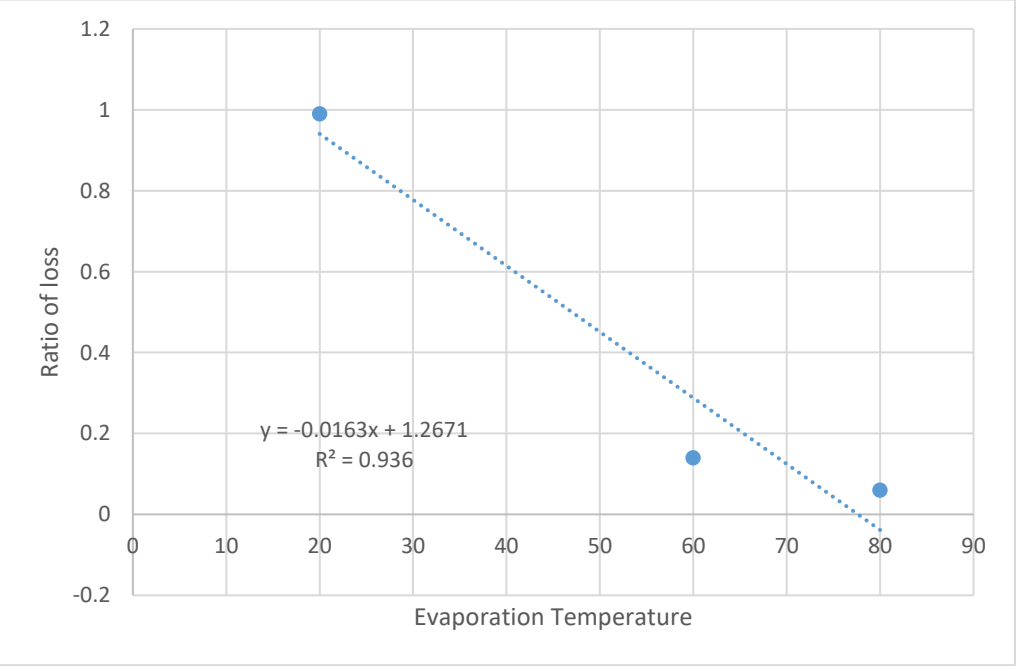

Figure 4.21: The normalized peak areas of the post-evaporation filter divided by the pre-evaporation filter for pinonaldehyde. The rate of pinonaldehyde evaporation determined by the ratio of compound loss.

The vapor pressures of each of these compounds show a logarithmic trend with their ratio loss slope. Taking the natural log of their vapor pressure shows a rough estimate at the vapor pressure and peak loss relationship as shown in Figure 4.10.

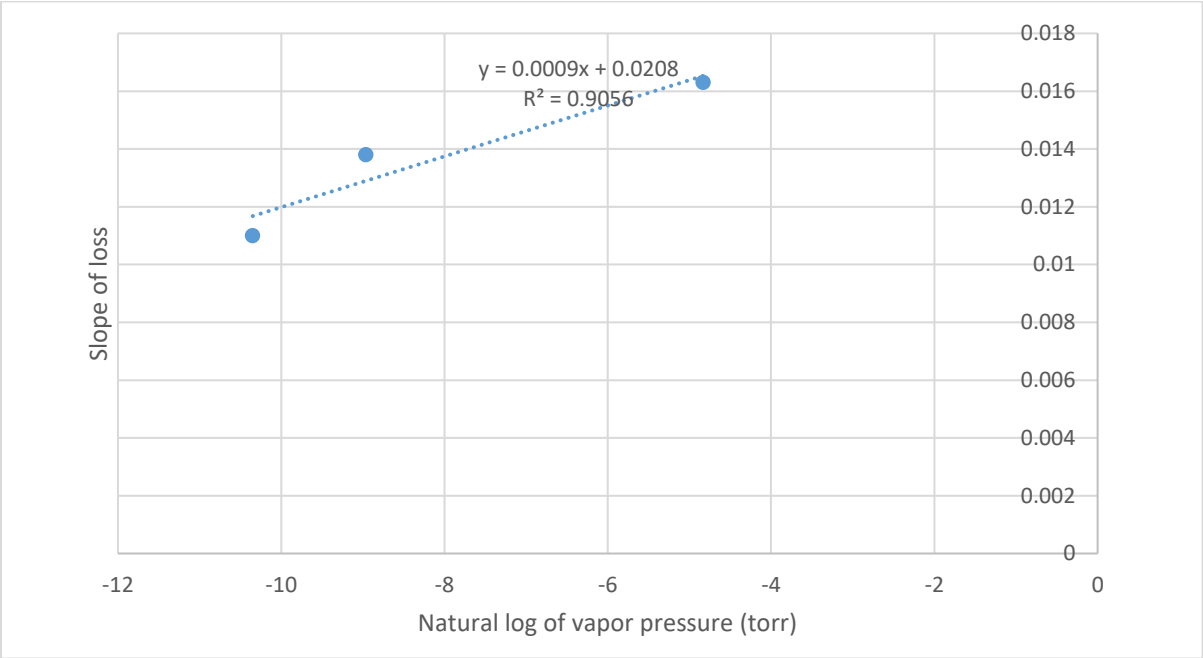

Figure 4.22: The natural log of vapor pressure graphed against their slope of loss. The trendline equation provides an estimate of a compound's vapor pressure.

By having the relationship present in Figure 4.10 we have an idea of how compounds' volatility relates to their evaporation rate in this experiment. Other compounds present in the chromatogram can be analyzed to determine their approximate vapor pressure.

4.5.1 Unknown Peaks vapor pressure estimation

With the relationship of loss from filter to vapor pressure the volatility of other, both identified and unidentified, α-pinene ozonolysis products could be evaluated. Four prominent peaks at m/z's of (+)191, (+)193, (+)207, and (+)209 were observed, determined to be ozonolysis products, and were semi-volatile based. Each had a clear decrease in signal in the post-evaporation filter as the temperature was increased. Table 4.6 shows the data of the unknown ions compared with the known compounds.

Table 4.6: Normalized peak data for unknown and known ions.

Compound	20 ºC	60ºC	80ºC	Slope	R^2 value
Pinic acid	Pre: 0.73 Post: 1.01	Pre: 0.87 Post: 0.96	Pre: 0.79 Post: 0.54	-0.011	0.9098
Norpinonic acid	Pre: 1.43 Post: 1.31	Pre: 1.74 Post: 0.81	Pre: 1.50 Post: 0.10	-0.0138	0.9758
Pinonaldehyde	Pre: 17.07 Post: 16.92	Pre: 11.94 Post: 1.71	Pre: 8.76 Post: 0.53	-0.0163	0.936
(+)191	Pre: 17.76 Post: 16.08	Pre: 9.77 Post: 1.74	Pre: 9.07 Post: 0.82	-0.143	0.9456
(+)193	Pre: 7.22 Post: 10.49	Pre: 5.94 Post: 2.72	Pre: 7.39 Post: 0.89	-0.0226	0.9924
(+)207	Pre: 42.66 Post: 46.87	Pre: 33.44 Post: 19.93	Pre: 35.51 Post: 7.74	-0.0144	0.9882
(+)209	Pre: 7.91 Post: 12.88	Pre: 5.78 Post: 4.95	Pre: 7.51 Post: 4.79	-0.0169	0.9853

The second, third, and fourth columns have the normalized peak area for the pre-evaporation filter and the post-evaporation filter.

Each compound has its own ratio of loss with temperature. Their slope of loss can be compared to the known compounds' slopes in order to compare their vapor pressures.

Table 4.7: Unknown ions slope of loss and calculated vapor pressure from Figure 4.10

Ion	Ratio loss vs temperature slope	Calculated vapor pressure (torr)[a]
(+)191	-0.0143	7.302×10^{-4}
(+)193	-0.0226	7.389
(+)207	-0.0144	8.160×10^{-4}
(+)209	-0.0169	1.312×10^{-2}

a: Calculated from equation in Figure 4.10

It is important to note that Table 4.7 utilizes a rough calculation of vapor pressures. This calculation comes from data points that were done a single time. The trendlines such as ratio lost slopes and the relation between natural log of vapor pressure and loss slopes only have 3 points each. In the future it would be desirable to have much more data in order to get a more accurate measurement. This data still does give an idea of the vapor pressures of these unknown compounds. Ions (+)191 and (+)207 have a lower vapor pressure than pinonaldehyde but higher than norpinonic acid. The (+)209 peak must have a slightly higher volatility than pinonaldehyde while the (+)193 peak is significantly higher. These conclusions can start to be drawn about these unknown species but with more data a better estimation will be made.

4.6 Conclusions

LC-MS was successful in identifying known semi-volatile compounds from the ozonolysis of α-pinene. In addition, various unknown ions were discovered which can lead to discovering more about the composition of the semi-volatile layer of SOA. Using the method of comparing how signal changes with temperature differences can lead to

estimating volatility. In the future there can be a much more accurate relationship between signal loss of a compound and its vapor pressure. With this information the volatility of SOA can also be determined through LC-MS.

CHAPTER 5 – CONCLUSIONS AND FUTURE WORK

5.1 Conclusions

LC-MS was the most successful out of the instrumental methods and shows the most promise going forwards. FTIR was tested for its ability to measure the functionality and volatility of SOA. However, there were many inconsistencies with data most likely caused by imperfect contact of the sample with the ATR crystal. GC-MS was also tested for the ability to identify individual species in the semi-volatile fraction of SOA. Derivatization of products before sampling was necessary which involved altering the structure of compounds with certain functional groups. Ultimately this procedure was too problematic as products were not able to be successfully identified from this change in structure. LC-MS was able to successfully identify several known compounds from the ozonolysis of α-pinene. LC-MS is able to locate individual species in SOA. In addition, a method was constructed in order to estimate volatility of unknown compounds observed by LC-MS.

5.2 Future work

The first objective in the future is collecting more data. The work on vapor pressure estimation relative to the slope of loss does not have enough compounds and tests completed to make an accurate conclusion. More known compounds should be tested and at least one more temperature should be studied. Also, as the 40 ºC temperature run could not be used it should be done again. Additional runs should be done for the known compounds to show this is repeatable. As the experiments have only been done one time each there are no error bars or standard deviation. The 4 runs at the

different temperatures should be completed for a minimum of 3 times each. Not only would more data give a better idea of vapor pressure for unknown peaks but it would make this estimation much more reliable.

The resin comparison should also be investigated further as that too needs more data points. More compounds and runs comparing the resins can show which would be ideal. A greater variation in compounds and their functional groups would give a better understanding into each resin's collection efficiency.

The unknown compounds that are seen by the LC-MS should also be further explored. Some prominent ions are already clear but there are many more species that we have not yet analyzed. Their molecular weight will be known and there will be an estimated calculation of their vapor pressure. More about these compounds may be determined which would help characterize the semi-volatile layer of SOA. Out of the three techniques tested LC-MS exhibited the most success. However, both FTIR and GC-MS may still provide significant insight to this study and may be explored further.

REFERENCES

1. Kroll, J. H.; Seinfeld, J. H., Chemistry of secondary organic aerosol: Formation and evolution of low-volatility organics in the atmosphere. *Atmospheric Environment* **2008**, *42* (16), 3593-3624.
2. Pope, C. A., III; Ezzati, M.; Dockery, D. W., Fine-Particulate Air Pollution ad Life Expectancy in the United States. *New England Journal of Medicine* **2009**, *360* (4), 376-386.
3. Harrison, R. M.; Yin, J. Particulate matter in the atmosphere: which particle properties are important for its effects on health? *Science of the Total Environment*. **2000**, *249* (1-3), 85-101.
4. Donahue, N. M.; Robinson, A. L.; Trump, E. R.; Riipinen, I.; Kroll, J. H., Volatility and Aging of Atmospheric Organic Aerosol. *Atmospheric and Aerosol Chemistry* **2012**. *339*, 97-143.
5. Jacob, D. J. Introduction to Atmospheric Chemistry. **2009** Princeton, New Jersey.
6. Hallquist, M. *et al*. The formation, properties and impact of secondary organic aerosol: current and emerging issues. *Atmos Chem Phys* **2009**, *9* (14), 5155-5236.
7. Seinfeld, J. H.; Pankow, J. F. Organic Atmospheric Particulate Material. *Annual Review of Physical Chemistry* **2003**, *54*, 121-140.
8. Zhang, J. Y.; Hartz, K. E. H.; Pandis, S. N.; Donahue, N. M.; Secondary organic aerosol formation from limonene ozonolysis: homogeneous and heterogeneous influences as a function of NO_x. *J Phys Chem A* **2006** *110* (38) 11053-11063.

9. Ervens, B. Turpin, B. J.; Wever, R. J. Secondary organic aerosol formation in cloud droplets and aqueous particles (aqSOA): a review of laboratory, field and model studies. *Atmos Chem Phys* **2011**, *11* (21), 11069-11102.

10. Lim, Y. B.; Tan, Y.; Perri, M. J.; Seitzinger, S. P.; Turpin, B. J. Aqueous chemistry and its role in secondary organic aerosol (SOA) formation. *Atmos Chem Phys* **2010**, *10* (21), 10521-10539.

11. Ng, N. L.; Kroll, J. H.; Keywood, M. D.; Bahreini, R.; Varutbankul, V.; Flagan, R. C.; Seinfeld, J. H.; Lee, A.; Goldstein, A. H. Contribution of first- versus second-generation products to secondary organic aerosols formed in the oxidation of biogenic hydrocarbons. *Environ Sci Technol* **2006**, *40* (7), 2283-2297.

12. Robinson, A. L. *et al*. Rethinking Organic Aerosols: Semivolatile Emissions and Photochemical Aging. *Science*. **2007**, *315*, 1259-1262.

13. Kroll, J. H.; Chan, A. W. H.; Ng, N. L.; Flagan, R. C.; Seinfeld, J. H. Reactions of Semivolatile Organics and Their Effects on Secondary Organic Aerosol Formation. *Environ Sci Technol* **2007**, *41*, 3545-3550.

14. Jacobson, M. C.; Hansson, H. C.; Noone, K. J.; Charlson, R.J. Organic atmospheric aerosols: review and state of the science. *Reviews of Geophysics* **2000**, *38*, 267–294.

15. Rudich, Y.; Donahue, N. M.; Mentel, T. F. Aging of organic aerosol: bridging the gap between laboratory and field studies. *Annual Review of Physical Chemistry* **2007**, *58*, 321–352.

16. De Gouw, J. A. *et al.* Budget of organic carbon in a polluted atmosphere: results from the New England Air Quality Study in 2002. *Journal of Geophysical Research—Atmospheres* **2005**, *110*, D16305.

17. Heald, C. L. *et al*. A large organic aerosol source in the free troposphere missing from current models. *Geophysical Research Letters* **2005**, *32*, L18809.

18. Heald, C. L. *et al*. Concentrations and sources of organic carbon aerosols in the free troposphere over North America. *Journal of Geophysical Research—Atmospheres*. **2006**, *111,* D23S47.

19. Volkamer, R. *et al*. Secondary organic aerosol formation from anthropogenic air pollution: rapid and higher than expected. *Geophysical Research Letters* **2006**, *33,* L17811.

20. Fraser, M. P.; Cass G. R.; Simoneit, B. R. T. Gas-phase and particle-phase organic compounds emitted from motor vehicle traffic in a Los Angeles roadway tunnel. *Environ Sci Technol* **1998**, *32* (14), 2051-2060.

21. Yokelson, R. J. *et al*. Emissions from biomass burning in the Yucatan. *Atmos Chem Phys* **2009**, *9* (15), 5785-5812.

22. Woo Jin An; Pathak, R. K.; Lee, B.-H.; Pandis, S. N. Aerosol volatility measurement using an improved thermodenuder: Application to secondary organic aerosol. *Journal of Aerosol Science* **2007**, *38* (3), 305-314.

23. Lee, B.-H.; Pierce, J. R.; Engelhard, G. J.; Pandis, S. N., Volatility of secondary organic aerosol from the ozonolysis of monoterpenes. *Atmospheric Environment* **2011**, *45* (14), 2443-2452.

24. Kidd, C.; Perraud, V.; Finlayson-Pitts, B. J. New insights into secondary organic aerosol from the ozonolysis of α-pinene from combined infrared spectroscopy and mass spectrometry measurements. *Phys Chem. Chem Phys.* **2014**, *16*, 22706-22716.

25. Isaacman, G.; Worton, D. R.; Kreisber, N. M.; Hennigan, C. J.; Teng, A. P.; Hering, S. V.; Robinson, A. L.; Donahue, N. M.; Goldstein, A. H. Understanding evolution of product composition and volatility distribution through in-situ GC x GC analysis: a case study of longifolene ozonolysis. *Atmospheric Chemistry and Physics* **2011**, *11* (11), 5335-5346.

26. Hung, H.-M.; Chen, Y.-Q.; Martin, S. T. Reactive Aging of Films of Secondary Organic Material Studied by Infrared Spectroscopy. *The Journal of Physical Chemistry* **2013**, *117,* 108-116.

27. Perraud, V., *et al*., Nonequilibrium atmospheric secondary organic aerosol formation and growth. *Proceedings of the National Academy of Sciences of the United States of America* **2012**, *109* (8), 2836-2841.

28. Gross, S.; Bertram, A. K., Products and kenetics of the reactions of an alkane monolayer and a terminal alkene monolayer with NO3 radicals. *Journal of Geophysical Research – Atmosphere* **2009**, *114* (D2), D02307/1-D02307/14.

29. Presto, A. A.; Huff Hartz, K. E.; Donahue, N. M., Secondary Organic Aerosol Production from terpene Ozonolysis. 2. Effect of NO_x Concentrration. *Environ Sci Technol* **2005**, *39,* 7046-7054.

30. Jaoui, M.; Kamens, R. M. Mass balance of gaseous and particulate products analysis from α-pinene/NO_x/air in the presence of natural sunlight. *Journal of Geophysical Research* **2001**, *106* (12), 12541-12558.

31. Schauer, J., *et al*. Development of an in situ derivatization technique for rapid analysis of levoglucosan and polar compounds in atmospheric aerosol. *Atmospheric Environment* **2015**, *123*, 251-255.

32. Mazurek, M.; Hawley, H.; Dukett, J.; Sagona, J. Sequential derivatization of polar organic compounds in cloud water using *O*-(2,3,4,5,6-pentafluorobenzyl)hydroxylamine hydrochloride, *N*,*O*-bis(trimethylsilyl)trifluoroacetamide, and gas-chromatography/mass spectrometry analysis. *Journal of Chromatography A* **2014**, *1362*, 16-24.

33. Doskey, P.; Flores, R. Evaluation of multistep derivatization methods for identification and quantification of oxygenated species in organic aerosol. *Journal of Chromatography A* **2015**, *1418*, 1-11.

34. Miyazaki, Y. *et al*. Chemical characterization of water-soluble organic carbon aerosols at a rural site in the Pearl River Delta, China, in the summer of 2006. *Journal of Geophysical Research* **2009**. *114*, D14208, doi:10.1029/2009JD011736.

35. Wilson, Nancy K.; Hannan, Steve W.; Chuang, Jane C. Field Comparison of Polyurethane Foam and XAD-2 Resin for Air Sampling for Polynuclear Aromatic Hydrocarbons. *Environ. Sci. Technol.* **1987**. *21,* 798-804.

36. Wania, F.; Lei, Y.; Hayward, S. Sorption of a diverse set of organic chemical vapors onto XAD-2 resin: Measurement, prediction and implications for air sampling. *Atmospheric Environment* **2011**. *45*, 296-302.

37. Larsen, B.; Bella, D.; Glasius, M.; Winterhalter, R.; Jensen, N.; Hjorth, J. Gas-Phase OH Oxidation of Monoterpenes: Gaseous and Particulate Products. *Journal of Atmospheric Chemistry* **2001**. *38*, 231-276.

38. Winterhalter, R.; Van Dingenen, R.; Larsen, B.; Jensen, N.; Hjorth, J. LC-MS analysis of aerosol particles from the oxidation of α-pinene by ozone and OH-radicals. *Atmospheric Chemistry and Physics Discussions* **2003**. *3*, 1-39.

39. Khaled, A.; Pawliszyn, Janusz. Time-weighted average sampling of volatile and semi-volatile airborne organic compounds by the solid-phase microextraction device. *Journal of Chromatography* **2000**. *892*, 455-467.

40. Fu, T.-M. *et al*. Global budgets of atmospheric glyoxal and methylglyoxal, and implications for formation of secondary organic aerosols. *Journal of Geophysical Research* **2008**, *113* (D15), JD009595.

41. Witkowski, B.; Gierczak, T. Early stage composition of SOA produced by α-pinene/ozone reaction: α-Acyloxyhydroperoxy aldehydes and acidic dimers. *Atmospheric Environment*. **2014**. *95*, 59-70.

42. Jenkin, M. Modelling the formation and composition of secondary organic aerosol from α- and β-pinene ozonolysis using MCM v3. *Atmospheric Chemistry and Physics* **2004**. *4*, 1741-1757

43. Meusinger, C. *et al*. Chemical and isotopic composition of secondary organic aerosol generated by α-pinene ozonolysis. *Atmospheric Chemistry and Physics* **2017**. *17*, 6373-6391.

44. Daubert, T.E., R.P. Danner. Physical and Thermodynamic Properties of Pure Chemicals Data Compilation. Washington, D.C.: Taylor and Francis, 1989.

45. US EPA; Estimation Program Interface (EPI) Suite. Ver. 4.1. Jan, 2010.

46. Claeys, M., *et al*. Formation of Secondary Organic Aerosols Through Photooxidation of Isoprene. *Science* **2004**, *303* (5661), 1173-1176.

47. Surratt, J. D., *et al*. Evidence for Organosulfates in Secondary Organic Aerosol. *Environmental Science and Technology* **2007**, *41* (2), 517-527.

48. Capouet, M.; Muller, J. A group contribution method for estimating the vapour pressures of α-pinene oxidation products. *Atmospheric Chemistry and Physics* **2006**. *6*, 1455-1467.

49. Bilde, M.; Pandis, S. Evaporation Rates and Vapor Pressures of Individual Aerosol Species Formed in the Atmospheric Oxidation of α- and β-Pinene. *Environmental Science and Technology* **2001**. *35 (16)*, 3344-3349.

50. Yu, J.; Cocker III, D.; Griffin, R.; Flagan, R.; Seinfeld, J. Gas-Phase Ozone Oxidation of Monoterpenes: Gaseous and Particulate Products. *Journal of Atmospheric Chemistry* **1999**. *34*, 207-258.

51. Sigma-Aldrich 2018. https://www.sigmaaldrich.com/united-states.html 2018.

52. Vingarzan, R. A review of surface ozone background levels and trends. *Atmospheric Environment* **2004**. *28*, 3431-3442.